Doctor of Engineering Thesis

Study on Engineering Properties of Soil Mixed with Discarded Tire Powder

March 2011

Hak Sam Kim

Abstract

Study on Engineering Properties of Freezing Soil Mixed with Discarded Tire Powder

Hak Sam kim

Yeungnam College of Science & Technology, 2011

Recently big building projects have increased the demand for crushed stone and gravel but they are hard to secure granular material of fine quality because the government's strict policies of environment and natural conservation have made developing stony mountains difficult.

This study, aiming at positive, effective use of discarded tire powder as soil material, instead of granular material of good quality in want, conducted a field experiment on the non-mixed and mixed soil (mixing ratio of tire powder 20%) in a concrete basin in order to investigate the effect of tire powder on inhibiting frost heave as the first step of the research. At the field experiment, frost heave amount, frozen depth, frost heave force, soil temperature, ground water level, etc. were observed. Also the frost heave suppressing effect of tire powder was evaluated quantitatively based on frost heave ratio and segregation potential.

As the second step of the study, tests of thermal conductivity, unfrozen water, ultrasonic wave and laboratory frost heave, etc. were carried out on the mixed soil of discarded tire to investigate its engineering characteristics.

First, test of thermal conductivity was carried out to analyze the thermal conductivity behavior according to temperature variance and mixing ratio using discarded tire powder of three different kinds in particle diameter. Besides, using pulsed Nuclear Magnetic Resonance (NMR) equipment, unfrozen water content of frozen soil was measured and expressed into the function of temperature. Also, by developing two-phase thermal conductivity model of soil particle and water for unfrozen soil proposed by Woodside, a new three-phase thermal conductivity model was proposed, consisting of soil particle, ice and unfrozen water, that can be applied even to the area of frozen soil.

For ultrasonic wave test, using pulse method, a kind of nondestructive method that can

evaluate dynamic characteristics of frozen soil, behavior of P wave (dilatational wave) and S wave (shear wave) of frozen soil was analyzed according to the change of -10 degree Celsius to 0 degree Celsius and mixing ratio of discarded tire powder, and unconfined compressive test was conducted on four kinds of mixed soil from discarded tire powder. Also, change in unfrozen water of frozen soil mixed with discarded tire powder was analyzed, and the relationships between unfrozen water content and elastic wave velocity as well as between elastic wave velocity and unconfined compressive strength were examined. In addition, using the measures of elastic wave velocity, against frozen soil mixed with tire powder, elastic constant, dynamic shear modulus, dynamic elastic modulus and Poisson's ratio were calculated.

In frost-heave experiment, aiming to examine the frost heave characteristics of mixed-soil according to the change of mixing ratio of discarded tire powder and to investigate the related frost heave suppressing mechanism, the author, based on the idea of change in coefficient of permeability by the mixture of discarded tire powder, first calculated unsaturated coefficient of permeability from the relationship between unfrozen water content in the low temperature below 0 degree Celsius and unsaturated water content in the normal temperature above 0 degree Celsius. Then, after considering the ice-impeding factor and ratio between the cross sections of soil and tire powder in the mixed soil, effect of tire powder reducing frost susceptibility was systemically investigated through calculating the permeability coefficient of frozen fringe.

Acknowledgments

I would like to express my deepest gratitude to my research supervisor, Dr. Teruyuki Suzuki, Professor of the Department of Civil and Environmental Engineering, Kitami Institute of Technology. His help and understanding has been invaluable toward the successful realization of this research. I sincerely acknowledge his painstaking academic guidance, fatherly disposition, and patience in ensuring that this research was carried to a logical conclusion. I will always be eternally grateful to him for the opportunity to learn many things and broaden my knowledge in many ways that I would not have thought possible.

Next, I would like to extend my gratitude to a former Professor Msami Fukuda of the Institute of Low Temperature Science, Hokkaido University for his guidance and expertise throughout all the stages of the studies described in this thesis. I also owe particular thanks to a former Professor Satoshi Akakawa, Department of Civil Engineering, Hokkaido University for his invaluable suggestions and discussions related to the frost heave analysis.

Particular thanks should also be given Dr. Sang Youl Suh, Professor of the Department of Civil Engineering, Yeungnam College & Technology, Dr. Sheng Yu of Lanzhou Institute of Glaciology & Geocryology, Dr. Takeshi Ishizaki of National Research Institute for Cultural Properties and Dr. Takashi Ono, Professor of the Department of Civil and Environmental Engineering, Hokkai-Gakuen University for their invaluable assistance in various way.

Special thanks are especially extended to Dr. Kazuo Takeda, Professor of Department of Agro-Environmental Science, Obihiro University of Agriculture and Veterinary Medicine, Dr. Satoshi Yamashita, Professor of the Department of Civil and Environmental Engineering, Kitami Institute of Technology, Mr. Dia Nakamura, Research Associate the Department of Civil and Environmental Engineering, Kitami Institute of Technology for their valuable advice and suggestions regarding my dissertation.

Finally, the author is deeply grateful to all the members of my family, including my parents, for their warm encouragement and support during my stay in Japan, and my wife, JaeHee, and daughters, BoHyeon and EunJae for their patience, encouragement and understanding.

Hak Sam Kim

Contents

List of Figures and Photographs

List of Tables

Chapter 1 Introduction

1.1 Background and Purpose of the study

Recently, as waste tire generation has increased dramatically with rapid growth of automobile industry at home and abroad, disposal of waste tire is emerging as a new issue. In case of leaving discarded tire as it is, it causes not only environmental problems such as harming the surrounding scenery, making natural habitat for vermin, danger of fire and human and material damages by fire, but also many other problems regarding its disposal, in our country's small territory, like difficulty in securing open-air storage yard. So from the perspective of resolving such environmental problems and reapplication of scrapped materials with economy, the current domestic situation calls for developing diverse technologies as well as researches for raising discarded tire recycling.

According to the fields of recycling domestic discarded tire published by Korea Tire Manufacturers Association[1)], for 2008, processing use such as powder or recapped tire (24.0%), thermal use such as cement kiln or incineration for cogeneration plant fuel (55%), and original form use such as civil works or export (13%), with nearly 92% of a total recycling ratio, and around 8% of remainder is not for processed. However, more than half of this recycling is focused on the field of thermal use. This means no more than a use as alternative fuel for oil under the effect of a high oil price, so it is urgent to develop a new field of use that can make the most of the characteristics of discarded tire for diverse fields.

In this regard, recently diverse researches are being made. They include mixed lightweight soil using discarded tire powder[2)], strength of concrete with discarded tire scrap[3)], concrete road pavement using discarded tire scrap[4)], stabilization of soft ground by tire mat[5)], soil reinforcement with tire cell[6)], construction of embankment using tire-clay mixed soil[7)], use of discarded tire for vibration decreasing material[8)], and use of discarded tire chip as soil material[9)]. Besides these, experimental studies are being published on carbon extraction from discarded tire or composite material of rubber plastic[10)] with a remaining stage with low economy, while in the above fields, there are a considerable restrictions to using a mass of discarded tire so without practical commercialization so far.

On the other hand, in the severe cold regions like Northern China or Siberia,

simultaneously with on-going maintenance of social infrastructure, technically by complication of the structures, countermeasure for frost heave of the ground is on the rise as an important pending issue.

For instance, most of Liquefied Natural Gas (LNG) receiving the highlight as an alternative for fossil fuel, which was chiefly responsible for global warming, is concentrated on the West Siberia. So far, to deliver the natural gas existing in abundance in the northern cold regions including Alaska and Siberia safely without failing to its needed place, buried-type natural gas pipeline has been partially used in permafrost, but as a result of not cooling the liquid gas, thawing of the surrounding frozen caused a deformation of the pipeline because of lost structural stability, which emits 2% of the entire output or 17% of the consumption in Japan into the atmosphere. This constitutes a double loss for future mankind because of not using the valuable natural resources and raising the greenhouse effect. Under this situation, north regions of Siberia and Alaska are all out for constructing a new pipeline for natural gas in more severe environments, proposing so far a chilled-oil pipeline that can transport it safely without thawing the permafrost. In this case, on the contrary, in non-permafrost, following the formation of a frozen layer called frost bulb, non-uniform frost heave will occur with a resultant large likelihood for causing the destruction of the pipeline, so it is desperately needed to develop a new countermeasure for frost heave to prepare for this.

Countermeasure for frost heave until now includes replacement by material with unlikely frost heave generation, installation of insulator on the ground, using additive, frost susceptibility through obstruction with subsurface flow, etc. However, these methods of construction have difficulty at use under water table as well as high price of material or possible decrease of inhibitive effect on frost heave by freezing and thawing.

Also, replacement method, currently much used, requires good-quality gravel, crushed stone, etc. as a replacement material. However under present domestic circumstances show, difficulty at securing foreshadows exhaust of material and rise in material cost, so developing its substitute material is in a desperate need.

From this viewpoint, if discarded tire powder can be used in a certain proportion as a replacement material for gravel or crushed stone, it will serve a double purpose in reusing wastes and developing a new anti-freezing material.

In this context, Lawrence et al.[11)] reported a possibility of using discarded tire scrap as an anti-freezing material for road based on the low thermal conductivity of rubber through

experimental study. According to their study results, using discarded tire scraps for under water table verified a noticeable decrease in freezing depth by insulating effect, but with a related problem that lowering strength of ground is inescapable by the compressive characteristic of discarded tire larger than soil.

Therefore, this study basically reviewed engineering characteristics of discarded tire powder in order to solve the above problems and further investigate the possibility as a new anti-freezing material instead of the existing granular material or tire scrap available to all civil works structure including chilled-oil pipeline in need countermeasure for frost heave.

1.2 Content of study

Recently big building projects have increased the demand for crushed stone and gravel but they are hard to secure granular material of fine quality because the government's strict policies of environment and natural conservation have made developing stony mountains difficult.

This study, aiming at positive, effective use of discarded tire powder as soil material, instead of granular material of good quality in want, conducted a field experiment on the non-mixed and mixed soil (mixing ratio of tire powder 20%) in a concrete basin in order to investigate the effect of tire powder on inhibiting frost heave as the fist step of the research. At the field experiment, frost heave amount, frozen depth, frost heave force, soil temperature, ground water level, etc. were observed. Also the frost heave suppressing effect of tire powder was evaluated quantitatively based on frost heave ratio and segregation potential.

As the second step of the study, tests of thermal conductivity, unfrozen water, ultrasonic wave and laboratory frost heave, etc. were carried out on the mixed soil of discarded tire to investigate its engineering characteristics.

First, test of thermal conductivity was carried out to analyze the thermal conductivity behavior according to temperature variance and mixing ratio using discarded tire powder of three different kinds in particle diameter. Besides, using pulsed Nuclear Magnetic Resonance (NMR) equipment, unfrozen water content of frozen soil was measured and expressed into the function of temperature. Also, by developing two-phase thermal conductivity model of soil particle and water for unfrozen soil proposed by Woodside, a new three-phase thermal conductivity model was proposed, consisting of soil particle, ice and unfrozen water, that can

be applied even to the area of frozen soil.

For ultrasonic wave test, using pulse method, a kind of nondestructive method that can evaluate dynamic characteristics of frozen soil, behavior of P wave (dilatational wave) and S wave (shear wave) of frozen soil was analyzed according to the change of -10.C to 0.C and mixing ratio of discarded tire powder, and unconfined compressive test was conducted on four kinds of mixed soil from discarded tire powder. Also, change in unfrozen water of frozen soil mixed with discarded tire powder was analyzed, and the relationships between unfrozen water content and elastic wave velocity as well as between elastic wave velocity and unconfined compressive strength were examined. In addition, using the measures of elastic wave velocity, against frozen soil mixed with tire powder, elastic constant, dynamic shear modulus, dynamic elastic modulus and Poisson's ratio were calculated.

In frost-heave experiment, aiming to examine the frost heave characteristics of mixed-soil according to the change of mixing ratio of discarded tire powder and to investigate the related frost heave suppressing mechanism, the author, based on the idea of change in coefficient of permeability by the mixture of discarded tire powder, first calculated unsaturated coefficient of permeability from the relationship between unfrozen water content in the low temperature below 0 degree Celsius and unsaturated water content in the normal temperature above 0 degree Celsius. Then, after considering the ice-impeding factor and ratio between the cross sections of soil and tire powder in the mixed soil, effect of tire powder reducing frost susceptibility was systemically investigated through calculating the permeability coefficient of frozen fringe.

1.3 Organization of this thesis

This thesis includes frost heave test on the non-mixed soil and mixed soil with tire powder at the field, and thermal conductivity test using thermal probe method, unfrozen water content test using NMR, ultrasonic test using sing-around method, and frost heave test using ramped freezing at laboratory.

This thesis consists of eight chapters in all, with each summarized as the following:

Chapter 1 introduces the background and purpose of the study as well as its composition.

Chapter 2 introduces the basic principle of frost heave along with its damage and countermeasure.

Chapter 3 describes the present status of discarded tire generation and its reuse, disposal and fields of reuse in Japan and Korea.

Chapter 4 evaluates a frost heave suppressing effect quantitatively using frost heave ratio and segregation potential from the result of field frost heave experiment for three seasons on the non-mixed section and mixed section with discarded tire powder.

Chapter 5 investigates the characteristics of thermal conductivity according to mixing ratio and temperature variation for three kinds of discarded tire powder and proposed three-phase thermal conductivity model applicable to mixed frozen soil using thermal probe method.

Chapter 6 analyzes the behavior of P wave and S wave of frozen soil according to the mixing ratio of discarded tire powder and temperature variation using ultrasonic, a kind of non-destructive method, and examines the characteristic relationships between unconfined compressive strength and elastic wave, unfrozen water content and elastic wave.

Chapter 7 calculates unsaturated coefficient of permeability and investigates the effect of discarded tire mixture for reducing frost susceptibility through calculating permeability coefficient for frozen fringe after considering ice-impeding factor, the ratio of cross section between soil and discarded tire powder in mixed soil to investigate the characteristics of frost heave in mixed soil according to the change of discarded tire powder mixing ratio and related frost heave suppressing mechanism through frost heave lab test.

Chapter 8 summarizes conclusions from all the tests conducted in this study.

Reference

1) www.kotma.or.kr/tire/tire-2.asp
2) Kim, Y. T. and Kang, H. S.: Mechanical properties of waste tire powder-added lightweight soil, Journal of the Korea Society of Civil Engineering, Geotechnical Engineering C, Vol. 28, No. 4, pp.244-253 (2008)
3) Choi, Y. H.: An experimental study on the changes of strength properties by level of concrete-mixed with wasted tire-chip, Seoul National University of Technology, Graduate School of Industry, Master thesis, pp. 2-35(2005)
4) Kim, N. S.: An experimental study on asphalt concrete utilizing waste tire, Journal of Korean Society of Hazard Mitigation Vol. 3, No. 2, pp. 89-97 (2004)
5) Bang, G. C.: A study on stability against settlement of revetment on soft ground reinforced by tire mat, Joongang University, Graduate School of Construction, Master thesis, p.79 (2006)
6) Gwon, G. S.: Numerical modeling of reinforced soil with tire cell, Inha University, Graduate School of Engineering, Master thesis, pp. 11-32 (2008)
7) Yoon, S. M., Prezzi, M., Siddlci, N. Z. and Kim, B. J.: Construction of a test embankment using a sand-tire shred mixture as fill material, Waste Management 26, pp. 1033-1044 (2006)
8) Kim, J. M., Lee, K. W., Cho, S. D. and Oh, S. Y.: Reduction Effect of Railroad Vibration by Utilizing Waste Tires", Journal of the Korean Society for Environmental Restoration and Revegetation Technology, Vol. 9, No. 1, pp. 31-40 (2006)
9) Yajimura, J., Ogura, K., Karmokar, A. K. and Yasuhara, K.: Mechanical evaluation of used tire rubber chips as geo-material, Journal of the Japanese Geotechnical Society, Vol. 1, No. 1, pp. 1-7 (2006)
10) Kim, J. G.: Development of the thermoplastic elastometer using waste tire, Geongsang National University, Graduate School of Engineering, Master thesis, pp. 5-25 (2006)
11) Lawrence, B., Humphrey, B. and Chen, L. H.: Field trial of tire shred as insulation for paved road, Proceedings of the tenth International Conference on Cold Region Engineering, pp. 428-439 (1999)

Chapter 2 Discarded Tire Generation and State of its Reuse

The aftermath of continued high prices of oil and economic depression since the second oil shock has raised concerns in discarded tire recycling, but it is urgent to develop diverse fields of reuse. Currently, discarded tire recycling is largely divided into three sections: processing use for rubber powder, reclaimed rubber, retread tire, thermal use to get thermal energy on cement kiln, dry incineration, and original form use for civil works and reclamation material.

Regarding the use of discarded tire, this chapter will look at the discarded tire generation, present state of reuse and technology of reusing discarded tire mostly in Japan and Korea.

2.1 Discarded tire generation and present of its reuse in Japan

Japan, the second largest country of automobile making with the same level of numbers of vehicle, 0.59 per head, as Germany or France, has been endeavoring for efficient disposal and reuse of discarded tire. According to the survey of Japan Automobile Tire Manufactures Association (JATMA)[1)], Japan's discarded tire generation for 2008 was around 106 million tires, with a total weight amounting to 1,056 million tons. This is the decrease of a million in amount, or 0.8% in weight compared to 2007, with detailed present condition shown in Table 2.1.

Looking at the present status of reuse against 2008, it comprises retread tire (3.6%), rubber powder (10%), fuel for cement production (13.4%), fuel for biomass generation fuel (45.7%), civil works (0.8%), export (14.9%), etc. All together, recycling rate is 89.3%, a similar level to 90.5% in 2007.

Of late, rise in oil prices has largely expanded demands for alternative fuel such as tree bark, Refuse paper & Plastic Fuel (RPF)[2)], discarded tire, and brought collapsing on a balance of supply-demand for discarded tire with confusion in the market. By its usage, cement kiln is annually on the decrease, while amount of discarded tire for paper making acutely increased 40% compared to 2005, as the planned biomass boiler gradually went into full-fledged operation.

On the other hand, exports of used tire and rubber chip have been slightly decreasing every year since 2005, which is considered due to the expanded use of domestic discarded tire in

the above-mentioned various area.

Table 2.1 Present condition of Japan's discarded tire recycling

(Unit: Weight/ton, Component ratio and Recycling rate/%)

Classification		2005year	2006year	2007year	2008year	
		Weight	Weight	Weight	Weight	Percentage
Processing use	powder	103,000	107,000	111000	106,000	10.0
	Retread tire	35,000	36,000	37,000	38,000	3.6
	Etc.	-	-	-	-	-
	Total	138,000	143,000	148,000	144,000	13.6
Thermal use	Cement kiln	181,000	168,000	148,000	141,000	13.4
	Dry distillation	343,000	407,000	459,000	483,000	45.7
	Total	524,000	575,000	607,000	624,000	59.1
Original form use	Civil eng.	32,000	11,000	11,000	8,000	0.8
	Export	213,000	196,000	180,000	157,000	14.9
	Etc.	22,000	20,000	17,000	10,000	1.0
	Total	267,000	227,000	208,000	175,000	16.6
Amount of total reuse		929,000	945,000	963,000	943,000	
Amount of non-practical use		93,000	111,000	101,000	113,000	
Amount of total discarded tire generation		1,022,000	1,056,000	1,064,000	1,056,000	
Recycling rate		90.9	89.5	90.5	89.3	

2.2 Discarded tire generation and its present state of recycling in Korea

According to the survey of Korea Tire Manufacturer Association (KTMA)[3)], amount of Korea's discarded tire generation for 2008 is around 30million with a total weight of 308,000 tons, which is a decrease of around a million tires in amount and 3.1% in weight, with detailed present condition of recycling shown in Table 2.2 Thermal use such as cement kiln, incineration by dry distillation, etc. was the most 55.7%, processing use into rubber powder, retread tire, rope etc. 24.0%, and use of an original form such as equipment on the used car for export 12.7%, etc. All together, recycling rate is 91.6%, which is a considerably lower than 98.1% in 2007.

Still, though even prior to the exchange rate crisis (1988), discarded tire recycling was very low, remaining at 40 to 50%, it has since risen greatly from the rapidly increasing demand for discarded tire (especially from cement industry) as one alternative fuel material caused by skyrocketing exchange rate, oil prices, etc.

With increased rates of using discarded tire for supplementary fuel of cement since the latter part of 1997 and with stopping of supplying to civil works for military camp since 1999,

disposal structure has changed in its order from using as an original form → processing → thermal use to the current thermal use → processing → using as an original form. That is, until 1998, discarded tire was mostly reused as the method of original form, but since 1999 when use as a heat source in cement factories drastically increased to 61%, it showed almost the same coefficient of utilization until 2008.

Table 2.2 Present state of recycling discarded tire in Korea

(Unit: weight/ton, Component ratio and recycling rate/%)

Classification		2005year	2006year	2007year	2008year	
		Weight	Weight	Weight	Weight	Percentage
Processing use	powder	25,008	33,092	40,126	46,042	15.0
	Retread tire	26,445	23,759	23,693	21,774	7.7
	Etc.	1396	2538	3,377	4,019	1.3
	Total	52,849	59,389	67,196	71,835	24.0
Thermal use	Cement kiln	170,521	173,299	188,083	164,708	53.5
	Dry distillation	5,425	5,922	3,744	6,855	2.2
	Total	175,946	179,221	191,827	171,563	55.7
Original form use	Civil eng.	7,939	7,075	6,564	4,899	1.6
	Export	30,463	26,099	27,276	33,926	11.1
	Etc.	-	-	-	-	-
	Total	38,402	33,174	33,840	38,825	12.7
Amount of total reuse		267,197	271,784	292,863	282,223	
Amount of non-practical use		7,875	11,206	5,636	25,703	
Amount of total discarded tire generation		275,072	282,990	298,994	307,926	
Recycling rate		97.1	96.0	98.1	91.6	

2.2.1 Fields of discarded tire recycling

Generally, disposal of discarded tire is divided into processing use, thermal use and an original form use. Current status of disposing of discarded tire for 2008 shows 24% for processing use, 55.7% for thermal use and 12.7% for original form use. Following is the detailed fields of use according to methods of recycling.

(1) Original form use: uses for reclamation, fishing banks, civil works, etc.

(2) Thermal use: uses for cement kiln, dry incineration, pyrolysis, etc.

(3) Processing use: uses of rubber powder or retread tire, etc.

(1) Original form use

-General landfill

Discarded tire can simply be reclaimed, too, as general wastes. Disposal by landfill not

only has limitations to securing a reclaimed land due to its shortage, environmental pollution, the local residents' avoidance, etc., but also discarded tire in the ground can rise up on the ground to make a habitat for mosquitoes, crack the soil, dry up the ground, and lead the reclaimed land to desolation[4].

-Constructing a military camp

Many portions of discarded tire were used for constructing a military camp. Discarded tire used for this purpose ran up to 12 million pieces, posing a danger to serious environmental pollution. Especially, in case of leaving alone after a camp relocated, it can damage the natural landscape and pollute the environment greatly in outbreak of a forest fire. These camps are mostly built in a green tract in the suburban areas, contributing to environmental destruction with a high risk of catching fire in case of attack by fire. Because of these problems, discarded tire use for constructing a military camp has no demand anymore and this use cannot be a fundamental disposal of discarded tire except for a makeshift simple reuse.

-Earth retaining structure using discarded tire

Though tire retaining wall is not good to look at, but using discarded tire can cut down construction cost, be installed even on a weak foundation, and reduce the term of works greatly because of simple construction. Besides, discarded tire including high-strength steels and diverse industrial fibers has such excellent durability in material that the life of related structures is estimated to be semi-permanent (approximately over 100 years). In a construction of earth retaining structure near Bradford, for example, they reaped a saving effect of 75% compared to ordinary retaining wall[5].

-Using discarded tire as an inside wall for a reclaimed land

When using discarded tire scrap for the foundation and inner wall of a reclaimed land, it has the effect of preventing the ground erosion, removing bad smell of wastes and keeping rivers around from pollution. Actually, the inner wall of a landfill located in city of Iowa, the U.S. was built using a million of discarded tires. Smashing tire scrap up into small pieces forming a drainage barrier to gather the waste water seeping from wastes in a place, they were used in place of sand in the method of sending the waste water back to the waste water

disposal plant by pump for purification.

-Using tire for fill material and improvement of soft ground

Unit weight for discarded tire scraps and powder are in the scope of 0.6~0.8g/cm^3 according to size, and a lightweight aggregate compared to the existing construction material such as cement, gravel, sand. Coefficient of permeability for the scrap of 0.2~0.3cm in particle diameter is between $4.92x10^{-2}$ and $1.13\ x10^{-2}$cm/sec, and it has excellent permeability and insulating effect with thermal conductivity one fourth of gravel or sand.

Besides, as a result of dissolution test, it has extremely less remitted heavy metal or organic matter than the standards for acceptable amounts, which means being environmentally safe. 6.5~15.7% of the thickness of discarded tire revealed the characteristics of immediate settlement and as a result of large scale shear test, internal friction angle was 22~26°, smaller than sandy soil as a weak point in this case. Using discarded tire scrap as fill material for a retaining wall has the effect of reducing earth pressure. With excellent permeability, it is good to use for fill material and especially suitable for use as a waterway filter. Also, with small unit weight, discarded tire scrap can also be used for improvement of soft ground. Actually, in the state of Wisconsin, U.S., they tried building lightweight embankment in the method of mixing discarded tire scraps and sand in a soft ground and surrounding it with geotextile.

(2) Thermal use

Heating value of discarded tire is around 9,000Kcal/kg. This high heating value can be used for pyrolysis in cement kiln, incinerator by distillation, etc.

-Cement incinerator

Using discarded tire for supplementary fuel of cement incinerator is showing a very notable result. Currently, the capacity for domestic cement companies to treat discarded tire using discarded tire input facilities is 133,000 tons, around 19 million pieces in amount based on a small discarded tire. With this facility capacity, cement companies can treat around 53% of domestic discarded tire generation annually (based on weight).

- Carbonization Incineration

Discarded tire has a higher heating value than subbituminous coal (around 6,500kcal/kg). Besides, containing a large amount of volatile substances, discarded tire has a very high availability for energy retrieval in the course of pyrolysis. To incinerate discarded tire, first, put the discarded tire chip in a carbonization incinerator with air controllable and ignite it to generate carbonization gas. This gas, mixed with air in a combustor keeping suitable temperatures, goes on with a rapid response of flame combustion. This process of carbonization gas burning is similar to burning ordinary combustion gas, generating a large amount of heat. Fig. 2.1 shows the flow sheet of carbonization incineration for ordinary discarded tire.

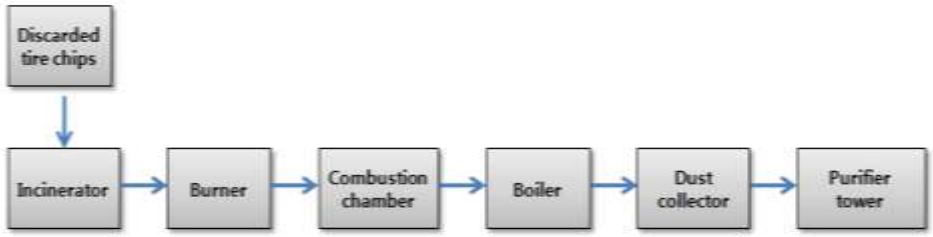

Fig. 2.1 Flow sheet of carbonization incineration for discarded tire

Generally, carbonization incineration is a technology for complementing problems of emitting many pollutants in direct incineration, with chief disposal of waste plastic, waste synthetic resins, waste rubber (discarded tire), etc. This system of carbonization incineration permits imperfect combustion at a low temperature and low oxygen to generate flammable gas, which was re-combusted in a second combustor to collect the generated heat[6].

Though domestic factories of leather, food processing and tire manufacture in installation of a carbonization incinerating facility use discarded tire for fuel in place of bunker C oil, but after the Ministry of Environment reinforced the test items for pollutants, emission criterion, etc. with “Regulations for installation standard of discarded tire carbonization incineration facility”, additional installation for this facility has not been made even with the existing facility idling, so the demand is decreasing every year.

For 2008, domestically 6,885 tons of discarded tire were treated with carbonization incineration, an increase of 83% compared to the previous year. On the other hand, according to the revised wastes management act, a small-size incinerating facility (under 25km per

hour), which causes an air pollution including dioxin, has been banned from installation and operation, so it considered difficult to use and dispose of discarded tire by small-size carbonization incinerator henceforth.

(3) Processing use

-Powder manufacture

Two typical methods of pulverizing discarded tire are those by machines and by cooling. Basic principle of mechanical pulverization is direct pulverization of discarded tire using a grinder, while pulverizing by cooling is cooling off discarded tire under -30 degree Celsius and then pulverizing it by adding mechanical power. At this time, liquid nitrogen is chiefly used for a refrigerant, and Fig. 2.2 shows the process of manufacturing discarded tire powder.

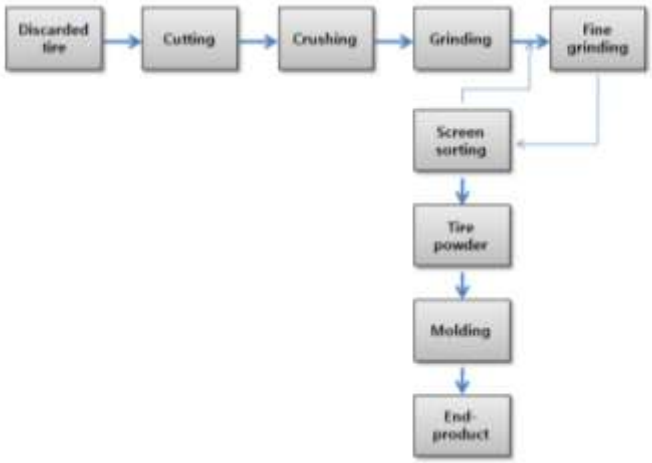

Fig. 2.2 Flow sheet of discarded tire powder

Mechanical pulverizing has a low rate of collection and difficulty of insufficient pulverization. Pulverizing by cooling however, can separate fibers, steels and rubbers effectively with a high degree of purity for pulverized rubber and can obtain fine particles, under 50 mash, which is hard to get under normal temperature. Also, with little transformation by heat or oxidization and satisfactory liquidity and pulverizing efficiency, it can process a large amount of tire. This is why pulverizing by cooling is chiefly used, and Japan or Germany is operating factories that can process 10,000 tons per year. This pulverizing matters because it comes to the significant prior stage to other ways of recycling

discarded tire and because the produced powder can be reused as the material for other products (i.e. retread tire, rope, block, etc.) However, since it uses high-priced liquid nitrogen, matters of profitability remain domestically to be solved and as its substitute, research on using LNG gas is being made.

-Retread tire

Reclaimed rubber means a treatment of processed rubber physically and chemically, and then providing it adhesive property and plasticity to make available for the same purpose as the material or unprocessed rubber. The simplest and clearest method of recycling waste rubber known so far is pulverizing as minute as possible by mechanical grinding, low-temperature cracking, etc. and then using it as rubber filler by chemical treatment, and retread tire uses this reclaimed rubber. This reclaimed rubber is mixed with new rubber and coated with the tread (the contact surface between tire and ground) part of tire (retread) to recycle tire. For manufacturing recycling tire, generally remold system and precure system are used.

Remold system is the method of removing moisture and foreign substances from reusable discarded tire and drying it and then chipping off the tread part and attaching pressed rubber sheet. It has a high speed and good look. Also precure system is the method of applying tread in advance, characterized by small installation investment and long life.

Retread tire, as a new tire is, is experiencing production depression by the economic slump and output for 2008 is presumed to be 2.1 million tires, a decrease of about 8% compared to the previous year. On the other hand, since discarded tire supplied to reclaimed tire manufacturer is processed into reclaimed tire to circulate in the market, it entails the burden of disposal cost for the final collection. But in case a manufacturer produces a reclaimed tire for exports, it can be refunded with the waste deposit according to an established rule of the Ministry of Environment[7)].

-Asphalt of discarded tire (Rubber asphalt)

Pavement of discarded tire asphalt is the concept of adding the component of discarded tire to Ascon and making up for the weakness of low-temperature brittleness and high-temperature viscosity of asphalt as well as using its viscosity and elasticity of rubber. As merits, it provides pavement with long life and excellent durability resisting on cracks, and the surface shows excellent sliding resistance with strength on the pushing and plastic strain.

Also, because paving with reduced thickness is possible, it can save aggregate, reduce noise vibration and harshness, and recycle a large amount of discarded tire.

As demerits, it requires special equipment, has to mix with oil or kerosene to raise the viscosity of asphalt because in case of thin pavement, the pavement is likely to be pushed along, and must scatter limewater to prevent adhesion after compaction[8]. Despite these weaknesses, it has a high value of usage because of excellent driving, low noise realization, and usability as a pavement material for regions of large temperature variance.

-Rubber concrete using discarded tire

Fig. 2.3 shows the flow of manufacturing rubber concrete. First, through process of desulfurization of rubber, elasticity is removed with added adhesive property and plasticity, and in rubber concrete, rubber solution is used as a bonding agent in place of the existing cement paste. Manufactured rubber concrete has excellent property (compressive strength 800kg/cm^2) compared to cement concrete with characteristics of light weight and resistance to noise, vibration and temperature variance[9].

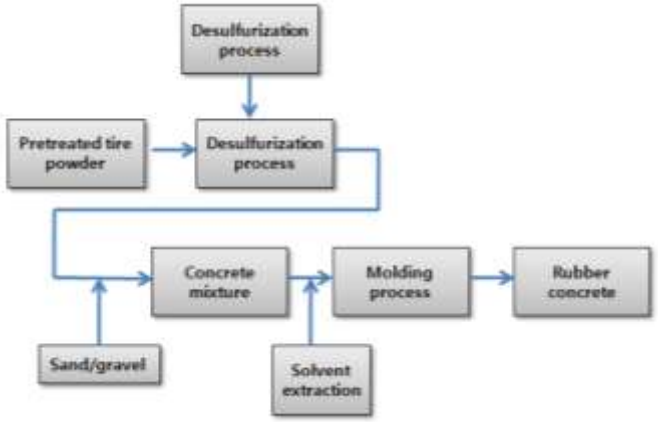

Fig. 2.3 Flow sheet of rubber concrete

Binder so far widely used as a construction material is cement hydrate with weaknesses of slow hardening time, low tensile strength, large drying shrinkage, poor chemical resistance, etc. Recently, a new example of binder supplanting the polymer cement with an aim to improve these drawbacks of cement concrete is appearing, and this is called polymer concrete.

According to an experiment that uses rubber liquid extracted from discarded tire as a new

binder for cement paste, this rubber cement reveals an excellent properties (compressive strength: existing concrete 300~400kg/cm^2, rubber cement 800kg/cm^2) compared to existing cement concrete. Besides, it can have economy and light weight from use of discarded tire together with excellent characteristics in effect of inhibiting noise and vibration and against temperature and moisture vibration.

-Permeability cement concrete using discarded tire powder

Another example of cement using discarded tire besides ordinary rubber concrete is permeability cement concrete. Currently, the material of asphalt pavement road has the drawbacks of frequent car accidents caused by hydroplaning, while the material of concrete pavement has the weakness of lower driving comfort than asphalt, in main property of a road. Besides, since these pavement road materials are almost treated as waterproof, harming the ecology of trees lining a street. Permeability cement concrete has a form of gap structure because of high viscosity of cement paste coated on the aggregate and, in case of adding discarded tire powder, shows improved permeability compared to the existing porosity concrete.

Such permeability pavement materials indicate the eco-friendly probability for plants to grow. Installing porosity cement that allows plants to grow on the soil, causes it to absorb moisture from rain and soil, a seed germinates and grows up. If such tree-planting is done by this growth, it can be used as soundproof facilities as well as handling the road slope stably, so permeability concrete is a very desirable material from an eco-friendly point of view. It can also reduce the hydroplaning of a road and raise the driving comfort with unique elasticity of rubber.

Reference

1) www.jatma.or.jp
2) www.e-rpf.jp
3) www.kotoma.or.kr
4) Hong, Y. K. and Jeong, K. G.: A study on recycling of waste tire, The Journal of Suwon University, Vol. 12, pp. 99-103 (1995)
5) Kim, H. T.: A study on soil-structure behavior using waste tyres, Journal of The Korean Geotechnical Society, Vol. 7, No. 4, pp. 99-103 (1991)
6) www.daehwan.co.kr/gas.htm
7) www.ikhr.or.kr
8) www.heart.civ.ac.kr
9) Jeong, K. H. and Jo, D. H.: Study on rubber-textile adhesion using condensed tannin, The Rubber Society of Korea Quarterly, Vol. 30. No. 1, pp. 32-42 (1995)

Chapter 3 Soil Freezing and Frost Heave Phenomenon

3.1 Freezing process on the ground

Pore water in soil freezes when it is below 0 degree Celsius in the ground. Such process of freezing can be considered a matter of thermal conduction in porous materials which involves phase change. Frozen thickness of the ground is determined by the elements of fall in temperature on the ground surface, thermal properties and permeability of ground, groundwater level while the surface temperature is determined by weather conditions such as temperature, wind speed and solar radiation, vegetation, amount of snowfall, etc. Thermal properties of the ground include thermal conductivity, specific heat and latent heat, which are affected by kinds, density, and water content of soil.

3.1.1 Analysis of the ground's freezing process

The ground's freezing process can be expressed by the analysis known as Neumann's solution, where it is assumed that semi-infinitely broad ground will be frozen. As an initial condition, the entire layer of the ground (frozen soil and unfrozen soil) is T_0 (> 0 degree Celsius) and freezing rapidly lowers surface temperature to T_s (0 <degree Celsius). In case T_s is lower than $T_{f,}$ a freezing temperature of the ground, freezing advances from the surface of the earth downward. This relation is put into Fig. 3.1. Here, freezing point means the boundary between frozen and unfrozen areas. In many cases, freezing front is not exactly the same as 0 degree Celsius face due to the influence of the salt in soil water, but here both are assumed to be in agreement. If under these conditions, equation of thermal conductivity is deducted for frozen and unfrozen soils, considering the latent heat of freezing front, frozen depth X can be expressed as below[1)]:

$$X = 2\gamma\sqrt{k_f t} \tag{3.1}$$

Where, k_f is thermal conductivity of frozen-soil layer, γ is a fixed number according to temperature conditions. Berggren, as a modification of Eq. (3.1), proposed the following[2)]:

$$X = \lambda\sqrt{2(\frac{k_f}{L})(T_f - T_S)t} \tag{3.2}$$

Where L is latent heat, λ is correction factor.

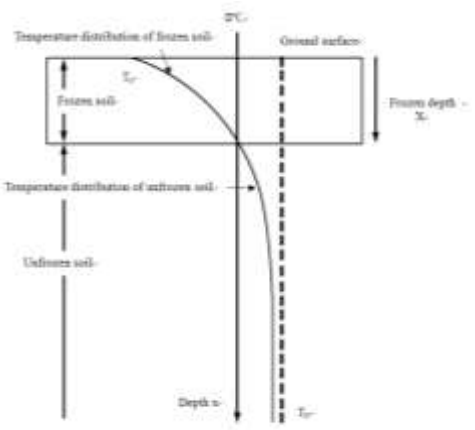

Fig. 3.1 Scheme of ground-temperature profile

3.1.2 Deduction of frozen depth using freezing index

In the previous section, we assumed that temperature on the ground surface lowers rapidly from T_0 to T_s and then remains at T_s. However, in open-air ground freezing, the temperature lowers gradually as winter begins, showing low values in freeze-up with severest cold and then rises toward spring. Here, if $(T_f - T_s)t$ in the right side of the expression is replaced by $T_s(t)$, a surface temperature changing with time, then this can be paraphrased as follows:

$$F = \int_{t_1}^{t_2} (T_f - T_S(t))dt \tag{3.3}$$

Where the predefined F is a freezing index, an important consideration in relation to ground freezing. Using F, Eq. (3.2) can be put into the following:

$$X = \lambda\sqrt{\frac{2k_f F}{L}} \tag{2.4}$$

Fig. 3.2[3)] shows the relationship between freezing index and frozen depth in Hokkaido region. Here, coefficient α is the one in $X = \alpha\sqrt{F}$, which generally has the value between

2.0 and 2.5. Coefficient α differs according to the kinds of soil, with large values for the ground of sand and gravel.

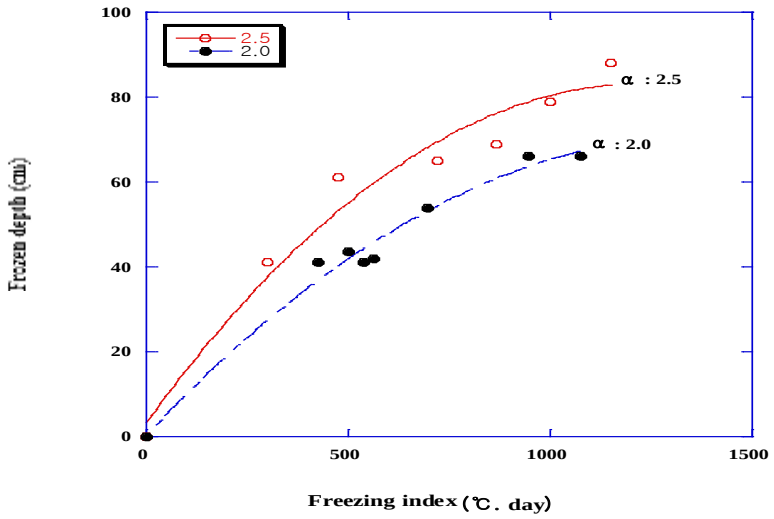

Fig. 3.2 Relationship between freezing index and frozen depth

3.2 Frost heave phenomenon

3.2.1 What is frost heave phenomenon?

If temperature continues below 0 degree Celsius for a long term, the ground expands. This is the result of the moisture moving onto the freezing front with a phase change into ice, which is called frost heave phenomenon. For instance, in so-called permafrost such as Siberia and parts of Canada, we can see small hills composed of ice called Pingo, which has been formed through 100 to 1000 years of time. Photo 3.1 shows the example of Pingo existing in the northwest region of Canada, which has grown up to 70m in height. Since this pingo is the result of forming a large layer of ice by pulling up moisture from unfrozen soil under the freezing front, pingo is another kind of frost heave phenomenon in this respect. Besides, in the morning of early winter, we can easily find needle ice on the ground surface. This needle ice is formed as a result of moisture moving onto the earth surface from underground and changing into ice in phase, with the same mechanism of ice lens growth in the ground.

Photo 3.1 Pingo

Photo 3.2 Needle ice

Photo 3.3 Section of natural frozen soil

Therefore, frost heave phenomenon can be conceived as the one of such needle ice being generated in the ground (Photo 3.2).

In a cold region like Hokkaido, there exists needle ice underground during winter. Photo 3.3 shows the section of frozen soil observed in the field site at Kitami Institute of Technology[4]. This picture, taken after the occurrence of frost heave phenomenon in the winter season, shows the forming of ice lens one upon another, an ice layer with several millimeter thicknesses in underground. This ice layer is called rhythmic ice lens.

Fig. 3.3 shows one of the results of frost heave amount and frozen depth observed from the same place at Kitami Institute of Technology[5]. The soil at field site is silty soil which has high frost susceptibility. Freezing began at the end of November, which has many days below 0℃ in daily mean air temperature, frost heave at the ground surface occurred a little later than ground freezing, and the amount of frost heave increased with the increase of frozen depth to a maximum freezing depth of 68 cm and a frost heave amount of 8 cm toward the middle of March.

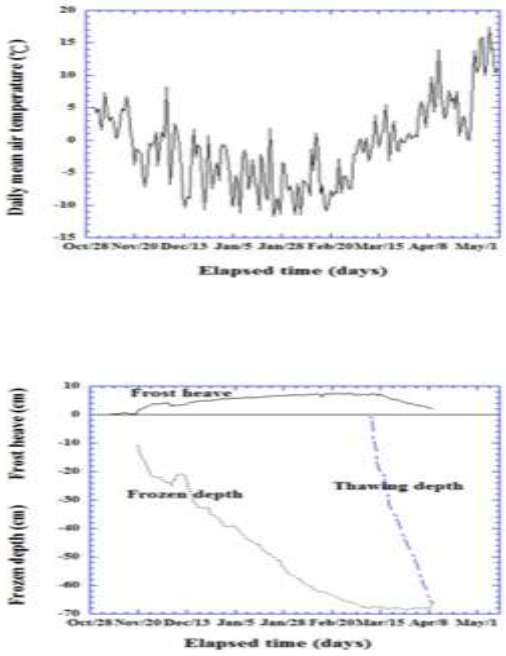

Fig. 3.3 Example of observing frost heave

3.2.2 Frost heave mechanism

Frost heave is the phenomenon of soil's freezing and expanding in volume as the result. Ground freezing responsible for this frost heave can be largely classified as two kinds. One

kind is in-situ freezing, in which pore water in the ground freezes in its own condition. When water changes into ice in phase, it involves around 9% of volume expansion. Thus, as soil freezes, it logically expands 9% in volume. However, supposing water takes up a ratio of 50% within soil, volume expansion doesn't go more than several percents. Also, in case of soil with a large permeability, volume expansion hardly occurs because excessive pore water created by freezing expansion exists on the unfrozen side. Therefore, in-situ freezing doesn't become a serious matter in terms of engineering.

The other kind is segregation freezing. This is the type of freezing in which pore water moves toward the freezing front from the side of unfrozen soil. In this case, as pore water changes into ice in phase, an ice layer in the frozen soil, called ice lens, forms and grows, with expansion of frozen soil as wide as ice lens. If water is supplied continually, it is possible to form a frozen heave of dozens of centimeters.

Since ground freezing goes on from the ground surface downward, moisture is supplied from unfrozen soil below. On the boundary between frozen and unfrozen soil, there concurrently exist heat to be moved to the ground surface, heat to be introduced onto the freezing front from unfrozen soil, and latent heat needed for water to freeze. When these heats are in equilibrium, the boundary stops moving, drawing the moisture in unfrozen soil onto the freezing front to form an ice layer (Fig. 3.4)[6].

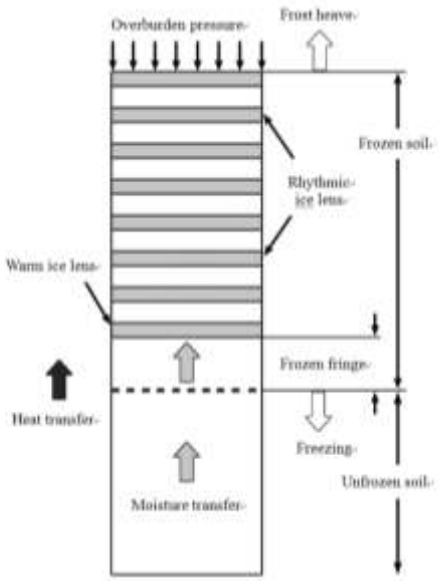

Fig. 3.4 Mechanism of frost heave occurrence for natural ground

Consequently, unfrozen soil under freezing front becomes dry and if moisture is not in a smooth supply, it further moves the boundary downward. Ice lens once again forms where enough water exists, and repetitions of this process heave up the ground. This is the basic mechanism for creating frost heave. It was also experimentally observed that temperature on the side of pore water in unfrozen soil moving in phase change to exist as ice lens is a little lower than 0 degree Celsius, the freezing point of water. In this ice lens, the area between growth face and 0 degree Celsius face is called frozen fringe (Fig. 3.4). This area consists of soil particles, unfrozen water film surrounding soil particles, and pore water. Photo 3.4 shows the ice lens occurred through an experiment with frost heave. In this photo, what is seen in black horizontally one upon another are the ice lenses.

Photo 3.4 Ice lens observed in the Laboratory

From descriptions so far, frost heave is the phenomenon composed of heat and moisture transfer, phase equilibrium, existence of unfrozen water film, supercooling water freezing, etc. Theories of frost heave are frequently introduced in literature, but studies have not yet clearly established its fundamental mechanism. Still, it is a well-known fact that the main cause of frost heave on the ground is the heat transfer following the generation of freezing expansion around freezing front.

3.2.3 Main elements affecting frost heave

Elements affecting frost heave phenomenon include lowered temperature of the ground

caused by its continued exposure to low temperature, temperature gradient in the direction of ground depth, soil easy to generate frozen heave, existence of groundwater that can be supplied to freezing front, load, and many others. However, soil, temperature and soil moisture are the most important elements. Each of these has the following characteristics:

(1) Soil

It is the general way to decide frost susceptibility by the size of soil particles. For instance, in case of sand with a particle size over 0.1mm, frost heave doesn't occur. Frost heave begins to occur with a particle size of 0.1~0.05mm and increases with a smaller size. There is a theory that the smaller particle size has, the more driving force to create frost heave increases, but in practice, frost susceptibility is the strongest in the range of 0.005~0.002mm. However, with a smaller particle size than this, frost susceptibility weakens on the contrary. It is because pore between soil particles narrows and the resultant poorer permeability makes it hard to supply moisture onto the freezing front. In terms of soil's coefficient of permeability, frost heave occurs from soil between 10^{-3} and 10^{-6}cm/sec, while outside of this range, frost susceptibility deceases.

There is the Cassargrand criterion, which has long been used for judging frost susceptibility based on a particle size. This criterion says, in case of sufficient moisture supply, that frost heave occurs for inhomogeneous soil when it contains over 3% of particles under 0.02mm, for homogenous earth, when it contains over 10%, while it is under 1% frost heave doesn't occur even if groundwater level exists around the ground surface. Frost susceptibility of soil is affected not only by a particle size but also by the shape and chemical constitution of the particle.

(2) Temperature

Too low temperature doesn't form an ice layer in the shape of lens, hardly creating frost heave. It is because a fast frost advance rate delays moisture supply onto freezing front. Temperature on the ground is another element to be considered, but what affects frost heave directly is heat balance at the freezing front. Experiment verified that the temperature at the face to exist in the form of ice by water moving from unfrozen soil under freezing front was a little lower than 0 degree Celsius. Frozen fringe is between the faces of existing ice and 0degree Celsius. In order for frost heave to occur, ground surface temperature, underground

temperature, temperature gradient, lowered temperature on the ground, etc. must meet certain conditions.

(3) Moisture

When water has moved from unfrozen soil onto freezing front and changed into water, frost heave occurs. At this time, if only water in unfrozen soil moves, it is called closed-system frost heaving; if underground water continually flows into unfrozen soil, it is called open-system frost heaving. In case of closed-system frost heaving, volume expansion occurs only within several percent, but in open-system frost heaving, even hundreds of percent volume expansion is possible.

Though, in order to move from unfrozen soil to freezing front, water must pass through capillary between soil particles, distance that water can move is almost the same as capillary rise in soil. Therefore, if water level is located deeper than capillary rise of unfrozen soil, this underground water cannot serve as a source of supply. That is why sufficient investigation on soil and underground water level is needed to grasp the characteristics of frost heave in advance. Unfrozen water content attached as moisture in soil to the surface of soil particles acts a large role, and especially behavior of unfrozen water in frozen fringe matters.

3.2.4 Frost heaving force

In order for frost heave to occur, pore between soil particles must be enlarged and water must come into the pore to make freezing. Frost heaving force is defined as the force to enlarge the gap between soil particles when frost heave occurs in the porous materials including water.

Because, in general, frost heaving force is large in clay with small particles but small in sand, Everette et al. [7], inferring from capillary rise, conceived that frost heaving force is generated by the ice-water surface tension within capillary made by soil skeleton. Theoretically, supposing the boundary between ice and water in curvature with the radius of r_{iw}, maximum frost heaving force of soil can be put into the following:

$$P_{\max} = P_i - P_w = \frac{2\sigma_{iw}}{r_{iw}} \tag{3.5}$$

Where, P_i and P_w mean the pressure of ice and water, respectively. When P_i=0, Eq. (3.5)

expresses the maximum absorption. The theory is simple because P_{max} is the own value of the tested soil, not depending on freezing rate or temperature. For Penner[8], there were cases of agreement in the comparison between experimental and theoretical values, but after the 1970's when high precise experiment became possible, he verified that test value tends to be somewhat larger than theory value.

Tkahasi et al.[9] fixed the sample completely and then froze it partially to find the maximum frost heaving force that occurs. The schematic diagram of experiment is shown in Fig. 3.5. Tkahasi et al. used clay to carry out experiment in the open-system condition where moisture was in supply. As the sample was frozen, frost heaving force gradually increased to converge to a certain value after a long time elapsed. On the long-term test of frost heaving force, in many cases, growth of ice lens was seen on the cooling plate. Fig. 3.6[9] shows the relations between temperature of ice lens found through experiment and frost heave force generated. From Fig. 3.6, it was verified that the following relationship exists between P_{max} (MPa), the maximum frost heave force, and T_c (degree Celsius), cooling plate temperature in the range of temperature 0 ~ -18 degree Celsius:

$$P_{\max} = -1.09T_c\,(MPa) \tag{3.6}$$

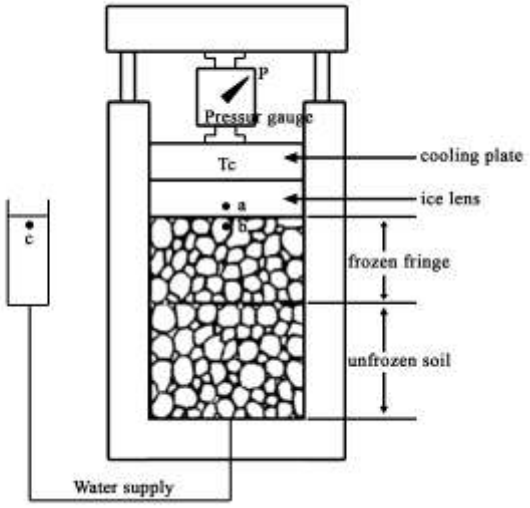

Fig. 3.5 Schematic diagram for experiment of frost heaving force

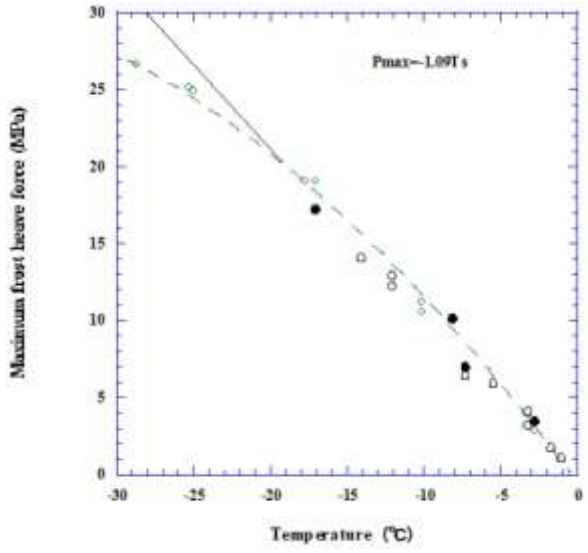

Fig. 3.6 Relations between maximum frost heaving force and cooling plate temperature

Now, let's consider the relations between maximum frost heaving force and temperature of ice lens growth side using the related equation for thermodynamics. In case the growth of ice lens has stopped, in a sufficient time elapse after the start of experiment, it is conceivable in Fig. 3.5 that chemical potentials between point a (ice), and point b (unfrozen water) are the same. That is:

$$\mu_i(P_i, T_i) = \mu_w(P_w, T_w) \tag{3.7}$$

From this condition the following expression can be obtained:

$$V_i P_i - V_w P_w = -L\frac{T_i}{T_m} \tag{3.8}$$

Where, V_i and V_w are the specific volume for ice and water, L is latent heat.

In Fig. 3.5, because soil particles partially receive the pressure ice receives, there is difference in pressure between Pi (point a) and Pw (point b). Eq. (3.8) is called the generalized Clausis-Clapeyron equation. However since point b is linked to water, pressure of water in the soil is defined by Pw, pressure of water at C, which exists in equilibrium. In Fig. 3.5, as pressure at C is equal to air pressure, it gives Pw=0. In this case, Eq. (3.8) can be put into follows:

$$P = -L\frac{T_i}{V_i T_m} = -1{,}12T_i(MPa) \tag{3.9}$$

Empirical Eq. (3.6) well agrees with Eq. (3.9). Tkahashi et al. attributed a smaller value from experiment in low temperature than Eq. (3.9) to the continuity of unfrozen water being lost in the low temperature[9]. From the results above, it is found that the maximum frost heaving force depends largely on temperature condition rather than on the soil property.

3.2.5 Unfrozen water

There is water that is not frozen in the temperature below 0 degree Celsius which is called unfrozen water around soil particles. Unfrozen water is linked to the pore water of unfrozen soil, and the thickness of this unfrozen water is known to be reduced as the temperature lowers. Fig. 3.7[10] is the schematic representation illustrating that the thickness of unfrozen water around soil particles depends on temperature. It shows that as temperature lowers, unfrozen water with a far-off distance from soil particles freezes first, which results in gradual decrease in the thickness of unfrozen water. Such existence of unfrozen water has a great effect on frost heave phenomenon.

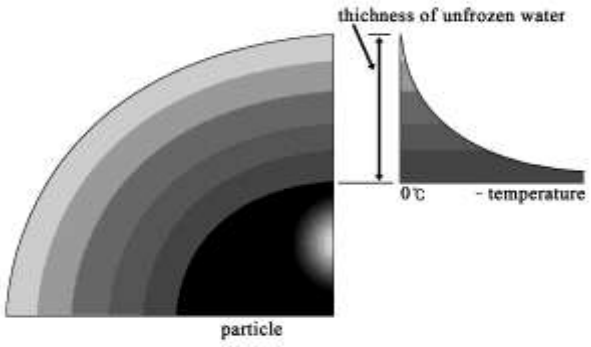

Fig. 3.7 Thickness of unfrozen water film around soil particles

Reason for existence of unfrozen water is still unclear and it is one of the big research tasks for the field of low-temperature science. However, it is a confirmed fact that unfrozen water has a lower chemical potential than bulk water. For unfrozen water, as the result of receiving the function of physical chemistry such as adsorption from the surface of soil particles, their

capillary pressure, pore water solute, etc. chemical potential can be expressed as the function of a distance from soil particles. Since unfrozen water with far-off distance from the soil particles has a larger chemical potential, it makes an early phase change into ice as temperature lowers.

Soil moisture turns into ice below 0 degree Celsius for sandy soil, but for fine-grained soil, some of it remains without freezing (i.e. unfrozen water). Profile of moisture left in soil was shown in Fig. 3.8[11].

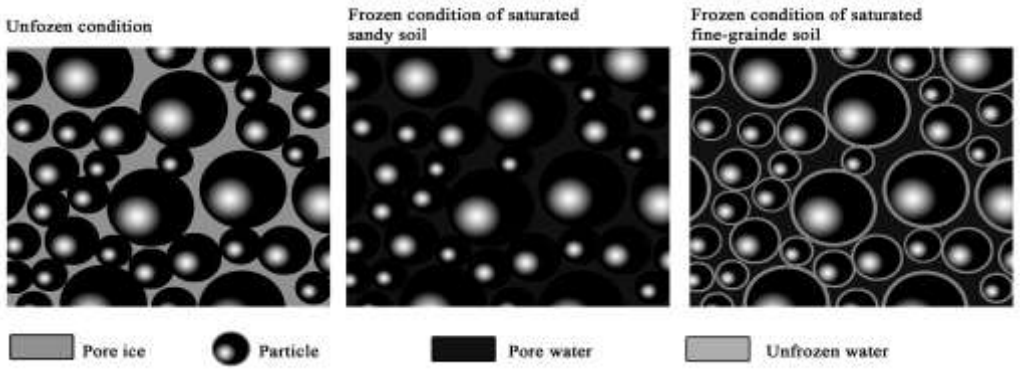

Fig. 3.8 Moisture distribution in unfrozen and frozen soil (difference between sandy and fine-grained soils)

In temperature above 0 degree Celsius, pore water exists around particles marked in a ball shape in Fig. 3.8, and as a result of almost all the pore water going through a phase change into ice at 0 degree Celsius, frozen sandy soil becomes a state of freezing characterized by high solidity like mortar. However, in the case of fine-grained soil below 0 degree Celsius, unfrozen water surrounds particles and frozen moisture outside unfrozen water, that is, pore ice is distributed as shown in Fig. 3.8. At this time, pore ice increases with lowered temperature, and together with it, unfrozen water goes into freezing with its part farther from soil particle first. Generally, fine-grained soil is dozens of millimeters at 0.01 degree Celsius, 10mm at -0.1 degree Celsius and several millimeters at -1 degree Celsius in thickness, where thickness of unfrozen water thins with lowering of temperature. To measure the amount of this unfrozen water, there are calorimeter method using the thawing heat of ice, NMR method using the difference of water and ice in motion within the magnetic field of atomic value for hydrogen, TDR using the difference of ice and water in permittivity, etc. For example, NMR method can find the amount of unfrozen water from the intensity of NMR signals, using the fact that intensity of signals are proportionate to the number of atoms for hydrogen in

unfrozen water.

3.3 Theory and model for ice lens growth mechanism[12)]

Soil consists of soil particles, air and water, and to investigate the growth mechanism of ice lens when soil freezes, it is most important to grasp characteristics in relation to the heat and moisture transfer in frozen soil according to the formation of ice lens, phase change into ice, etc. From this point of view, the author is going to introduce the current representative theories and models for frost heave.

3.3.1 The capillary theory

The capillary theory, which dominated both experimental and theoretical research in the 1960's, 1970's and part of the 1980's, and was also termed primary frost heaving by Miller, was used to describe heaving pressure and ice lens formation in granular materials. Theoretical data for developing the theory are provided by Gold, Everett, and Everett & Haynes, the last-mentioned of which have created theory-based models and modifications of the equation. Experimental research has been conducted by Penner, Sutherland and Gaskin, Holden et al. and Williams.

According to the capillary, the flow of water to the freezing front is caused by the pressure difference at the curved interface between the solid and liquid phases. The magnitude of this pressure difference varies for each side of the interface in the balanced state, due to surface tension, the difference being derived from the Young-Laplace equation as follow:

$$\Delta p = \mu c = \pm(1/r_1 + 1/r_2) \tag{3.10}$$

Where μ is surface tension, r_1 and r_2 are the main surface curve radiuses. The plus sign is used in the equation when phase 1 is on the concave side and the minus sign when it is on the convex side. When the ice-water interface is presumed to spherical, the pressure difference is:

$$\Delta p = p_i - p_w = 2\mu_{iw}/r_p \tag{3.11}$$

Where r_p is pore radius. This equation can be used to describe the pressure conditions

under which ice can penetrate into the pore system. According to the capillary theory, an ice lens will only grow at the freezing front, i.e. the equation may be used to determine when segregated ice (ice lens) or pore ice occurs at a given temperature.

The freezing point depression, i.e. the temperature at which ice crystals begin to enlarge and the ice lens begins to form, can be calculated by inserting the basic capillary model Eq. (3.11) into the Clausius-Clapeyron equation. Thus the freezing point depression is obtained by the equation:

$$\Delta T = (2\mu_{iw} \cdot T_0 \cdot V_w) / r_p \cdot L \tag{3.12}$$

If the pressure difference between ice and water conforms to Eq. (3.13), the ice lens may penetrate through the pore system and create pore ice without displacing soil particles:

$$P_i - P_w \geq 2\mu_{iw} / r_p \tag{3.13}$$

If the pressure difference confirms to Eq. (3.14), the ice lens will not be able to penetrate into the adjacent pore, in which case ice will displace the soil particles, forming segregated ice:

$$P_i - P_w < 2\mu_{iw} / r_p \tag{3.14}$$

According to the capillary theory, pore-size is of major importance in the freezing process and freezing occurs only if the ice forms outside the pores. It is also suggested in the model that an ice lens will only grow at the freezing front when its development is contingent on the inability of the ice-water meniscus to penetrate a pore with a radius smaller than r_p at a given temperature.

The basic capillary Eq. (3.10) can also be derived from theoretical considerations of the chemical potential of ice and water phases by means of thermodynamic equations.

The heaving pressure is obtained in the capillary in terms of the pressure caused by the ice lens, employing equation (3.15)

$$P_i = P_w + 2\mu_{iw} / r_p \tag{3.15}$$

The maximum pressure difference is dependent only on soil characteristics and not on temperature, temperature gradient or frost penetration rate.

It was apparent by the early 1070's that the capillary model of ice lens growth severely underestimates the maximum heaving pressure attainable in non-colloidal soils. Miller claimed that the ice lens grows on the colder side, somewhat beyond the zero isotherm and arrived later at the conclusion that the only kind of ice segregation that could occur according to the sample capillary model, which he termed the primary heaving model, was the formation of needle ice at the soil surface.

3.3.2 The secondary frost heave theory

The secondary frost heaving theory, which was introduced by Miller in 1972, involves the growth of an ice lens at that point in the frozen zone where the effective stress on the soil particle is zero. Miller refers to the zone between the freezing front and the growing ice lens as the frozen fringe. In his earlier experiments, Hoekstra observed the ice lens as the frozen fringe to grow behind the freezing front in saturated clay and granular soils. The frozen fringe is the zone between the warmest ice lens and the unfrozen soil. Experiments have yielded a frozen fringe thickness of 2-4 mm in a silt soil.

The principal idea behind the secondary frost heave model is that ice is a rigid body moving in the direction of heat flow, i.e. ice flow, water flow and heat flow all occur in a freezing soil. The principle of continuity yields the conclusion that ice flow in ice lens is equal to the ice flow and water flow in frozen fringe, and that these together equal the frost heave. As claimed by Miller, the frost heave rate and ice flux are one and the same thing, i.e. the ice phase moves as a continuous rigid body with a uniform linear velocity equal to the observed heave rate. Pore ice movement, which may be accompanied by a simultaneous net flux of liquid water through films and ice-free pores, is viewed as a regelation process involving the continuous liquid phase that lies between the pore ice and the mineral particles which bind the pores. Regelation involves continuous phase changes, a locally circulating liquid flow and an associated circulation of latent heat being released and reabsorbed by these changes. A significant factor in the physical examination of the freezing process is the stress between phases. Miller divides neutral stress, which constitutes the second factor in Terzaghi's total stress as used in the geotechnical description of unfrozen soils, between the

pore ice and pore water, using a suitable stress partition factor:

$$P = \sigma_c + \sigma_n = \sigma_c + \chi \cdot p_w + (1-\chi) \cdot p_i \qquad (3.16)$$

Where P is the overburden pressure, σ_c effective stress, σn neutral stress and χ the stress partition factor. According to the segregation freezing theory, heave occurs when the neutral stress exceeds the overburden.

The secondary frost heave theory describes the formation of a new ice lens as a physical process (Fig. 3.9). There must be a temperature drop in order for the heaving process to begin. As the temperature falls, p_i and σ_n rise. When the maximum σ_n value reaches σ, the minimum σ_c value reaches zero, fulfilling the condition for initiating a new lens, which will form at the level at which the ice pressure p_i exceeds the load pressure σ.

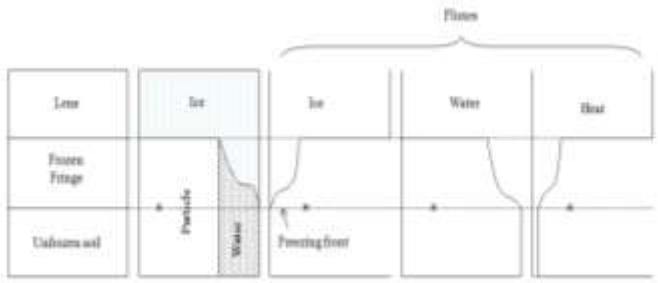

(a) Schematic representation of condition near the freezing

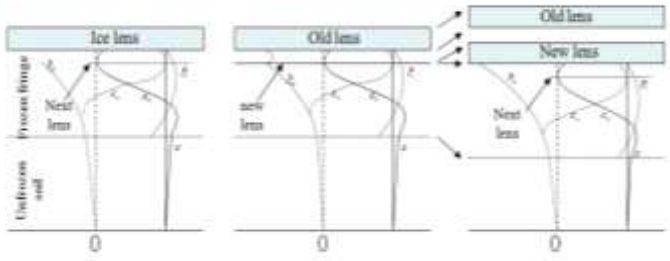

(b) Stress profiles in a freezing soil

Fig. 3.9 Principles of the secondary frost heave theory. a) Schematic representation of condition near the freezing front when secondary heaving is in progress. b) Stress profiles in a freezing soil. Left, situation before the initiation of a new lens; middle, situation just after a new lens has been established; and right, situation before initiation of another new lens

As soon as the new lens is established, however, its pressure cannot exceed σ, as that is the load imposed on the ice of the new lens. Thus p_i drops as the new lens is established, while σ_n drops and σ_c rises above zero, inhibiting the loss of any more particles into the moving ice. Pi remains constant and equal to σ at the base of the new lens, but as the temperature continues to fall, p_i rises below the new lens, and the lens initiation cycle is eventually repeated at a lower level.

Heaving pressure can also be calculated from the theory of secondary frost heave. The pressure prevailing on the freezing front is that caused by the ice alone, its maximum value indicating the heaving pressure. The maximum heaving pressure during secondary frost heave is dependent only on the lowest temperature at the lower surface of the ice lens and the pore water pressure, as indicated by Eq. (3.17):

$$P_{\max} = \gamma_i (p_w / \rho_w + L\Delta T / T) \tag{3.17}$$

Where γ is density.

The theory of secondary frost heave is used in the case of fine-grained soils dominated by secondary frost heave, as in a number of mathematical frost heave models e.g. Miller, Gilpin, Black & Miller.

3.3.3 The adsorption force theory

Freezing has also been described in terms of the adsorption force theory. Physically, the role of the adsorption water layer as a driving force for frost heave was also emphasized by Taber and Beskow. The theory originates from the idea that the film water adsorbed on soil particles on soil particles can build up an internal solid-like stress and freezing draws pore water to the freezing front to maintain the thickness of the adsorbed water film, generating a suction force that draws water to the freezing front where the heaving pressure pushes up the overburden. This suction is attributed to the molecular forces created in adsorbed film, the equilibrium thickness of which is determined by the adsorption forces exerted by the particles and the ice as water molecules become attached to the base of the ice lens.

The freezing of water, which generates suction, will be termed segregation freezing, which means that the heterogeneous film of water adsorbed between the particle surface and the ice surface freezes. In contrast, the freezing of homogeneous free pore water will be termed in

situ freezing, since this mechanism does not create suction, i.e. the in situ freezing front advances as in situ freezing progresses.

According to Takagi, there is also another freezing area which he calls the zone of diffused freezing, the lower boundary of which is the site of in situ freezing. This boundary does not contribute to frost heave, but governs the availability of water to the freezing zone. The upper boundary of this region is located in the place where the ice grows, causing frost heave. The model is incomplete, however, and has not yet been tested for its practicability.

3.3.4 The osmotic theory

Horiguchi presented an osmotic model for frost heaving in a normally consolidated, saturated soil which has no solute in its pore water. The theory sets out from the pressure difference caused by the concentration between the diffusion layer surrounding the soil particles and the pore water. The flux of water depends on the temperature gradient and pressure gradient of the liquid phase in the transitional zone. (cf. frozen fringe). The model takes account of the effect of overburden pressure, mass and heat flux on the rate of frost heaving due to ice segregation.

3.3.5 The segregation potential concept

Konrad and Morgenstern introduced the concept of segregation potential SP, defined as the ratio of the water migration rate to the overall gradient in frozen fringe, to characterize a freezing soil. The mechanics of frost heave can be regarded as a problem of impeded drainage to an ice-water interface at segregation freezing front. The driving potential arises from the substantial suction generated at the ice lens according to the thermodynamics of phase equilibrium and from the impediment to water flow caused by the low permeability frozen fringe. Permeability is a function of the unfrozen water content of the fringe. According to the segregation potential theory, the flow of water v(t) to the growing ice lens at the time of formation of the final ice lens in a freezing soil is proportional to the overall thermal gradient, grad $T_f(t)$, in the frozen soil. The constant of proportionality is termed the segregation potential SP(t) in the equation

$$v(t) = SP(t) grad T_f(t) \tag{3.18}$$

Where grad $T_t(t)$ is the overall temperature gradient in the frozen fringe.

Segregation potential can be defined from both frost heave laboratory tests and in situ measurement, provided that the temperature gradient of the partially frozen soil and the flow of water to the freezing front are known. The water intake rate can be calculated from the frost heave rate by observing the expansion of water, the porosity of the unfrozen soil and the amount of unfrozen water at the segregation temperature. Segregation potential is also used as a criterion in the frost susceptibility classification of soils, its magnitude being dependent on the load imposed on the specimen. According to Konrad and Morgenstern, segregation potential decreases exponentially with increased load.

One considerable advantage offered by segregation potential is that it can be used to calculate the magnitude of frost heave. It has been used to calculate both seasonal frost and frost heave in an artificially frozen soil. The method only allows calculation of frost heave occurring in a non-stationary state.

3.3.6 The hydrodynamic theory

Hydrodynamic models involve an approach to freezing using combined models of mass and heat transfer. The basic equation is that of Clausius-Clspeyron, which is used to calculate the pressure of the moving unfrozen water in a partially frozen soil, the ice lens being assumed to form behind the freezing front. The model is based on adaptations of equations developed to describe heat and water flow in unfrozen soil. Water flow is normally assumed to occur only in the liquid phase, and the liquid pressure is defined by the Clausius-Clspeyron equation and the transport coefficients related to the unfrozen water content. Water moves in accordance with the law of Darcy, which is modified to take account of the ice component when calculating the hydraulic gradient. Frost heave takes place when the ice content exceeds a given percentage of the pore content. The location of ice lens or ice enrichment zone is then simply the depth at which the divergence of the water flux is greatest.

3.4 Examples of damage from frost heave

Frost heave by soil or a base rock has a great effect on the road, tunnel, retaining wall, slope, etc. in winter season. This phenomenon can cause damages of a crack in surface, bumpy road, overturning of retaining wall, collapse of slope, destruction of structure, etc.

Examples of damage to the road from frost heave include ones caused by frost heave itself from the expansion of subgrade soil in winter and decrease in bearing capacity or shear strength in the spring caused by the thawing of an ice layer existing beneath the road.

3.4.1 Damages to the road from frost heaving

It is, as the damage to the road from frost heave itself, the uneven upheaval of the pavement side in a cross direction of a road (Photo 3.5), caused by ice lens occurring on the subgrade. This generally occurs at maximum in the middle of a road, causing a great crack around the center line of the road as shown in Photo 3.5. During the cold winter months, hard shoulder of a road can be insulated to some degree by snowfall, but for the center part of the road, on which snow won't pile up on the surface due to continued traffic, it is out of the question to expect the effect of insulation from snowfall. Consequently, frozen depth and frost heave amount are larger on the central part of a road than on hard shoulder, and tensile stress occurs on the road surface, which can end up with destruction of the road. For asphalt pavement, this destruction agrees to the construction joint around the central part of a road,

Photo 3.5 Destruction of pavement by freezing

and is notably characterized by the generation lengthwise on the road.

During the thawing period of spring, the frozen ground begins to thaw from the surface, and as a result, the road is the condition of saturation. Especially, because a frozen layer still exists beneath the surface, the thawed water is hard to seep underground, which remarkably

reduces the strength of the road ground. In case the vehicle runs on such a road, it increases the tensile stress and normal strain to asphalt or concrete pavement, destroying the pavement and resulting in a crack in the road face (Photo 3.6) and settlement of the road.

Photo 3.6 Road destruction following the lowered bearing capacity in thawing period

3.4.2 Damage to retaining wall from frost heave

Photo 3.7 shows the L-type experimental retaining wall against frost heave installed on the embankment slope within Kitami Institute of Technology. In this photo, for retaining wall A, a heat insulator was installed behind it, while for retaining wall B, only used soil with frost susceptibility for backfill material

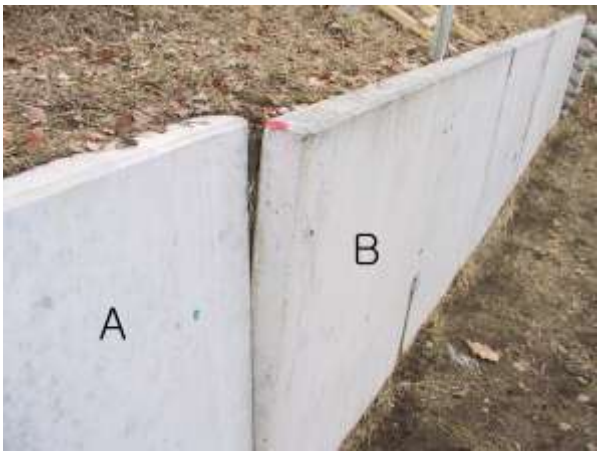

Photo 3.7 Damage to embankment slope from frost heave

After 11 years, it is seen that retaining wall B has been considerably protruded forward. This result is considered because freezing penetrated deeply into the backfill material composed of frost susceptible soil and formed ice lens, which led to volume expansion (frost heaving force) toward the retaining wall and its protrusion. If repeated freezing and thawing continues each year, then it is estimated that the effect of frost heaving force working horizontally will gradually increase the distortion of the wall leading it to destruction after all.

Photo 3.8 shows the damage from frost heave to the retaining wall of a park cemetery located in Ashibetu city of Hokkaido. This place consists of terrace using a slope, and L-type concrete retaining wall was used to make the site in a terrace form. As shown in this photo, as the result of repeated freezing and thawing for several years of winter after using it, the retaining wall has leaned greatly. Moreover, asphalt pavement behind the wall is serious in surface destruction, with gravels and soil disengaged from the pavement scattered around on the ground.

Photo 3.8 Damage to a park cemetery from frost heave

3.5 Countermeasure against frost heave

Frost heave phenomenon occurs when factors such as soil, temperature, underground water, have met at the same time. Therefore, frost heave can be prevented or inhibited by removing or improving at least one of these factors. General countermeasure includes replacing frost susceptible soil with soil hard to generate frost heave (replacement method), installing a insulating layer under the roadbed to minimize the temperature fall of subgrade soil and frozen depth as a means to reducing frost heave (insulation method), applying additives such

as cement, lime, etc. in mixture to soil in frost susceptibility to improve the nature of soil or lower its freezing point (stabilization method), installing an obstruction layer such as vinyl sheet, asphalt, etc. on subgrade to obstruct the water in ground rising up toward frozen front as a means to inhibiting frost heave (cutoff method), etc. Of these, the most popularly used one today on the site is replacement method.

3.5.1 Replacement method

In replacement method, replacement depth is generally decided to prevent destruction both by road surface and frost heave and by lowered bearing capacity for road and roadbed in thawing spring season. To prevent frost heave, this method opts to substitute quality material that keeps off frost heave up to the maximum frozen depth (frozen depth in the year coldest of this past 10 years). This can also prevent the pavement destruction by lowered bearing capacity for subgrade in the spring season of thawing. However, due to economic reasons and construction experience, replacing it up to 70% of the maximum frozen depth is usually used. The replacement depth found this way is compared with the entire depth with the sum of surface, base and subbase courses and pavement of subgrade together found without considering frozen depth. If replacement depth is larger, materials like sand, volcanic ash, gravel, etc. unlikely to cause frost heave are added for the difference. This section is called anti-frost layer and considered part of the subgrade.

Replacement material must meet the quality and standard suitable for the purpose of usage, comprising quality materials that keep off frost heave. Following is the standard for granular material that frost heave does not occur:

(1) Sand: under 6% passage through a sieve of 0.075mm
(2) Gravel: Under 9% passage of 0.075mm sieve of 4.75mm sieve for all samples
(3) Rubble: Under 15% passage of 0.075mm sieve of 4.75mm sieve for all samples
(4) Mixed gravel and rubble: Under 12% passage of 0.0075mm sieve of 4.75mm sieve for all samples
(5) Volcanic ash: Under 20% passage of 0.075mm sieve without weathering and with good drainage and under 4% ignition loss. Also defined as materials that have proved difficulty with frost heave occurrence through a frost heaving test.

3.5.2 Insulation method

Insulation method is the method of minimizing the temperature fall of subgrade by installing a insulating layer beneath roadbed to prevent the damage to a road from frost heave. It is recently much used as a method to counter frost heave from the road and airport pavement.

Insulating material has many kinds according to use. But for preventing frost heave, it must have low thermal conductivity with continued insulation effect. In addition, quality of insulator, its strength, durability, adsorption, change in quality according to a long-term traffic load, etc. must be reviewed sufficiently. Especially, because insulating material in subgrade is likely to lower in its insulating effect and strength with progress of dampness according to time elapse, care should be taken in opting for a insulating material. Currently, compressed Styrofoam (thermal conductivity of 0.034W/m.K) is the only material that meets these conditions. As conventional compressed Styrofoam is made of impervious material, water always exists over an insulating layer, but a new insulating material in pervious material has now developed to make up for the existing drawbacks to a degree. This method can relieve frozen depth when installing insulation layer in a shallow position, but also causes a problem of reduced bearing capacity. So it is necessary to review the proper position, depth, etc. of an insulating layer.

3.5.3 Cutoff method

Frost heave phenomenon occurs when moisture moves from lower to upper part on the contrary direction to gravity to form ice lens on the frozen front. Frost heave is inhibited by obstructing the soil moisture moving to freezing front. Cutoff method includes ways of obstructing moisture to move to freezing front by making a cutoff layer with assembled material (coarse-grained soil), metal, vinyl, asphalt, etc. that keep off capillary rise. Though these methods can obstruct the moisture moving to freezing front from lower section but it also result facilitating frost heave because it makes moisture moving downward from the surface by rainfall remain in the upper section of the cutoff layer. So to solve this problem, geotextile (non-woven) is much used.

3.5.4 Stabilization method

It is considered that mixing cement, lime, etc. with frost susceptible soil in proper amount is effective in inhibiting frost heave to a degree by the effect of mutual cohesion of soil

particles, freezing point fall of pore water, adsorption increment of soil particle, permeability decrease, etc.

Generally cement is used mainly for a sandy soil and lime is much used for cohesive soil, while on the ground with high moisture content quick lime is effective. This method has the biggest drawback in a high likelihood for occurring problems in long-term effect continuity according to the function of freezing and thawing, high water content in subgrade soil, and difficulty in mixing admixture uniformly in frost susceptible fine-grained soil, which necessitates the choice of proper additive according to a soil.

Reference

1) Jumikis, A. R.: Thermal soil mechanics, Rutgers University Press, pp. 236-246 (1966)
2) Berggren, W.P.: Prediction of temperature distribution in frozen soil, Transaction, American Union, pp.71-77 (1943)
3) Ishizaki, T. and Akagawa, S.: Soil freezing and geotechnical engineering- 2. Soil freezing and frost heave phenomenon, Journal of Soil and Foundation, Vol. 534, pp. 59-62 (2003)
4) Sato, A.: A study on effective use of unsuitable soil in cold region, Kitami Institute of Technology, Doctoral thesis, pp.98-110 (2009)
5) Murata, E.: Characteristics of slope behavior on freezing-thaw process, Kitami Kitami Institute of Technology, Doctoral thesis, pp.98-110 (2009)
6) Miyata, Y. : A macroscopic frost heave theory, Graduate School of Engineering, Hokkaido University, Doctoral thesis, pp.9-16 (2000)
7) Everett, D.H.: The thermodynamics of frost damage to porous solids, Trans, Faraday soc. 57, pp.1541-1551 (1961)
8) Penner, E.: Heaving pressure in soil during unidirectional freezing, Canadian Geotec hnical Journal, Vol. 4, No. 4, pp. 398-408 (1967)
9) Takashi, T., Ohrai, T., Yamamoto, H. and Okamoto, J. : An experimental study on maximum heaving pressure of soil, Snow and Ice, 43, pp. 207-215 (1981)
10) Akagawa, S.： Frost heave process of porous materials and its macroscopic ice lens initiation mechanism, Snow and Ice, Vol. 66, No. 2 (2004)
11) Akagawa, S.： Cold region railway engineering course finial report, Graduate School of Engineering, Hokkaido University, pp. 6-9 (2003)
12) Kujala, K.: Factors affecting frost susceptibility and heaving pressure in soil, University of Oulu, Doctoral thesis, pp.22-28 (1991)

Chapter 4 Field Experiments for Reducing Frost Susceptibility Using Discarded Tire Powder

4.1 Introduction

In cold regions, the ground is subjected to severe winter temperatures and freezes from the soil surface to a certain depth. During soil freezing, frost heave tends to occur in specific soil types under particular ground conditions. More specifically, frost heave results from the formation of successive ice lenses in subgrade soils. Roads, buildings, railways, pipelines, and other infrastructures are designed to prevent damage from frost heave; however, due to frost action, roads are often damaged by upheaval of the surface. The most common method of protecting roads from frost heave is to replace frost susceptible materials with non-susceptible soils.

In some areas it is rather difficult to obtain an adequate supply of sandy materials from local resources which, in turn, makes road construction in areas with cold winters expensive. In attempts to find alternatives, several different materials have been added to on-site frost-susceptible soil to make the road frost tolerant. Fukuda et al.[1)] added ordinary cement to silty soil. Thompson[2)] and Ono et al.[3)] also reported similar applications. Other methods include installing geotextiles[4,5)] or embedding thermal insulating material into the subgrade[6)].

There are some common disadvantages among these applications that make their practical use difficult. First, the cost of the materials employed is higher than that of non-frost-susceptible soil. Second, new machinery and techniques for installation or mixing on site remain undeveloped. Third, the duration of these methods' effectiveness has not been determined. Even considering these disadvantages, there is still a demand for new applications from industry and society to improve the performance of roads during winter conditions.

Huge numbers of tires are being discarded every year due to rapid modernization throughout the world. The recycling rate for discarded tires is low, and a great many used tires are being discarded into landfills or open stockpiles. Therefore, a variety of handling methods for these tires are urgently needed. One popular use of discarded tires is to embed them as insulation layers in road subgrades as mentioned above to limit the depth of frost penetration[7)]. However, embedded tire layers cannot support the stress surcharge derived

from heavy vehicles, giving rise to large settlement. The authors propose a novel method to overcome these disadvantages. A frost-susceptible soil is mixed with granulated rubber powder at a fixed soil-to-powder ratio. The authors firmly believe that using a soil-powder mixture, not only will total heave be reduced, but many waste tires can be recycled. With reduced frost heave, the operational life of engineering structures.

The present study evaluates the effectiveness of tire powders in reducing frost heave and the total heave reduction efficiency achievable with the application of tire powder-soil mixtures. The evaluation focuses on frost heave ratio, thermal conductivity, permeability and segregation potential parameters, based on the results of field tests conducted over three winter seasons.

4.2 Testing conditions

The authors conducted a field experiment using powdered tires in Tomakomai, which is located about 50 km south of Sapporo, Hokkaido. The area is situated at the bottom of a small basin where temperatures are quite low in clear weather. The daily mean air temperature drops to 0 degree Celsius starting in late November, and does not rise above 0 degree Celsius again until mid-March every year.

The freezing index and daily mean air temperature in the winter of 1996-1997 are shown in Fig. 4.1 as an example of the field conditions. The total freezing index amounted to 367 °C·days that winter. The monthly mean air temperature was 3.2 degree Celsius in November, -1.6 degree Celsius in December, -3.5 degree Celsius in January, -3.7 degree Celsius in February, -0.5 degree Celsius in March, and 4.9 degree Celsius in April. The minimum air temperature was -8.5 degree Celsius on January 25, 1997.

To eliminate extraneous effects, the field test was carried out in a waterproof concrete basin 5 m long, 5 m wide, and 1.75 m deep (Fig. 4.2).

First, non-frost-susceptible soil (sand) was backfilled and tamped into the bottom of the basin to a depth of 35 cm to maintain a uniform water distribution. Then a 100-cm deep layer of silty soil was added. Above this second layer, the apparatus was divided into two sections. One was a non-mixed section filled with silty soil, while the other contained silty soil mixed with 20% tire powder by weight. The third layer in both sections was 40 cm deep. After each

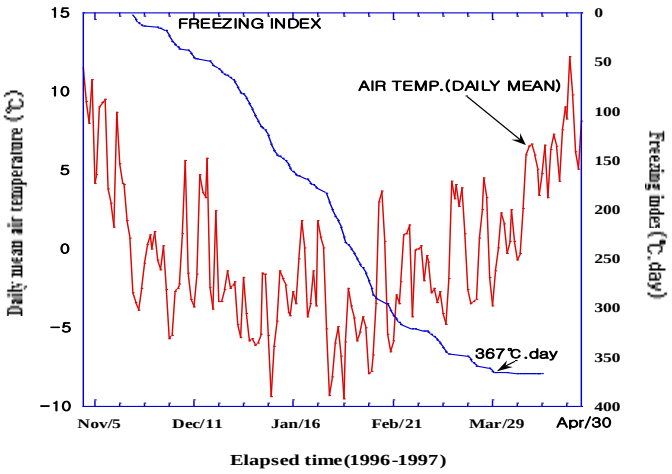

Fig. 4.1 Field test thermal and frost conditions

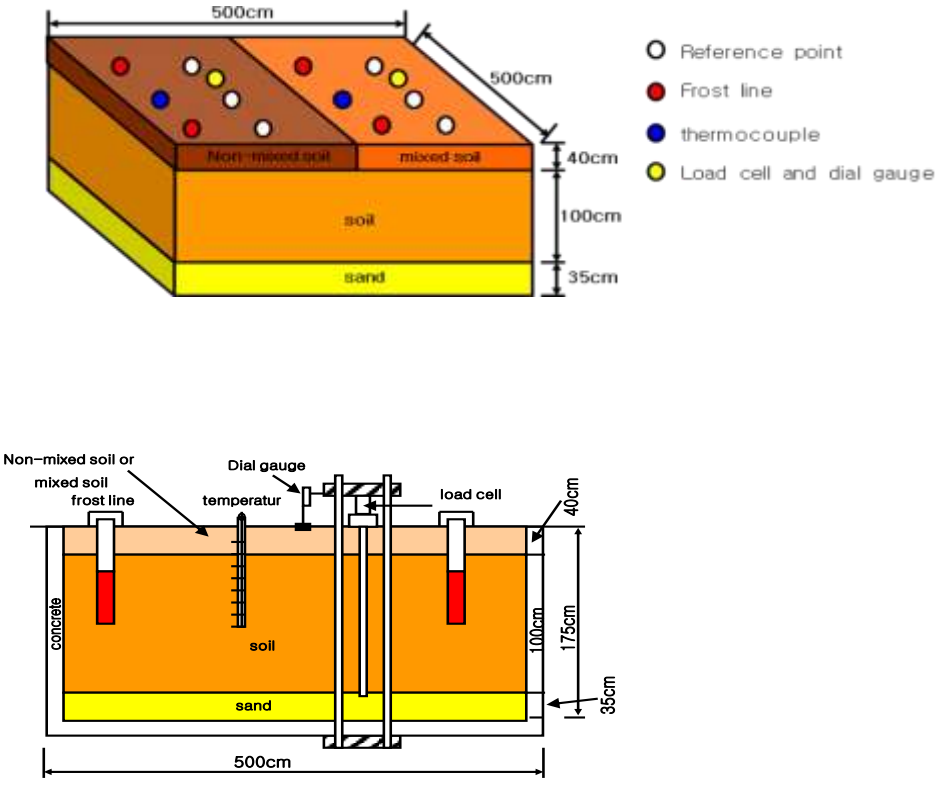

Fig. 4.2 Schematic diagram of field test installation (not to scale)

soil layer was placed in the basin, it was compacted using a vibrating ram. The maximum frost penetration depth was estimated to be about 40 cm.

To obtain the maximum freezing effect, snow was cleared from the site to eliminate the insulating effect of a snow cover. The soil used in the test is frost susceptible and is classified as SF. Fig. 4.3 shows the particle size distribution of soil and recycled tire powder. The specific surface area is 54 m^2/g and the specific gravity is 2.66. The plastic limit is 38% and the liquid limit is 46%. The granulated rubber powders used were uniformly graded and had a nominal maximum size of 2.1 mm and a minimum size of 1.1 mm. The granules were irregular in shape and were made using a cooling crusher after maintaining tire chips at -120 degree Celsius for 15 min. The specific gravity of the powder is 1.22.

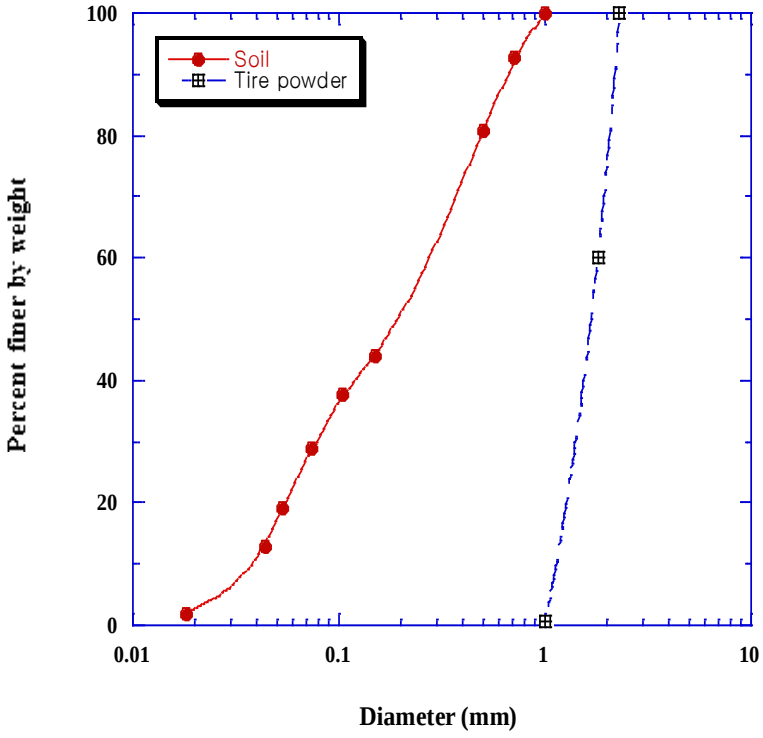

Fig. 4.3 The particle size distribution of soil and recycled tire powder

4.3 Measurements

In the test layer, a variety of sensors and instruments were installed to measure temperature profiles in each layer, the water level in the pool and the amount of frost heave. Water

content profiles were also analyzed by core sampling using a boring machine. The measurement methods employed are described below.

4.3.1 Soil temperature

Soil temperatures were measured at the center of each test section using thermocouples which were attached to the external surface of a 3-cm diameter vinyl pipe at 5 or 10 cm intervals from the soil surface to a depth of 200 cm. The pipe was inserted into a 3-cm diameter hole in the soil. Though the pipe rose together with the heaving of the ground surface, the spacing of the thermocouples did not change throughout the measurement period. Temperatures measured by the thermocouples were recorded in 4-hour intervals with a digital data acquisition system.

4.3.2 Frost penetration

Frost penetration was determined using a thin transparent tube filled with a 0.01% methylene blue dye solution in each test section. This frost tube was sheathed from above and suspended down into another open topped pipe with a slightly larger diameter, which was embedded vertically in the soil with its top protruding from the ground surface. The frozen depth was measured once a week.

4.3.3 Frost heave amount

The frost heave amount was measured using an engineer's level and a dial gauge. Measurements using the level were carried out once a week and the displacement detector recorded data every 4-hour during the freezing period.

4.3.4 Groundwater level

The water level in the basin was measured by reading the level of a buoy floating in a pipe connected to and placed close by the basin. No water from outside the basin was added after the soil began to freeze.

4.4 Results of the field experiment

4.4.1Frost heave characteristics

The data observed during the test for frost heave, penetration of freezing front, frozen depth and groundwater level for the mixed and non-mixed sections, along with the elapsed time in the three successive winter seasons from 1996 to 1999 are summarized in Figs. 4.4 to 4.6. The freezing index of the first season was a little warmer (367°C·days) than the following two seasons, 413°C·days and 439°C·days, respectively.

For the 1996 to 1997 season, ground freezing began around the end of November. After that, the ground surface continued to rise and reached its highest point of 7.9 cm in the mixed section and 12.7 cm in the non-mixed section on March 10, 1997 (Fig. 4.4). By that time the measured maximum depth of frost penetration in the non-mixed section was 42 cm and the

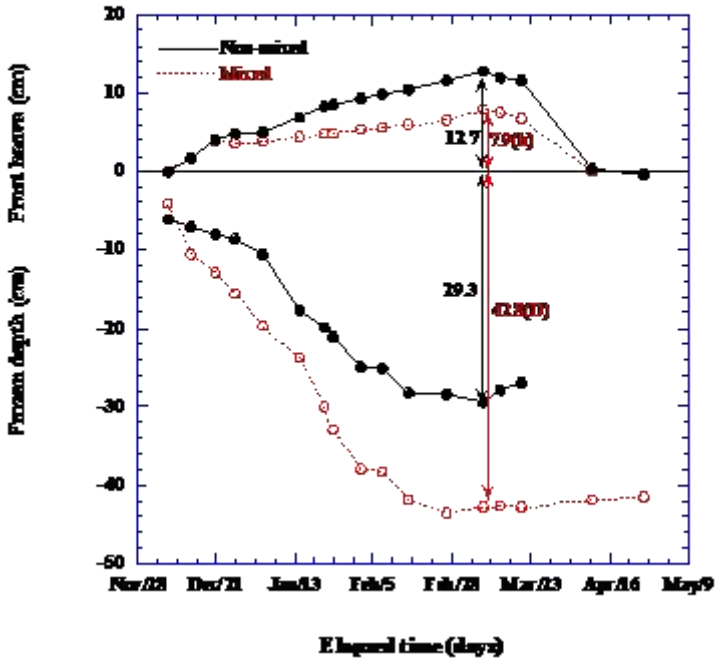

Fig. 4.4 Results of observation in the field during the winter of 1996~1997

depth of frost penetration in the mixed section was 50.7 cm. The freezing front continued to penetrate into the ground until February 28, 1997 and became nearly stationary thereafter. On March 10, 1997 the freezing front reached its deepest level of 42.8 cm (mixed section) and 29.3 cm (non-mixed section). The frost heave ratios of the mixed and non-mixed sections, (maximum frost heave height divided by maximum frozen depth) were 18.5 and 46.9%

respectively. The heave ratio of the mixed section was less than half that of the non-mixed section.

For the 1997 to 1998 season (initial groundwater level 5 cm below the ground surface), ground freezing began around December 15. The maximum measured heaves were 5.8 cm in the mixed section on March 16 and 13.3 cm in the non-mixed section on February 24. The maximum frozen depths were 42.4 cm (mixed) and 27.6 cm (non-mixed) yielding heave ratios of 13.7% (mixed) and 48.9% (non-mixed). Complete melting occurred on April 27. The ground water table continued to fall considerably as heaving progressed, reaching the tank bottom (178 cm below the initial ground surface) on February 17 and rising suddenly with the onset of thawing after March 24 (Fig. 4.5).

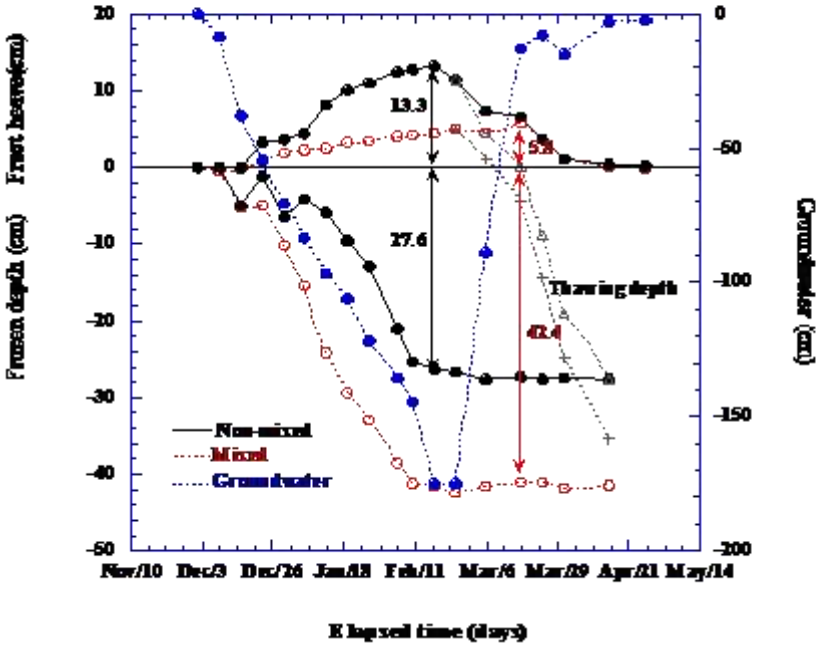

Fig. 4.5 1997~1998 winter field observations

The mean heaving rate was about 2.1 mm/day from December 15 to February 17 (non-mixed) and 0.63 mm/day from December 15 to March 17 (mixed). The heaving process in the mixed section was much slower than that in the non-mixed section, while the frost penetrated deeper in the mixed soil than that in the non-mixed soil.

For the 1998 to 1999 season (initial groundwater level 35 cm below the ground surface), ground freezing began around December 15. The maximum heave heights were 9.6 cm (mixed) on March 1 and 23.3 cm (non-mixed) on February 12. The maximum frozen depths were 37.6 cm (mixed) and 17.1 cm (non-mixed). The heave ratios were 24.2% (mixed) and 59.1% (non-mixed). Complete melting occurred on April 26. The groundwater table rose due to ground surface thawing between December 7 and December 14. It then proceeded to fall considerably as heaving progressed, reaching a depth of 130 cm below the initial ground surface on February 14 after which it remained stable then suddenly rose as thawing began after March 26 (Fig. 4.6).

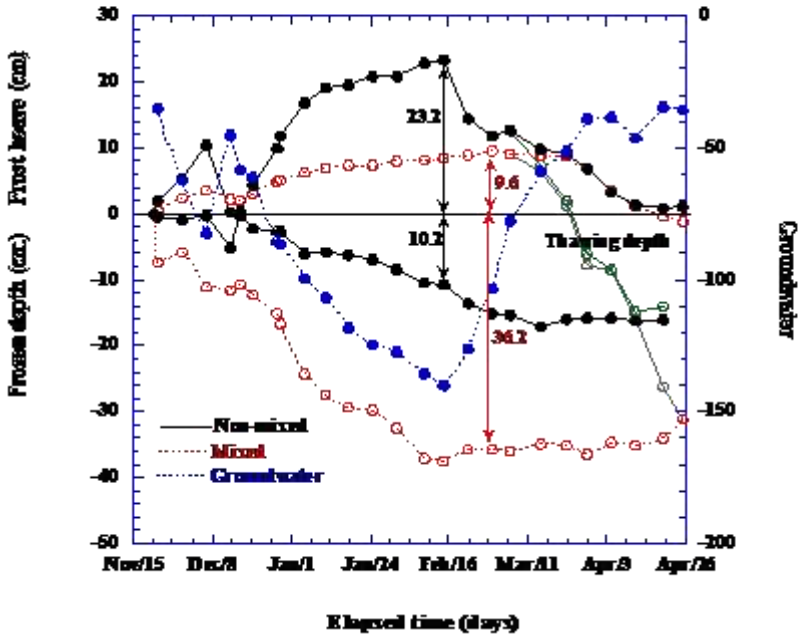

Fig. 4.6 1998~1999 winter field observations

The mean heaving rates were about 4.2 mm/day from November 22 to February 15 (non-mixed) and 1.3 mm/day from November 22 to March 1 (mixed).

The heaving rate from the onset of winter to the middle of December this season was very high due to the intensive growth of an ice column at the ground surface. The ice column, which was observed in the field, was 2 cm thick in the mixed section and 6 cm thick in the non-mixed section. The frost front of the mixed section penetrated deeper than that of the non-mixed section. Such a difference of freezing front shows that the volumetric water

content decrease caused by the granulated rubber powder-soil mixture has an effect on the latent heat caused by ice segregation.

4.4.2 Thermal characteristics

The maximum frozen depth, defined as the thickness from the original ground surface before frost heave to the freezing front for the 1996~1997, 1997~1998 and 1998~1999 winters is shown in Fig. 4.7. The frozen depth beneath the mixed section ranged from 37.6 cm to 42.8 cm. On the other hand, the frozen thickness beneath the non-mixed section ranged from 17.1 to 29.3 cm. The addition of the granulated rubber powder increased the frozen depth of the mixed section about 66% compared to the non-mixed section. This indicates that the granulated rubber powder is not effective in reducing the frozen depth and that the decrease of the heave achieved by mixing the rubber powder in is not produced by an insulation effect but some other factor.

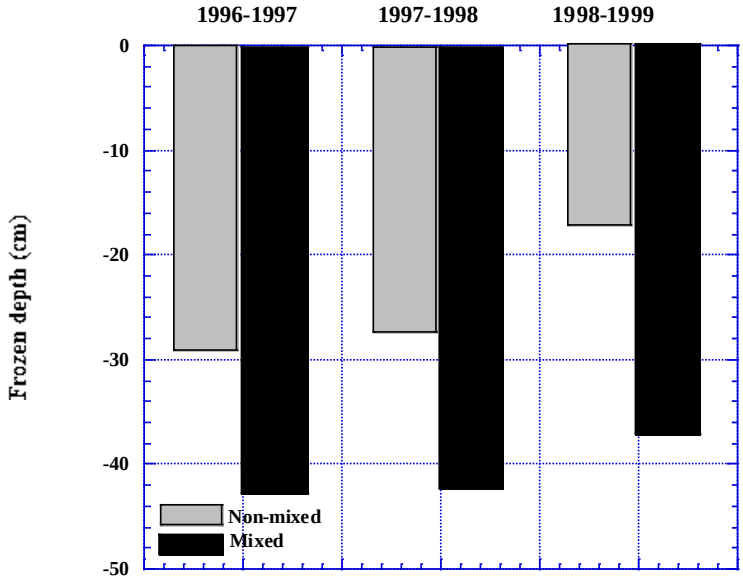

Fig. 4.7 Maximum frozen depth

A comparison of the freezing front, representing the boundary between the frozen and unfrozen zones in both sections is shown in Fig. 4.8 (1996~1997 season). The freezing front in the non-mixed and mixed sections reached levels of 42 and 50.7 cm, respectively, below the ground surface on March 10. The freezing front in the mixed section penetrated more

rapidly than in the non-mixed section until the beginning of the spring thaw in both sections. However, the results shown in Figs. 4.6 and 4.7 are quite different from Humphrey's result [8,9]. This is thought to arise from a diminution of latent heat due to the water-repellent properties of the tire material and the decrease of unfrozen water content in the mixed soil. It is also clear that if tire powder is mixed with a soil, the rubber powder does not function as an insulator, even though the thermal conductivity of rubber is much lower than that of soil.

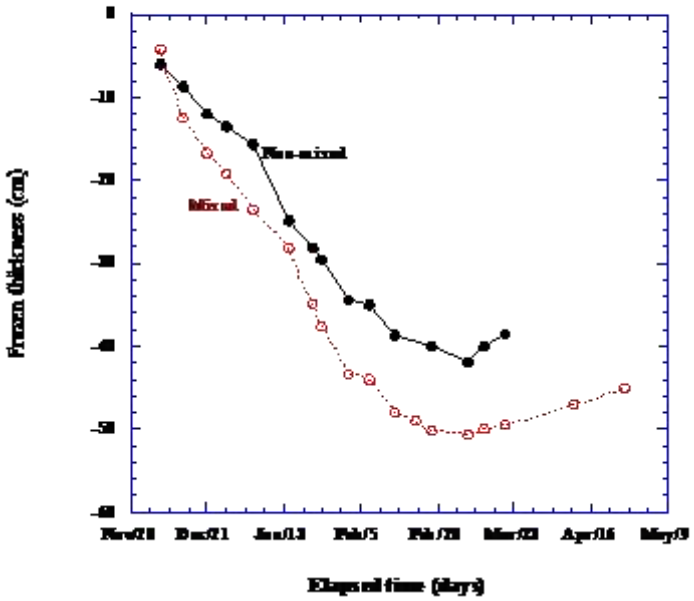

Fig. 4.8 Frost front depth comparison, 1996~1997 season

4.4.3 Volumetric water content analysis

Core samples 5 cm in diameter, extending from the ground surface to about 100 cm deep, were taken from both sections on March 5, 1998 and March 5, 1999 (during freezing), using a boring machine with a high-speed rotating edge. The samples were examined to investigate their layered structures. Slices were taken at intervals of 2.5 and 5.0 cm. The volumetric water content (θ) of each frozen sample was obtained by calculating its wet density (ρ_t), using the difference between its weights in air and kerosene, its water content(w) and the density of water(ρ_w); $\theta=\rho_t \cdot w/(\rho_w(1+w))$. The sample's volumetric water content is shown in Fig. 4.9.

Fig. 4.9 shows that the volumetric water content near the surface in the mixed section was 52%, compared to 65% in the non-mixed section before freezing. It increased to 68% (non-

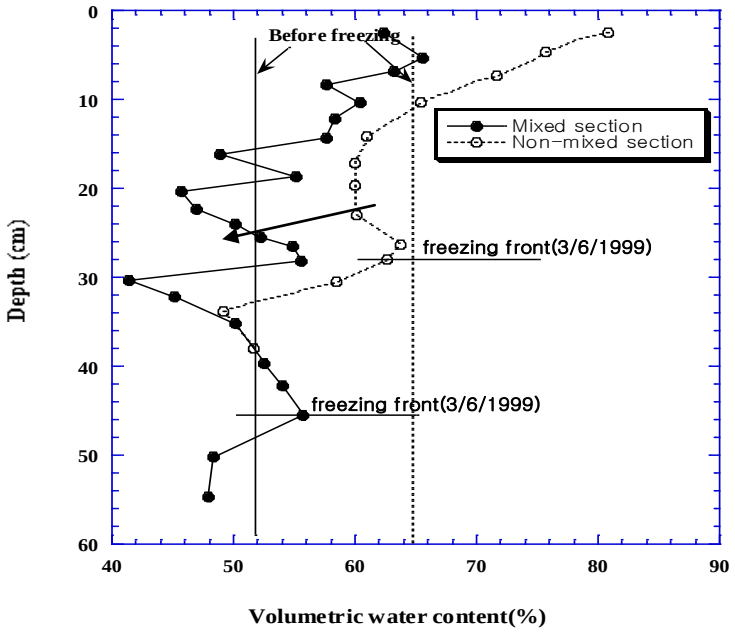

Fig. 4.9 Vertical distribution of volumetric water content

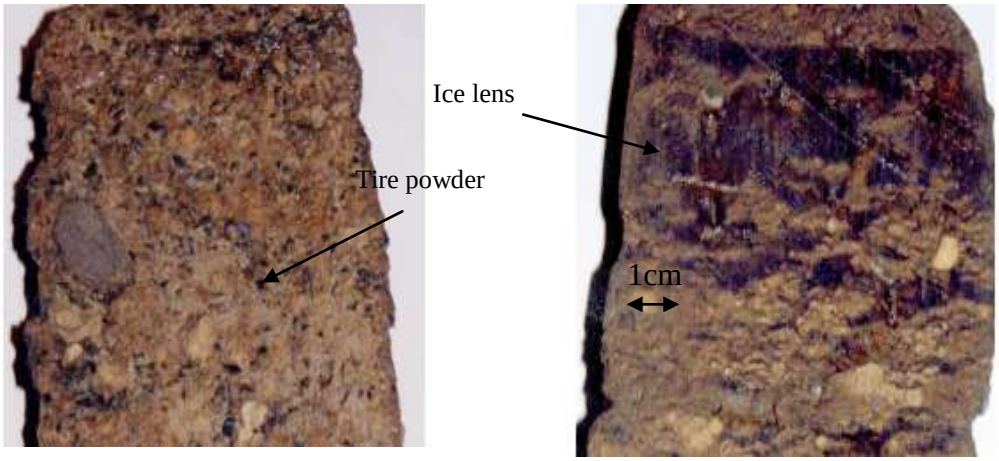

(a) Mixed section (b) Non-mixed section

Photo 4.1 Occurrence of ice lenses in mixed and non-mixed soil

mixed) and 81% (mixed) including an ice column that developed at the surface, but was smaller in an unfrozen layer immediately below the freezing front. The increase of the volumetric water content in the frozen layer corresponds to the presence of ice lenses. Ice

lenses 2 to 3 mm thick were detected in the frozen core of the non-mixed section, but hardly any ice lenses were visible in the frozen core of the mixed section, as shown in Photo. 4.1.

4.5 Discussion

There are several mechanisms by which frost heave may be reduced when granulated rubber powder is mixed with soil. In order to understand which mechanisms are responsible for the reduction, we investigate frost heave considering thermal conductivity, and the permeability of the tire powder-soil mixture, Then, in the last part of this chapter, we analyze the effect of the addition of tire powders to the soil based on segregation potential theory.

4.5.1 Evaluation of the tire powder mixture using frost heave ratio

Frost heave ratio is usually defined as the ratio of frost heave height to maximum frozen depth (See Fig. 4.4 h/D). The calculated frost heave ratios for the three winters of the study are shown in Table 1. The difference in frost heave ratio between a mixed medium and a non-mixed medium is clearly shown in Table 4.1. In our three year field experiment, the frost heave ratio decreased about 64% as a result of mixing tire powder with surface soil.

Table 4.1 Frost heave ratios in mixed and non-mixed sections (%)

Year	1996-1997	1997-1998	1998-1999	Mean
Mixed site	18.5	13.7	24.2	18.8
Non-mixed site	46.9	48.2	59.1	51.4

The thermal and hydraulic properties of a soil material affect the degree of its frost susceptibility. The thermal conductivity of tire powder-soil mixtures was measured for various mixing ratios. In Fig. 4.10, the thermal conductivities of these tire powder-soil mixtures are plotted for both frozen and unfrozen conditions as a function of mixing ratio (tire powder to dry soil by weight). When frozen, thermal conductivities decrease slightly as mixing ratio increases. This implies that frozen depths may be shallower for a mixed soil than for soil with a higher value of thermal conductivity such as a non-mixed soil. Differences in frozen layer thickness between the two test conditions, both of which have the same freezing

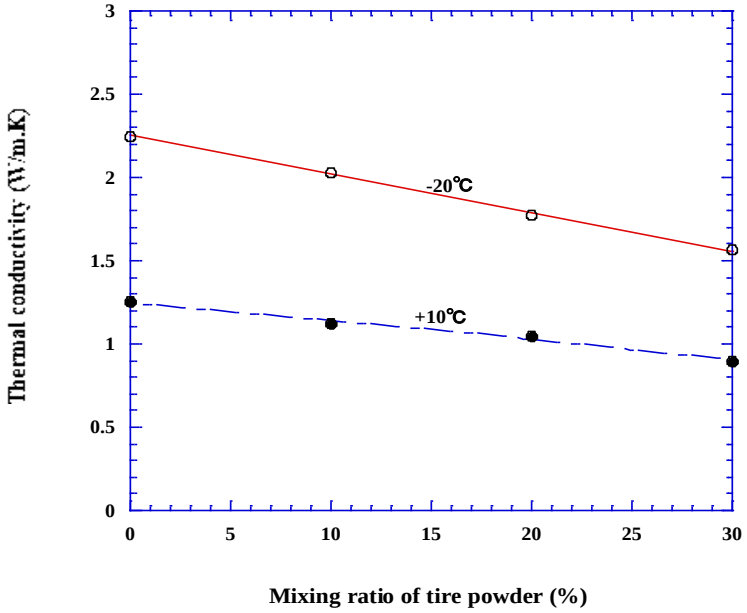

Fig. 4.10 Relationship of thermal conductivity to tire powder mixing ratio

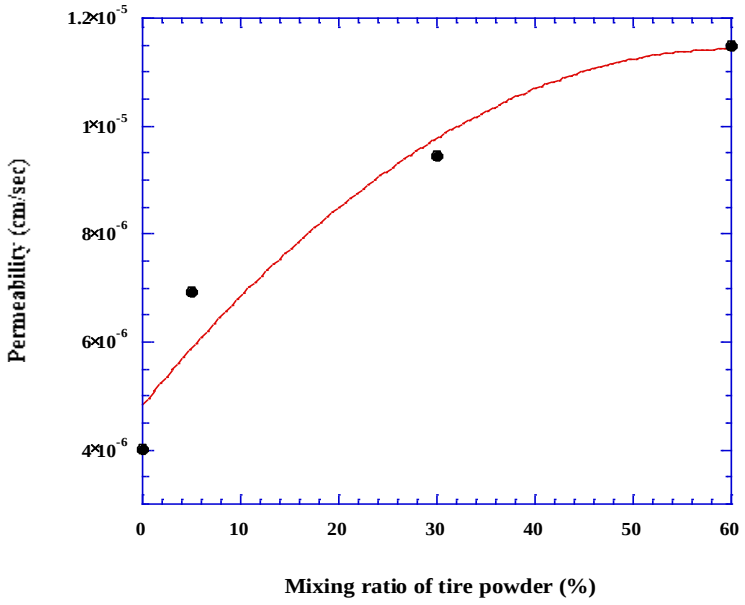

Fig. 4.11 Permeability as function of tire powder mixing ratio (unfrozen state)

index, might be caused by this property.

The permeability of soils in their unfrozen state was measured for different tire powder/soil mixing ratios. The results are shown in Fig. 4.11. The permeability of samples with tire powder added is twice to three times that of non-mixed soil.

In general, soils with higher frost susceptibility have higher permeability. This result implies that soil permeability is not the determining factor for frost heave if the values differ only by a factor of 2 to 3.

The comparisons of thermal conductivity and permeability between tire powder-mixed and non-mixed soils do not appear to conclusively explain the mechanism whereby frost heave is reduced. To try to discover the factor responsible for the reduction in frost heave achieved by mixing powdered tires into soil, the results of the field experiment were examined based on the so-called segregation potential (SP) theory proposed by Konrad[10,11]. The results of this analysis are given in the next section.

4.5.2 Evaluation of the tire powder mixture effect using the SP theory

According to the Segregation Potential (SP) theory, an ice lens grows somewhere inside frozen soil, slightly behind the freezing front, which is the warmest isotherm at which ice can exist in the soil pores. The growth of the ice lens depends mainly upon the temperature gradient in its vicinity. In the simplest form of the model, the segregation potential is given by:

$$V=SP\cdot gardT \tag{4.1}$$

where V is the velocity of water intake (mm/s) and gardT is the temperature gradient adjacent to the growing ice lens (°C/mm).

- Temperature gradient near frozen fringe

An example of a soil temperature profile observed during the field experiment is shown in Fig.4.12. Each temperature in the profile was calculated using mean daily temperatures recorded at 4-hour intervals.

In this study, we assume the space between the location where the temperature is 0 degree Celsius and the nearest upper thermocouple to be the frozen fringe, and calculate temperature

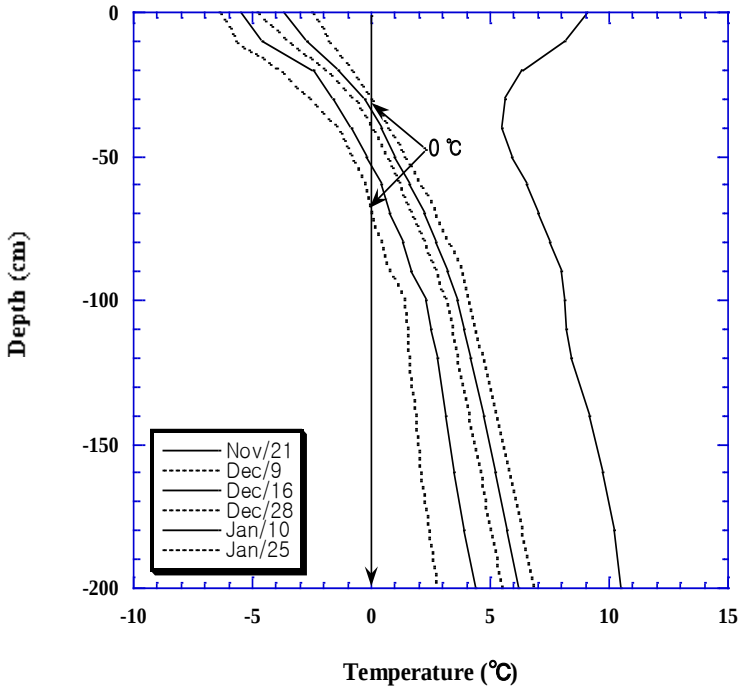

Fig. 4.12 Test section temperature profiles for the1997~1998 winter season

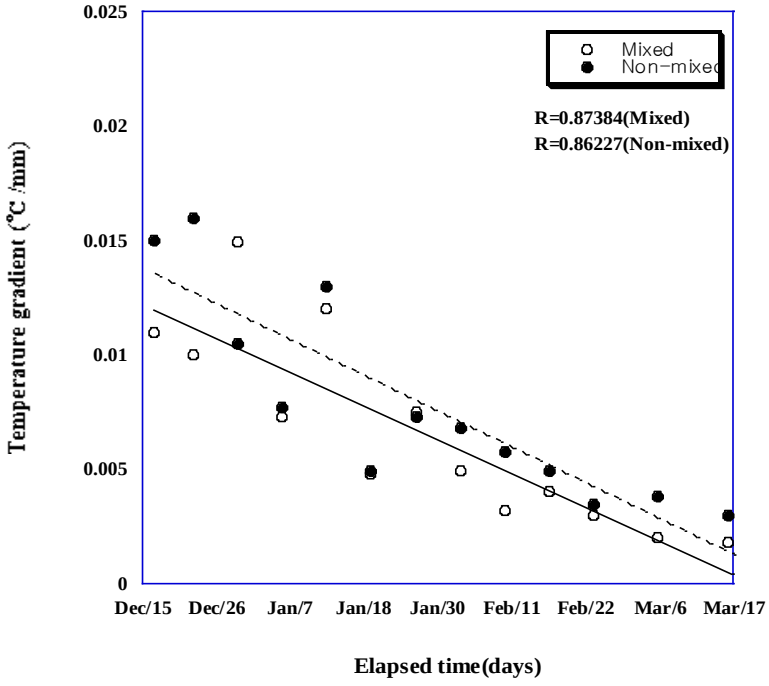

Fig. 4.13 Temperature gradients for the 1997~1998 winter season

gradients using temperature data at these points during the freezing period. The slope of the temperature profile then becomes the temperature gradient near the frozen fringe because of temperature profile interpolation. The relationship between daily temperature gradients and elapsed time for both sections is shown in Fig. 4.13. Fitting the data to the plots, we obtain values for the time-dependent function grad(t)=A-B(t), where grad(t) is the temperature gradient in the frozen fringe, t is elapsed time (days), and A and B are constants. The temperature gradient of both soils tended to decrease gradually as temperatures fell starting in the middle of December, although individual temperature gradients for both test conditions varied considerably within a range of 0.015~0.003 °C/mm.

-Velocity of frost heave and velocity of water intake

Eq. (4.1) shows that the velocity of water intake and temperature gradient are proportional to the SP value for a soil. The relationship between velocity of frost heave and velocity of water intake can be described by:

$$V = (1/1.09)\times dh/dt \quad (4.2)$$

where dh/dt is the frost heave velocity. By substituting Eq. (1) into Eq. (2), the velocity of frost heave can be expressed as follows:

$$dh/dt = 1.09\cdot SP\cdot gradT \quad (4.3)$$

Thus the result that differentiated frost heave amount measured in 7 day interval by time (Fig. 4.5) becomes the velocity of frost heave. Similarly ground surface frost heave rates calculated for both test sections plotted against elapsed time are shown in Fig. 4.14. The relationship between elapsed time to heave rate was then obtained by fitting data to f(t)= C-D(t) where C and D are constant. In the early stages, the frost heave rate of both soils was very high, then generally decreased as time passed.

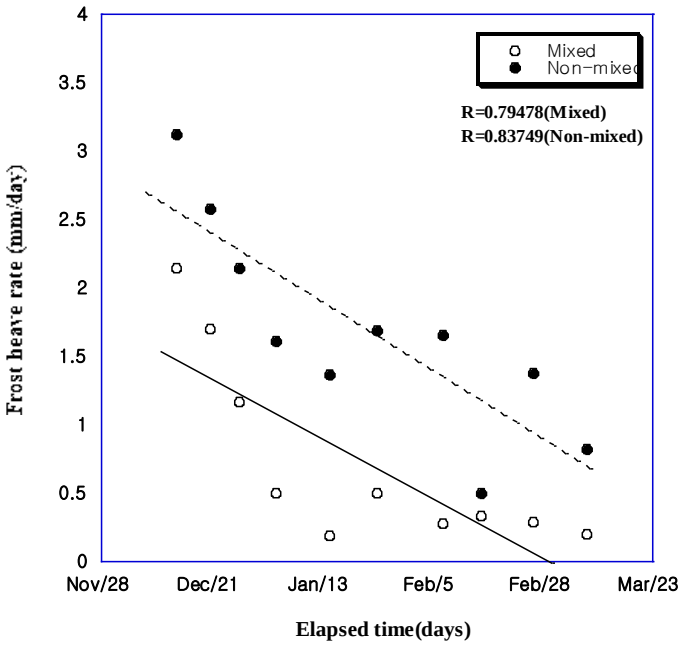

Fig. 4.14 Frost heave rates for a winter season of 1997~1998

-SP comparison of mixed and non-mixed soil

Based on the procedures outlined in sections 5.2.1 and 5.2.2, SP was calculated by substituting the temperature gradient and velocity of frost heave into Eq. (4.3). The one to one correspondence of temperature gradients and frost heave velocities calculated for the same points in time are shown in Fig. 4.15. Calculated SP and the results of a simple linear regression on mixed and non-mixed soil for three winters from 1996~1999 are shown in Table 4.2 and Fig. 4.15.

Table 4.2 SP values obtained by linear regression for three winters from 1996-1999

(units: $mm^2/s \cdot day$)

Type	1996–1997	1997–1998	1998–1999	Mean
Non-mixed section	167	249	264	225
Mixed section	121	59	54	78

The difference in frost susceptibility between the tire powder-mixed and non-mixed soil is clearly visible using SP values. The SP value of a soil depends on soil type and two other

external conditions, overburden pressure and pore water pressure at the frost front. In our field experiments, these conditions are the same in the mixed and non-mixed sections throughout the whole freezing periods as both sections are located in one waterproof pool. SP differences depend solely on soil characteristics or properties other than thermal conductivity and permeability.

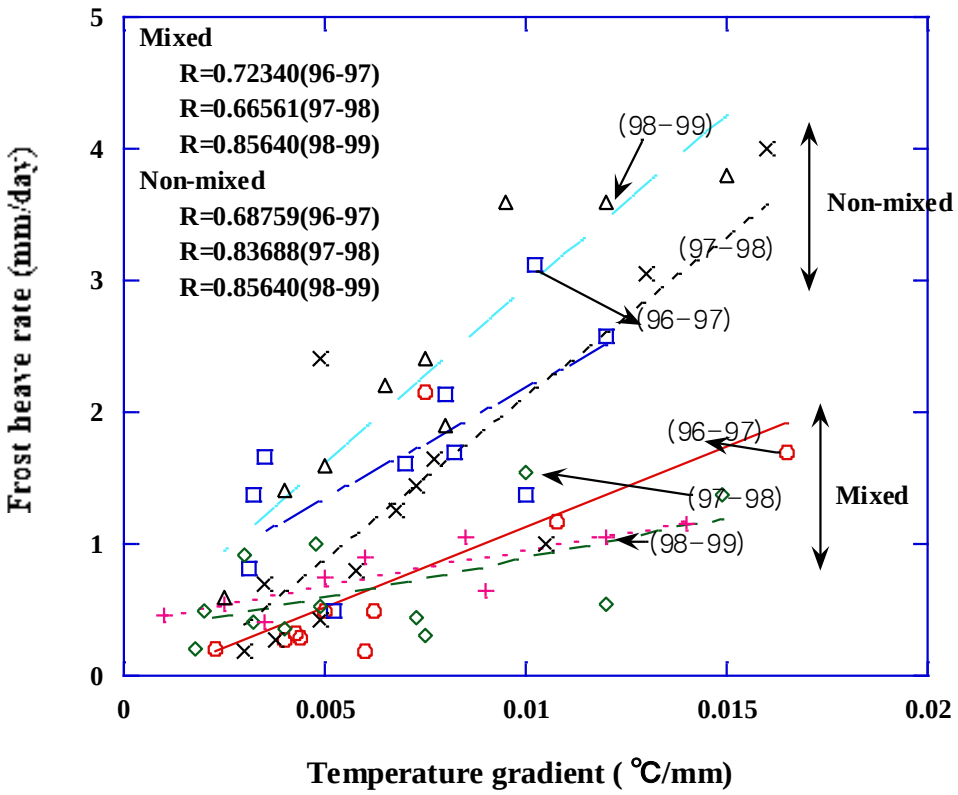

Fig. 4.15 Relationship between frost heave rate and temperature gradient

4.6 Summary

Field trials were conducted over three winters (1996~1999) to investigate the effect of granulated rubber powder as a new frost heave restraint material. The following conclusions can be drawn from the results of the research:

1. The frost heave reductions achieved by mixing powdered tires into soil were not due to the insulating effect of rubber.

2. The frost front in the mixed section penetrated deeper than in the non-mixed section. This may be a latent heat diminution effect caused by water-repellent properties of the rubber and decreased specific surface area in the mixed soil.

3. Our 3-year field experiment found that mixing soil with granulated tires (20% by weight) reduced the frost heave ratio by about 75%.

4. The segregation potential (SP) value of the soil decreased 65% by mixing 20% tire powder by weight into the soil. This large SP difference explains how the frost heave of mixed soil is restrained by the addition of powdered tires.

References

1) Fukuda, M.,Yamamoto H.and Izuta H.: The evaluation of reducing method of total heave amounts using soil-cement mixtures, Ground Freezing 91, pp. 417-424 (1991)
2) Thompson, M. R.: Durability and frost resistance of lime and cement stabilized soils, Proc. of Symposium on Frost Action on Roads, Vol. 2, pp. 201-203 (1973)
3) Ono, T. and Kawaabe, K.: Frost heave control using cement-stabilized method, The 40th Japan National Conference on Geotechnical Engineering, Hakodate, pp.1209-1210. (2005) (in Japanese)
4) Henry, K. S.: Laboratory investigation of the use of geotextile to mitigate frost heave, CRREL Report 90-6, p. 28 (1990)
5) Tsuchiya, F. and Yokota, S., "Frost heave mitigation by means of capillary breaks using geotextiles, Proceedings of Hokkaido Branch of the Japanese Geotechnical Society, No.38, pp.1-6 (1998) (in Japanese)
6) Dunphy, W.J.: Experimental insulation of a subgrade in Hampden, Main. *Proc*. Of Symposium on Frost Action on Road, Vol. 2, pp. 329-338 (1973)
7) Robert, A. E., Richard, J.R. and Dana, N. H.: Gravel road test sections insulated with scrap tire chips. Special Report 94-21 (1994)
8) Humphrey, D. N.: Field performance of tire chips as subgrade insulation for rural roads, Proc. of the Sixth International Conference on Low-Volume Roads, Transportation Research Board, Vol. 2, pp. 77-86 (1995)
9) Humphrey, D. N.: Civil engineering application of tire shreds, The Scrap Tire Management Council at Rubber Recycling '98, p.16 (1995)
10) Konrad, J. M. and Morgenstern, N. R.: The segregation potential of a freezing soil, Canadian Geotechnical Journal, 18: pp. 482-491 (1981)
11) Konrad, J. M., "The influence of heat extraction rate in freezing soils", Cold Regions Science and Technology, 14: pp. 129-137 (1987)

Chapter 5 Thermal Conductivity of Discarded Tire Powder-Soil Mixture

5.1 Introduction

Currently, LNG development from Siberia is under way as a joint project among Korea, Japan, China and Russia for its highlighted utility as a new energy source in the 21st century. On the section of Irkutsk-Beijing-Tianjin about 2,900km long, selected as the subject route, full-dress chilled pipeline construction work is soon beginning with an expectation of active participation from domestic construction-related companies henceforth[1)].

Besides, it was verified through the primary subsurface investigation that most of the route for planned pipeline construction belongs to seasonal permafrost region except some part of Siberia. That means, for building pipelines in this area, it is indispensable to investigate a frost heave characteristics in order to protect the pipeline structure from the effect of ground freezing caused by the continuous transfer of -20 degree Celsius natural gas through the pipeline. Also, to investigate the frost heave phenomenon on the ground, what matters the most is to estimate the thermal conductivity of frozen soil.

Since thermal probe method to measure the thermal conductivity of soil at normal temperature was developed, many related test formulas on the factors of affecting the thermal conductivity of soil were proposed. However, empirical formulas by Kerstern[2)] and Johansen[3)] are popularly used. Kerster's formulas measures thermal conductivity for silt, clay, and sandy soil using dry density and water content, but they are known as not applicable for dry soil and gravel.

Though Johanson's formula is close to the measured results, because of its need for unfrozen water, quarts content as parameters for estimating thermal conductivity, it is considered difficult to use practically, with ±25% margin of error in any way[4)]. Moreover, regarding the thermal conductivity at low temperature (below 0 degree Celsius), that is, for frozen soil, while domestic researches are being made fragmentarily in a very limited range[5,6)], they are on progress in diverse fields overseas[7,8,9)].

Of the existing thermal conductivity models, typical models for unfrozen soil include De Vries model[10)] in application of Maxwell's electric conductivity and series-parallel model[11)] expressing the macro-thermal conductivity for soil, while those for frozen soil

representatively include Farouki model[12] and Fukuda model[13], with a comparative review between measured and model-calculated results for thermal conductivity.

Currently, besides building a chilled-oil pipeline, designing a freezing-related civil structure such as use of artificial ground freezing, LNG tank construction, etc. must reflect the element of thermal conductivity. Since such structure always involves both areas of frozen and unfrozen soil, it is desired to use the model that can manage thermal conductivity successively for two areas of frozen and unfrozen soil. Up to now, however, no cases have been found that propose the pertinent model for thermal conductivity.

From this perspective, in this study, on the side of reusing the discarded tire, a kind of industrial by-product, after pulverizing it under 4mm, the first-phase process was established to review the potential applications for new anti-frost material to partially supplant the existing ant-frost layer, and then, for anti-frost inhibitor of aforementioned chilled-oil pipeline. First, this study was aimed to grasp the thermal conductivity characteristics of soil-tire powder mixture according to temperature change. Also Unfrozen water content was measured, using NMR (Pulsed Nuclear Magnetic Resonance) equipment, and expressed into the function of temperature. Besides, by developing the two-phased (soil particle and water) thermal conductivity model for unfrozen soil proposed by Woodside, we proposed a new three-phased model consisting of soil particle, ice and unfrozen water, which, considering the existence of unfrozen water, is applicable even to the area of frozen soil.

5.2 Decision on thermal conductivity model

Finding a thermal conductivity for two-phase state depends on how to weigh it out between solid and liquid. Many models of thermal conductivity so far can apply and weigh out thermal conductivity for solid and liquid using several methods, which are called a distribution model, including arithmetic mean, geometric mean and harmonic mean (Fig. 5.1).

By two phases, soil and thermal conductivity for liquid λ_T, λ_s, λ_w, soil volume fraction n, and liquid volume fraction (1-n), arithmetic mean, geometric mean and harmonic mean can be expressed as follows:

$$\text{arithmetic mean:} \quad \lambda_T = n\lambda_S + (1-n)\lambda_W \tag{5.1}$$

geometric mean: $\lambda_T = \lambda_S^{\,n} \times \lambda_W^{(1-n)}$ (5.2)

harmonic mean: $\lambda_T = \dfrac{1}{\dfrac{n}{\lambda_S} + \dfrac{1-n}{\lambda_W}}$ (5.3)

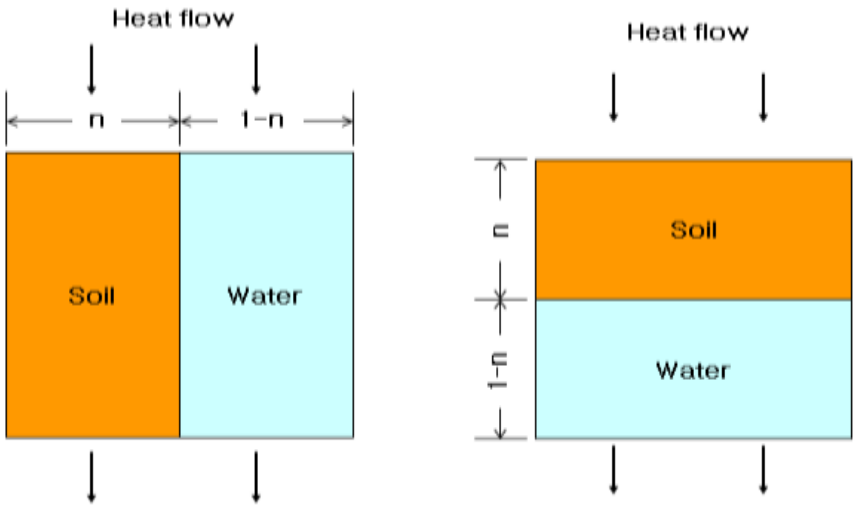

(a) Arithmetic mean model (b) Harmonic mean model

Fig. 5.1 Arithmetic mean model and harmonic mean mode[l1)]

Eq. (5.1) was put into as a parallel model with heat flowing separately in constant proportion between soil and liquid as shown in Fig. 5,1(a), Eq. (5.3) as a series model as in Fig. 5.1(b), and Eq. (5.2) as a form of logarithm from Eq. (5.1). With difficulty in explaining two-phase thermal conductivity using the above basic equation, serial-parallel model, which is a combined form of Eq. (5.1) and (5.3), is widely used. This model was shown in Fig. 5.2, and as shown here, thermal mobility was assumed to be three cases: ①part (b) with soil particle in direct contact, ② part (C) consisting of liquid, and ③ part (a) consisting of soil particle and liquid.

That is, assuming that heat simultaneously flows through the three passages, two-phase thermal conductivity (λ_T) can be expressed as the following on the condition of Fig. 5.2:

$$\lambda_T = \frac{a}{\frac{D}{\lambda_S} + \frac{1-D}{\lambda_W}} + b\lambda_S + c\lambda_W \qquad (5.4)$$

Where a, b, and c represent the ratio of parts relevant to ③, ①and ②, and d is a ratio that soil particle takes up in a. Eq. (5.4) is what Woodside et al.[11] applied the equation proposed by Wyllie et al.[14] to explain the electric conductivity of conductive particles for calculation of thermal conductivity of soil particles. For application of Eq. (5.4) into a model of soil thermal conductivity, the following relations exist in Fig. 5.2 for the 4 fixed numbers.

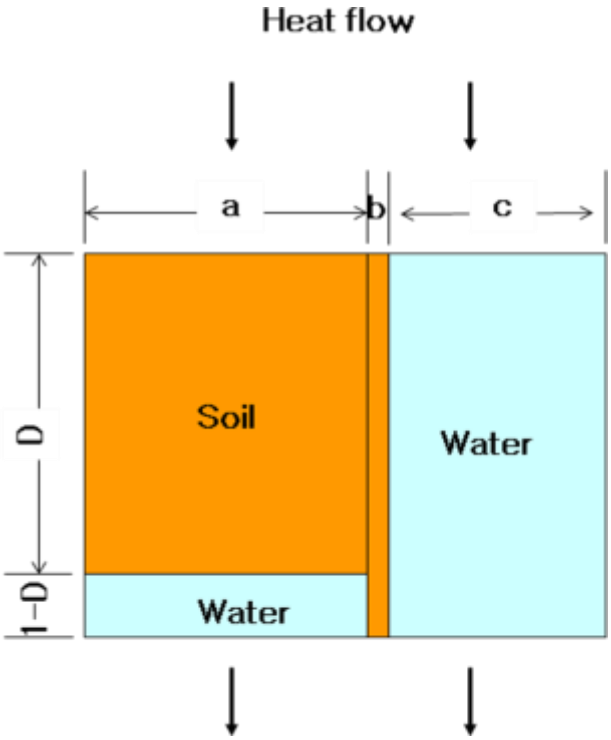

Fig. 5.2 Serial-parallel model [11]

$$a + b + c = 1.0 \qquad (5.5)$$

$$a \cdot d + b = n \qquad (5.6)$$

Since it is impossible to infer the 4 fixed numbers from Eqs. (5.5) and (5.6) alone, we can decide them using several experimental methods. Since b is the ratio of thermal conductivity by the contact of soil particles, it produces $\lambda_w \fallingdotseq 0$ in a vacuum if thermal conductivity for liquid is neglected, leading to the expression of $b = \lambda_T/\lambda_s$ in Eq. (5.4).

According to research result of Kimura[15], b stands in the rage of 10^{-3}~10^{-5}, minuscule

enough not to be considered practically. Substituting b to 0 gives three unknowns a, c, and d. Here, Woodside[11] proved on an experimental basis that if 1-n is ranged between 0.2 and 0.6, it bears the relation d=n/(n+0.03).

This study, by applying the simplified serial-parallel model proposed by Woodside (Fig. 5.3), is going to review a thermal conductivity model, available not only to unfrozen condition but also to frozen condition, on the subject of discarded-tire mixed soil. Eq. (5.7) was induced through the same development process as the serial-parallel model in Eqs. (5.1) and (5.3), by applying the model of Fig. 5.3.

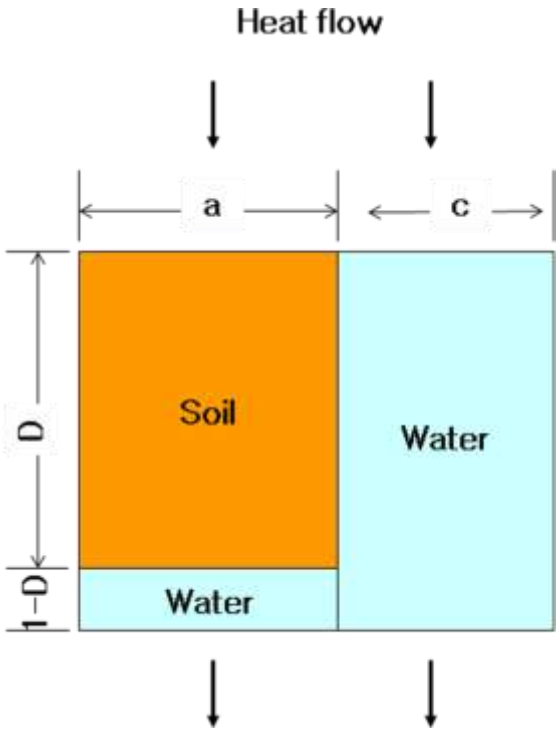

Fig. 5.3 Simplified serial-parallel model[11]

$$\lambda_T = \frac{a}{\frac{D}{\lambda_S} + \frac{1-D}{\lambda_W}} + C\lambda_W \tag{5.7}$$

5.3 Experimental apparatus and method

5.3.1 Physical properties of each sample

To estimate the thermal conductivity characteristics, tests on physical properties were carried out including density, particle size distribution, specific surface area, etc. Sample used

for this thermal conductivity experiment was the one with high frost susceptibility, gathered from the outskirts of Tomakomai city, Japan. It had specific gravity 2.66, specific surface area 54m^2/g, liquid limit 46% and plastic limit 38%, while unified soil classification system

Table 5.1 Basic physical properties of each sample

Remarks	Mixing ratio(%)			
	0	10	20	30
Specific gravity (Gs)	2.66	2.38	2.21	1.97
Maximum dry density(rd_{max})	1.79	1.69	1.51	1.36
Optimum moisture content($w_{opt,}$ %)	19.3	18.2	17.1	14.9
Liquid limit(LL, %)	46	41	-	-
Plastic index($I_{p,}$ %)	8	14	-	-
Specific surface area(m^2/g)	54	-	-	-
Soil classification(USCS)	SC	SC	SC	SC

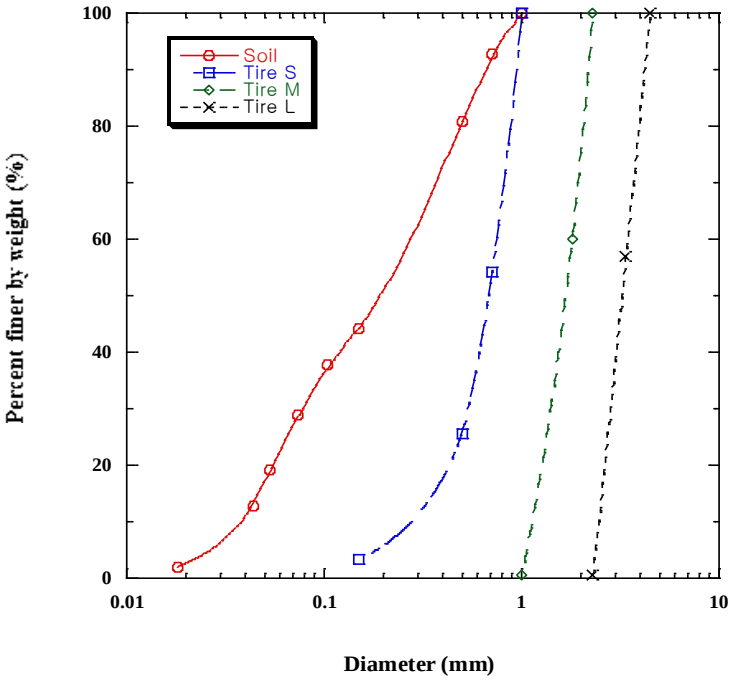

Fig. 5.4 Particle size distribution curve of the tested sample

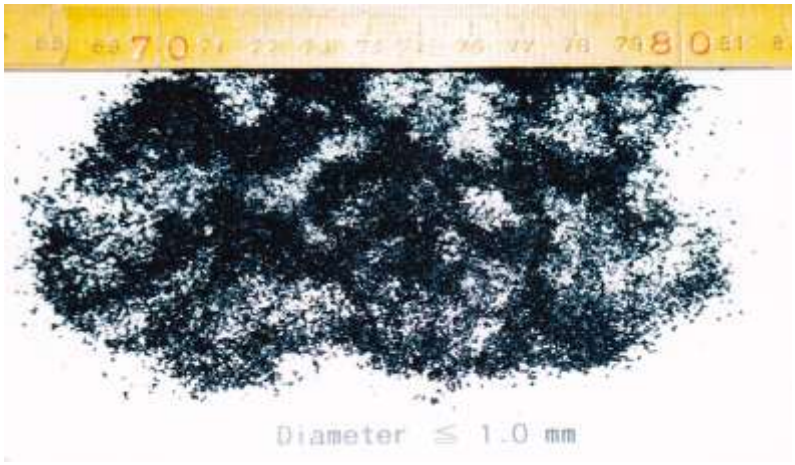

(a) S type

(b) M type

(c) L type

Photo 5.1 Picture of discarded tire powder

verified it as SC. Basic physical properties of the tested sample were illustrated in table 5.1 and Photo. 5.1, respectively, and particle size distribution curve was shown in Fig. 5.4.

5.3.2Thermal conductivity measurement of sample

Thermal conductivity measurement was performed using thermal probe method, a kind of unsteady-state method. Thermal conductivity measured by thermal probe method is the one including the effect of convection, radiation, moisture and vapor transfer, but because the effect of convection and radiation between soil particles is small and because it is possible to neglect the effect of moisture and vapor transfer in measurement by keeping the temperature increase of probe, so we considered heat transfer in soil chiefly due to conduction. Fig. 5.5 and 5.6 show the distribution of measuring equipment and the structure of thermal probe for thermal conductivity. Measuring equipment consists of thermal probe, constant voltage system, relay, A-D converter, microvolt meter, computer, and low-temperature constant bath controllable within the range of ±0.005 degree Celsius. On-off for probe voltage and data collection and processing were carried out with a computer.

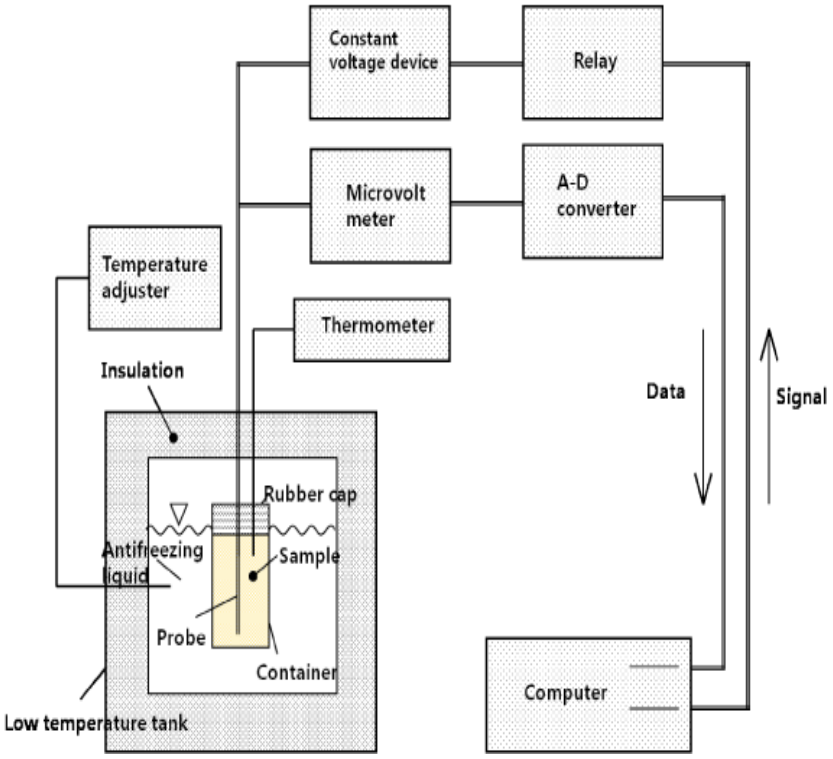

Fig. 5.5 Schematic diagram of thermal conductivity measuring equipment

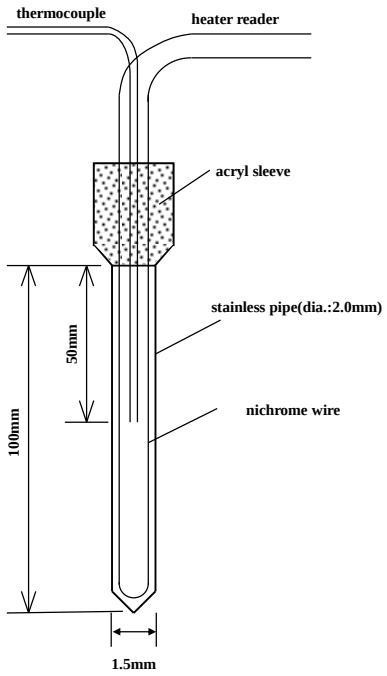

Fig. 5.6 Structure of thermal probe

For a probe used in this study, T type thermocouple with an electric heater (heater resistance R = 12.59 Ω) and temperature sensor was inserted in the stainless steel tube 2.0mm in external diameter and 100mm in length, fixed and insulated by paraffin inside. Temperature was measured from two spots – central part and upper part of the probe (standard temperature) – for electronic force, generated by the temperature difference between these two spots, and rising temperature.

Fig. 5.7 shows one example of rising temperature ΔT of the probe in measurement, with voltage adjusted to the rising temperature ΔT within 1 degree Celsius. If rising temperature ΔT is allowed to be larger than 1 degree Celsius, this will form a big temperature gradient inside frozen soil, along which it is likely that moisture diffusion will occur and heat besides conductivity will move. Also, if rising temperature ΔT is made too small, it can stop the heat from flowing in the sample, so it was kept within 1 degree Celsius to prevent that.

In thermal probe method, we measured the temperature of the probe with thermocouple when a constant amount of heat was added continuously in DC power and inside the probe in a heater line, letting the current flow by controlling the computer and automatically measuring the temperature change in the probe. At this time, temperature change in the probe according to time elapse can be expressed with the function of thermal conductivity.

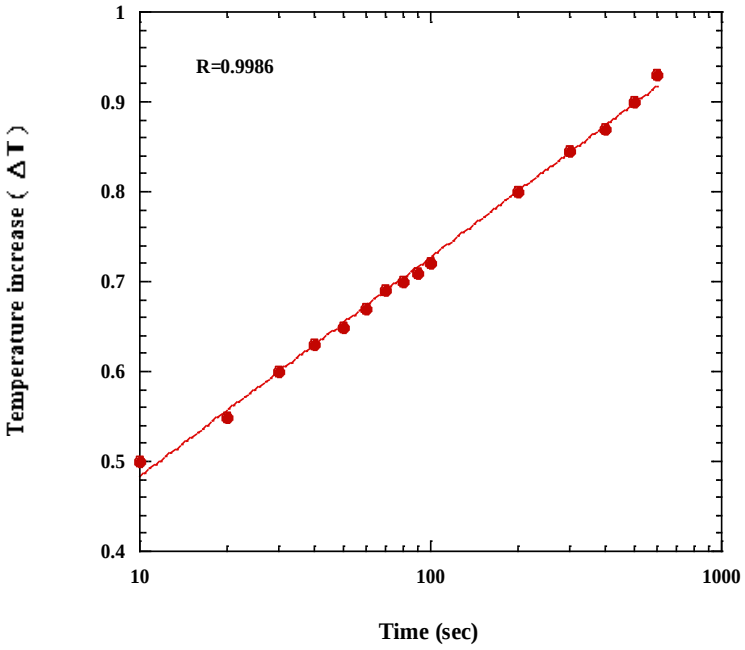

Fig. 5.7 Temperature curve of the probe test

Eq. (5.8) shows the relation that has found thermal conductivity using the above principle of measurement.

$$\lambda = \frac{Q}{4\pi} \times \frac{\ln t_2 - \ln t_1}{\Delta T} \qquad (5.8)$$

Where, λ is thermal conductivity (W/m.K), Q, heat flux per unit length of probe)(W/m), t_1 and t_2, hour, and ΔT, rising temperature (degree Celsius) of the probe from t_1 to t_2. For Incline of rising temperature $\Delta T/(\ln t_2 - \ln t_1)$, we used the slant of the straight line obtained from method of least square, using the data collected between 6 seconds and 600 seconds after the beginning of measurement.

Before measuring thermal conductivity, certain ratios of discarded tire powder (0, 10, 20, and 30%: weight ratio) were mixed with dried sample uniformly in a container. The tested sample (water content: 70% basis) was saturated using the 24-hour vacuum pump and then was filled up to the level of 10cm in a cylindrical plastic container 12cm in external diameter and 15cm in height. After the probe was vertically inserted in the center of upper-part sample,

rubber cap was used to prevent the drying of sample and temperature effect on the upper part. During the experiment, temperature in the sample was adjusted using low-temperature constant bath and, to minimize the moisture transfer in cooling, the sample was rapidly cooled off to -20 degree Celsius and then thermal conductivity was measured according to temperature change by raising the temperature stage by stage to final 10 degree Celsius. For one temperature, we measured three times for every two-hour and then, when changing the set temperature, thermal conductivity was not measured until the changed temperature was neglected for 24 hours.

5.3.3 Measuring unfrozen water content

Unfrozen water content, that is, water not frozen in the frozen soil, was measured using pulsed nuclear magnetic resonance. In measuring Pulsed NMR, after we applying magnetic field to the sample of frozen soil for a certain time, we used the fact that ice existing as a solid and unfrozen water as a liquid have different relaxation process for proton in hydrogen atoms. That is, FID (Free Indication Decay) detected after 40μs, when decrease of proton for ice has ended, is caused by liquid proton, and since the intensity of FID is proportionate to the number of protons. It is possible to find unfrozen water content quantitatively by measuring this signal.

The sample was put in a 25mm sample tube so that saturated soil might be a certain dry density and it was rapidly made to freeze using the low-temperature constant bath which kept at -20℃ in advance so that ice might be formed uniformly without water moving in the sample. After confirming the temperature in the sample reached a certain temperature and letting it rest overnight, we measured FID signal. By measuring the vibration magnetic field with 90° slanting from the axis parallel to magnetic field (90°pulsed) every 0.2 second, we recorded the maximum value of FID signal for 40μs. At each set temperature, measurement was taken 5 times with application of the mean values. After finishing measurement, it was carried out with a changed temperature for low-temperature thermostat with its repetition until 5 degree Celsius.

5.4 Experimental results and considerations

5.4.1 Unfrozen water content

Unfrozen water content is generally expressed as the volume ratio of unfrozen water that exists in the unit sample volume. Fig. 5.8 shows the result of change in unfrozen water content according to temperature change of discarded-tire-powder mixed soil measured by Pulsed NMR equipment.

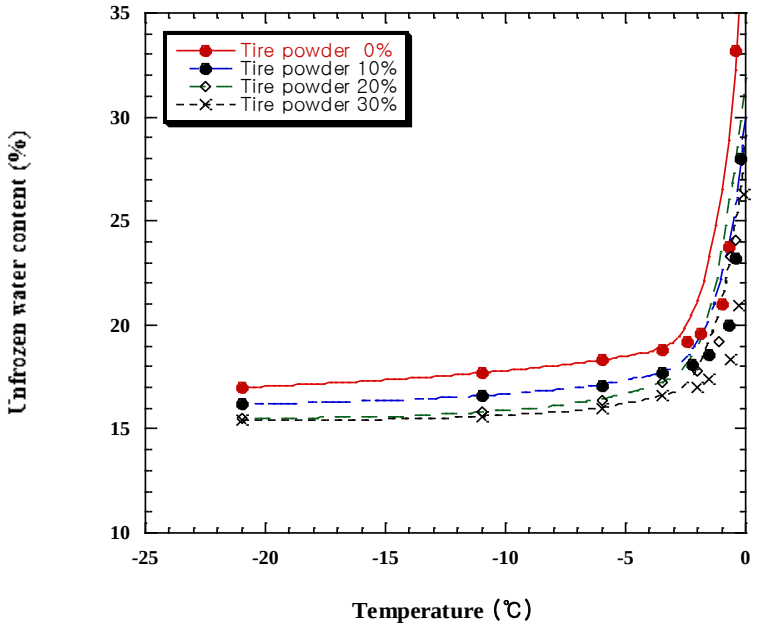

Fig. 5.8 Temperature change of unfrozen water content in frozen soil

Table 5.2 Coefficient a and b, correlation efficient r for unfrozen water content (θu) of each sample

Mixing ratio (%)	a	b	r
0	23.408	-0.136	0.844
10	20.825	-0.107	0.923
20	20.620	-0.115	0.949
30	18.966	-0.092	0.932

Unfrozen water content rapidly decreases between 0~-5 degree Celsius with lowering temperature, but decreases slowly under -10 degree Celsius. As the research by KICT[16] found out the relations between temperature and unfrozen water content, this study, also, was able to express the relations into the Eq. (5.9), an exponent function of temperature, from the result of Fig. 5.8. Coefficients a and b or each sample and correlation coefficient r, obtained

by method of least square from measured values were put into Table 2, and each curve in Fig. 5.8 shows the unfrozen water content calculated using the fixed numbers of experimental value. Also, as shown in Table 5.2, when the relations between temperature and unfrozen water content in the area below 0 degree Celsius on the four kinds of mixed soil, correlation coefficient r for each turned out to be 0.844~0.949.

$$\theta_u = a \cdot |T|^b \tag{5.9}$$

Where, θu is unfrozen water content (%), $|T|$, absolute value for soil temperature, a and b are fixed numbers. Unfrozen water can largely be divided into super-cooling water that is free water, confining water caused by the function of soil particles and water with its freezing point fallen by dissolved matters. Generally, the chief reason for unfrozen water is considered due to the effect of absorbed water that forms a hydration layer by combination with the surface of soil particles[17], and it is considered that a lowering sample temperature decreases chemical potential of confining water and weakens confining stress of soil particles, and consequently it turns into ice beginning with pore water distanced away from soil particles. Noting this fact, Dillon[18] and Anderson[19] clarified the relations in the difference of unfrozen water content according to kinds of soil by inducing specific surface area of soil, which is generally known to be deeply related to particle size distribution curve.

Besides, Fig. 5.8 shows that, with an increase of discarded-tire-powder mixing ratio, unfrozen water content tends to decrease, and this result is considered chiefly due to the decrease of unfrozen water content in the unit volume of mixed soil. That is, it is considered that unfrozen water content by unit volume of mixed soil has decreased in proportion to discarded-tire-powder mixing ratio because discarded tire powder cannot form absorbed water on the surface of powder particles and simply lets them drain by its typical characteristics.

5.4.2 Relations among mixing ratio, temperature change and thermal conductivity

Fig. 5.9 (a) ~ (c) shows the variation of thermal conductivity (λ) when, with the variable of

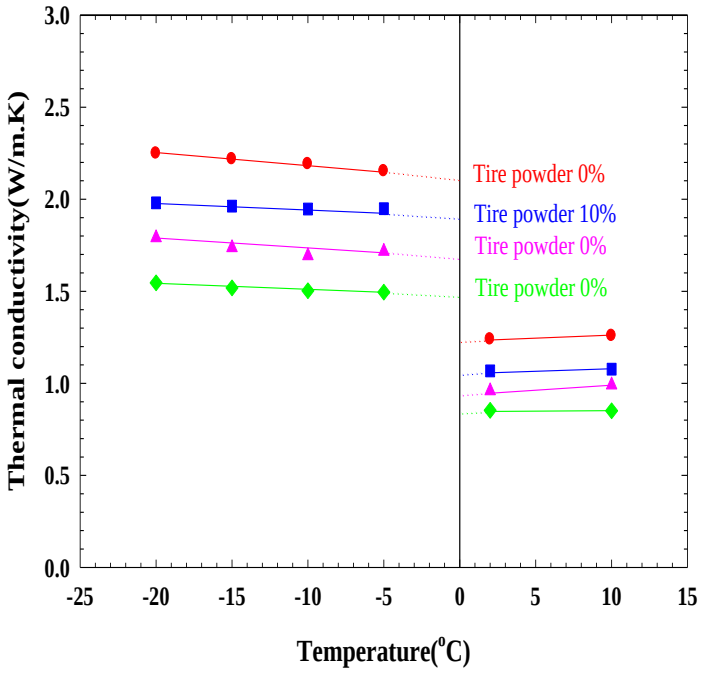

(a) S type

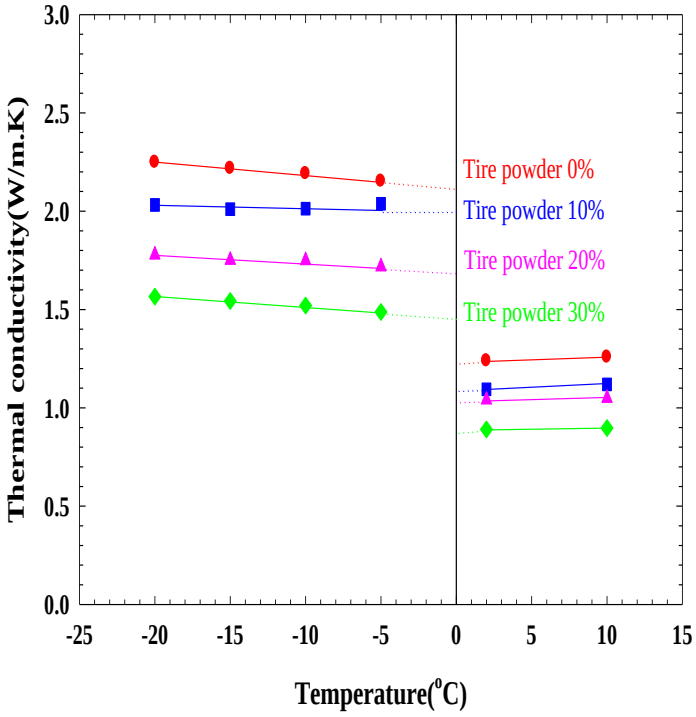

(b) M type

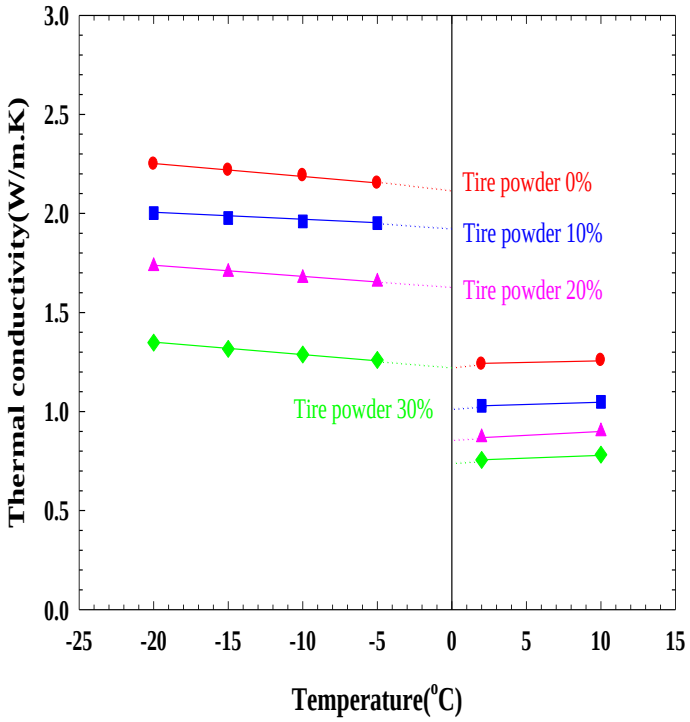

(c) L type

Fig. 5.9 Relations between temperature change and thermal conductivity

mixing ratio of discarded tire powder, sample temperature is changed into -20 ~ +10 degree Celsius. Where, mixing ratio of discarded-tire powder was put into the weight ratio of discarded tire powder included in the weight of mixed soil sample (discarded tire powder (g)/weight of the total mixed soil (g)). Hereunder in this thesis, mixing ratio of discarded-tire powder was simply expressed into mixing ratio.

In Fig. 5.9 (a) ~ (c), thermal conductivity shows a little increase or almost the constant value with an increase of sample temperature in the unfrozen area above 0 degree Celsius. It also shows, however, that below 0 degree Celsius, as the moisture in the sample freezes, thermal conductivity has increased drastically and that in case of lowering temperature further, the value of thermal conductivity increases gradually. A large change in thermal conductivity by freezing around 0 degree Celsius indicates the result of phase change from water with a thermal conductivity of 0.6w/m.K into ice with 2.3w/m.K. Besides, a gradual

increase in thermal conductivity with the lowering temperature of sample in a freeze reflects the effect of gradual phase change from unfrozen water into ice, as shown in Fig. 5.8. That is, difference in the change span of thermal conductivity according to temperature change is the result of the difference in the ratio of moisture changing into ice in the sample. Besides, regardless of mixing ratio, as the sample temperature lowers from -5 to -20 degree Celsius, increase span ($\Delta\lambda$) in thermal conductivity for all samples turned out to be 0.04~0.08W/m.K. Also, as mixing ratio increases from 0% to 30%, for instance of -20 degree Celsius, thermal conductivity decreased about 38.3% from 2.25w/m.K to 1.39w/m.K (based on L powder). Such results are considered chiefly due to the effect of discarded tire powder with thermal conductivity of around 0.2W/m.K lower than that of soil, and the decrease in unfrozen water content in the entire sample according the mixture of powder.

Both for the frozen and unfrozen states, it shows that as powder increases, thermal conductivity decreases. That is, as the mixing ratio increases 1% at -20 degree Celsius, thermal conductivity decreases 0.029w/m.K, while at +10 degree Celsius, it was around

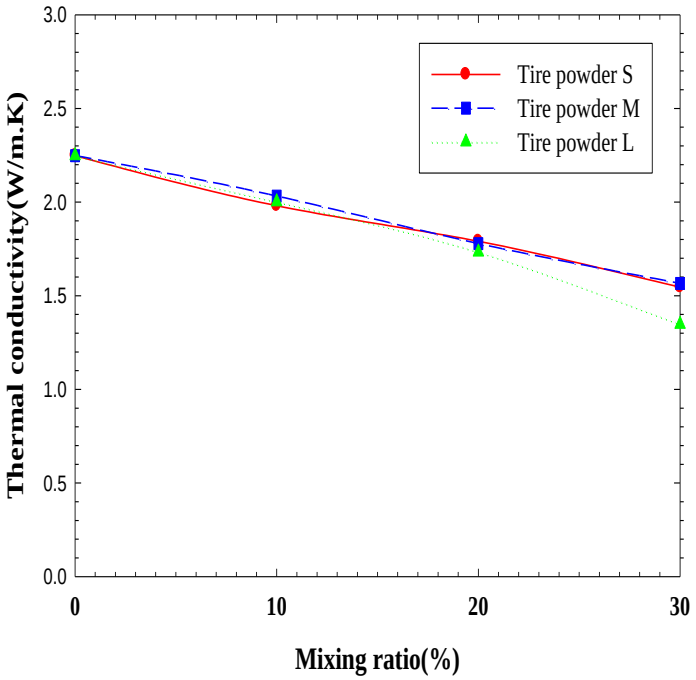

Fig. 5.10 Relations between discarded-tire size and thermal conductivity

0.016w/m.K on the average, about half of the thermal conductivity at -20 degree Celsius.

Generally, frost protection of using tire scraps for the ground consists in inhibiting frost advance with insulation effect. In case of using discarded tire powder, however, as shown in this study, it is predictable from the result of Fig. 5. 9 (c) that there is no significant insulation effect in the mixture of around 30%.

Fig. 5.10 shows the relations between mixing ratio and thermal conductivity at -20 degree Celsius along with the change of thermal conductivity according to the powder size of S, M, and L. Though up to a mixing ratio of 20%, it reveals almost the same thermal conductivity regardless of powder size, thereafter as mixing ratio gradually increases, thermal conductivity tends to decrease. Especially, at a mixing ratio of 30%, L powder decreased 0.21W/m.K in thermal conductivity relatively more than S or M powder. Such a result is considered due, for S and M powder mixed soil, to heat transfer made by the mutual connection of each ice as pore water existing between soil particles or powders is changed into ice in phase, but for L powder (30%) mixed soil, to unsmooth heat transfer resulting from the ice in the pore being separated by powder.

5.5 Proposal of thermal conductivity model for mixed soil

As the result from the previous chapter, thermal conductivity according to increase of mixing ratio and temperature change shows a constant tendency and unfrozen water content in frozen soil can be expressed with a function of temperature. From these, it is considered possible to construct a thermal conductivity model from three phases of soil particles that compose frozen soil, ice and unfrozen water.

As for thermal conductivity model for soil, diverse ones have been proposed until now, but this study developed the serial-parallel model with two phases of soil particles and water for the area of unfrozen soil proposed by Woodside[11] to propose a three-phase model of soil particles, ice and unfrozen water that can handle frozen soil in an effort to review a thermal conductivity model successively available from unfrozen to frozen soil.

Fig. 5.11 shows the thermal conductivity model proposed in this study. Based on the model in Fig. 5.3, for unfrozen soil, soil particle part was separated into soil and powder (Fig. 5 11 (a)), and for frozen, while soil and powder have no structural change, water being separated into ice and unfrozen water in a certain ratio according to temperature was expressed in Fig. 5 11 (b). Also, heat flow in the mixed soil was directed up to down as shown with an arrow in

the diagram, with a supposition that heat flow is delivered through mixed soil and water, and in mixed soil, soil particles and powder exist in parallelism. Here, moisture in mixed soil was treated with transformation into ice in serial order up to down as the direction of heat flow. By applying the same method as the induction of Eqs. (5.1) and (5.3), unfrozen soil thermal conductivity λ_{mu}, and frozen soil thermal conductivity λ_{mf} for mixed soil were

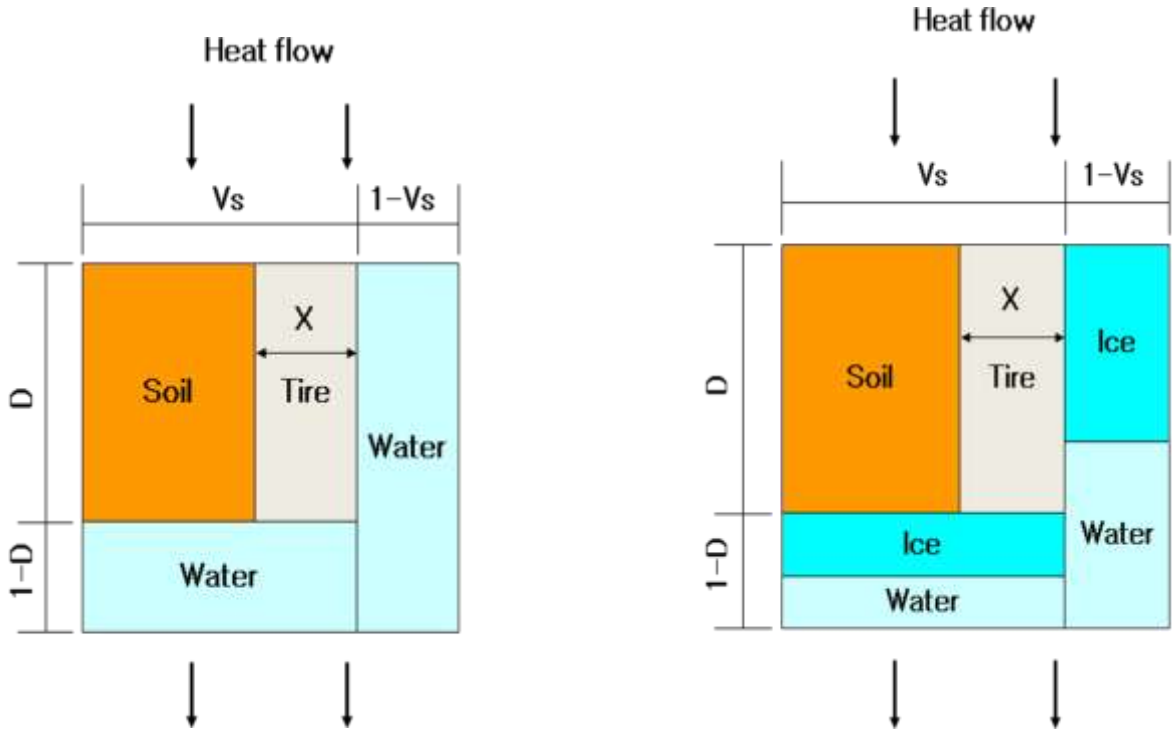

(a) unfrozen condition (b) frozen condition

Fig. 5.11 Proposed thermal conductivity of mixed soil

induced from conditions of proposed model of Fig. 5.11.

$$\lambda_{mu} = \frac{a}{\frac{D}{\lambda_t(\frac{\gamma_s}{\gamma_t})^{\frac{2}{3}}X + \lambda_s(1-(\frac{\gamma_s}{\gamma_t})^{\frac{2}{3}}X} + \frac{1-D}{\lambda_w}} + c\lambda_w \tag{5.10}$$

$$\lambda_{mf} = \frac{a}{\frac{D}{\lambda_t(\frac{\gamma_s}{\gamma_t})^{\frac{2}{3}}X + \lambda_s(1-(\frac{\gamma_s}{\gamma_t})^{\frac{2}{3}}X} + (\frac{1-D}{\lambda_w}\times\frac{\frac{d\theta_u}{dT}}{\theta_0} + \frac{1-D}{\lambda_i}(\frac{\theta_0 - \frac{d\theta_u}{dT}}{\theta_0}))} + \frac{c}{\frac{1}{\lambda_w}\times\frac{\frac{d\theta_u}{dT}}{\theta_0} + \frac{1}{\lambda_i}\times\frac{\theta_0 - \frac{d\theta_u}{dT}}{\theta_0}} \tag{5.11}$$

Where, λ is thermal conductivity, $\theta_{0,}$ volumetric water content of unfrozen soil, $d\theta_{0}/dT$, unfrozen water content at -T degree Celsius, Υ density, X powder mixing ratio, lower suffix m, s, t, w, and i, mixed soil, soil, tire powder, water, and ice, and u and f, unfrozen and frozen soil. Also, a, c and D are the experimental constants decided from the basic conditions (density, water content and volume) of each sample after finishing the experiment.

Eq. (5.11), if satisfying the relation $d\theta_{0}/dT=\theta_{0,}$ volumetric water content for unfrozen, becomes Eq. (5.10), and by substituting $d\theta_{0}/dT=\theta_{0,}$ mixing ratio (X)=0, becomes the same as equation (5.7). Besides, since Eq. (5.10) and (5.11) were for mixed soil (soil + discarded tire powder), the item of$(\Upsilon s/\ \Upsilon t)^{2/3}$ was added compared to Eq. (5.7). This is the reflection of the difference between soil and discarded tire in density on the model of Fig. 5.10 and 2/3 was applied here to convert volume into cross section since thermal conductivity is based on the heat amount that passes through a unit area in a unit time while density of each sample is based on unit volume.

Also, in Eq. (5.11), $d\theta_{0}/dT$ is the expression of unfrozen water content at -T degree Celsius. It is also considered possible to use the related data from Diagram 8 or use by directly substituting Eq. (5.9) for Eq. (5.11).

To apply the model proposed in this study, it is needed to decide, among the variables, the volume ratio n from mixed soil, and further we leave the state of partial saturation, that is, a matter of four-phase thermal conductivity model including air, for a future assignment to address.

5.6 Summary

In this study, to appraise the thermal conductivity of soil mixed with tire powder, we carried out unfrozen water experiment using Pulsed NMR and thermal conductivity experiment using thermal probe method. Conclusions from the results of this study are as follows:

1. Unfrozen water content in frozen soil was measured using Pulsed NMR equipment. As the result, relations between temperature and unfrozen water content were expressed into exponent of temperature for the area below 0 degree Celsius.

2. As powder mixing ratio increases thermal conductivity decreased, with 1% increase of mixing ratio based on -20 degree Celsius thermal conductivity decreased 0.029W/m.K, and at +10 degree Celsius, it was about 0.016W/m.K mean, around half of thermal conductivity at -20 degree Celsius. Also, at the same mixing ratio, very similar thermal conductivity was measured regardless of the particle size.

3. By developing the two-phase model of thermal conductivity for unfrozen soil, soil particles and water, proposed by Woodside, we proposed three-phase model consisting of soil particle, ice and unfrozen water, which can be applied also to frozen soil area, as well as a concrete method of calculation for three-phase model.

References

1) Suh, S. Y.: An experimental study on the dynamic characteristics of frozen soil, Journal of The Korean Geotechnical Society, Vol.19, No.1, pp. 229-236 (2003)
2) Kersten, M. S: Thermal properties of soils, University of Minesota, Institute of Technology, Engineering Experiment Station, Bulletin, No. 28 (1949)
3) Johansen, O. T.: Thermal conductivity of soil, Cold Regions Research and Engineering Laboratory, pp. 177-223 (1977)
4) Bi, C., Suzuki, T., Swada, S. and Yamasita, S.: Measurement of the thermal conductivity of crusher-run layer, Hokkaido branch, Japanese Geotechnical Society, Technical Report Vol. 44, pp. 15-20 (2004)
5) Kim, Y. J., Shin J. W. and Shon S.M.: An experimental study on the king Seajong station and Siberian frost soil, Journal of Korean Geo-Environmental Society , Vol.10, No.2, pp. 5-12 (2009)
6) Kim, H. S.: A study on the measurement of thermal conductivity of frozen soil by the thermal probe method, Journal of the Research Institute of Industrial Technology, Vol.13, pp. 62-73 (2001)
7) Tokumoto, I.: Coupled water and heat transport in an aggregated andisol at a soil-freezing field, Doctoral thesis, Iwate University, pp. 68-83 (2006)
8) Takahashi, K. and Suzuki, H.: Development of specific heat and thermal conductivity for ground material, 43th Proceedings of the Japanese Geotechnical Engineering, pp. 547-548 (2007)
9) Jaff, M., Robert. S., John, S. and John, M.: Characterizing the two-dimensional thermal conductivity distribution in sand and gravel aquifer, Soil Science Society of America Journal 70, pp. 1281-1294 (2006)
10) De Vries, D. A.: Thermal properties of soils, Physics of environment, North Holland Pub. Co. Amsterdam, pp. 210-235 (1963)
11) Wooside, W. and Messmer, J.H.: Thermal conductivity of porous media 1. Unconsolida tion sand, Journal of Apply Physics, 32, pp.1688-1699 (1961)
12) Farouki, O. T.: Evaluation of methods for calculating soil thermal conductivity, US Army Crops of Engineers, CRREL Report 82-8 (1982)

13) Fukuda, M.: Measurements of thermal conductivity of frozen soils, Low Temperature Science, series A, Physical Sciences, 34, pp.249-252 (1976)
14) Willie, M.R. and Southwick, P.F.: J Petrol. Technology, 6, 44 (1954)
15) Kimura, M. : Thermal conductivity of a filling layer, Chemical Engineering, 21, pp.472-480 (1957)
16) Kim, Y. J. and Hong, S. S.: A study on the frost penetration depth and insulation methods in pavement, Korea Institute Construction Technology Report, pp. 50-53 (2003)
17) Kinosita, S.: Physics of frost heave, Singita Press, pp. 83-88 (1982)
18) Dillon, D. M. and Anderson, O. B.: Prediction unfrozen water contents in frozen soils, Canadian Geotechnical Journal, 3(2), pp. 53-60 (1966)
19) Anderson, D. M.: Prediction unfrozen water contents in frozen soils from surface area measurements, Highway Research Record, 393, pp. 12-16 (1972)

Chapter 6 Dynamics Characteristics of Frozen Soil with Discarded Tire Powder

6.1 Introduction

Currently, despite the discarded tires are specified as industrial waste, there are many cases of fly-tipping of them without appropriate process or recycling, which becomes one factor of environmental aggravation. As part of solution of this environmental issue and recycling of waste matter being of utility value, various technology development and research have been being conducted to increase the recycling rate of the tire powder. For one of associated research, a study is being conducted using discarded tires as materials for the ground[1,2,3,4)].

Kim et al. proved the effect of the tire powder for a frost heave resistant material through field and laboratory experiments[3,5)]. Other than properties of frost heave of freezing soil mixed with used tires powder, the grasp of dynamic properties is also an important problem. While various studies related with mixed soil of used tire powder have been in progress in normal temperature[6,7)], studies on freezing soil mixed with used tire powder at below 0℃ are very insignificant.

Generally, frozen soil is comprised of four phases: soil particle, ice, unfrozen water, and air. Among these, unfrozen water has a great influence on dynamic properties of frozen soil. The lower temperature causes unfrozen water to be transformed into ices and the strength of frozen soil increases. In other words, parts of pore water remain as unfrozen water even in the temperature below 0℃, which decreases ice content of sample and consequently it has an influence on the strength of frozen soil. As a method to examine the strength of this frozen soil, unconfined compressive test has mainly been used up to now. However, since the difference of strength in frozen soil is big in accordance with the change of temperature and in general, the failure phenomenon is significantly influenced by partial non-uniformity at inside of frozen soil, there are many difficult cases to grasp general properties of dynamic nature. To complement these defects of compressive test, studies using elastic wave which is a kind of nondestructive test have been reported since 1970's[8,9)].

This study conducted the measurement of propagation velocity of elastic wave and unconfined compressive strength of frozen soil by the change of mixing ratio of tire powder between -10℃ and 0℃ using an ultrasonic pulse method as one of nondestructive methods

which can evaluate dynamic properties of frozen soil. Moreover, it grasped unfrozen water content characteristics of frozen soil mixed with tire powder and closely examined the relationship between unfrozen water content and the velocity of elastic wave, as well as between the velocity of elastic wave and unconfined compressive strength. Additionally, dynamic elastic constant, dynamic elastic modulus, dynamic shear modulus, and Poisson's ratio of frozen soil mixed with tire powder are calculated by the velocity of elastic wave in order to use as basic data required upon the use of tire powder as a frost heave resistant material in near future.

6.2 Contents of experiment

6.2.1 Properties of soil and discarded tire powder

The specimen used for this study is sandy loam which is one of the representative soils in Korea and collected from the neighborhood of Daegu city which had lots of sand as a component and showed $36m^2/g$ for specific surface area and $2.62g/cm^3$ for the density. The tire powder was triturated by using a crusher after freezing them for 15 minutes at -120 degree Celsius with liquid nitrogen. Then the tire powder from which particles more than 2mm in diameter were removed by using sieve was used after separating metal elements from used tire powder using a strong magnet.

Table 6.1 Basic Properties of each sample

Properties	Mixing ratio of tire powder (%)			
	0	10	20	30
ρ_s (g/cm^3)	2.62	2.30	2.14	1.93
γ_d (g/cm^3)	1.82	1.75	1.49	1.39
w_{opt} (%)	18.8	17.2	16.2	15.3
WL (%)	34.7	32.5	31.2	-
I_p (%)	12.1	18. 2	22.8	-
Soil classification	SF	SF	SF	-

This study used specimen mixed with four kinds; soil 100%, soil 90% + tire powder 10%, soil 80% + tire powder 20%, soil 70% + tire powder 30% in weight ratio. For each specimen, particle size distribution curves, basic properties, and a sample for ultrasonic experiment is shown in Table 6.1, Fig. 6.1, and Photo 6.1 respectively

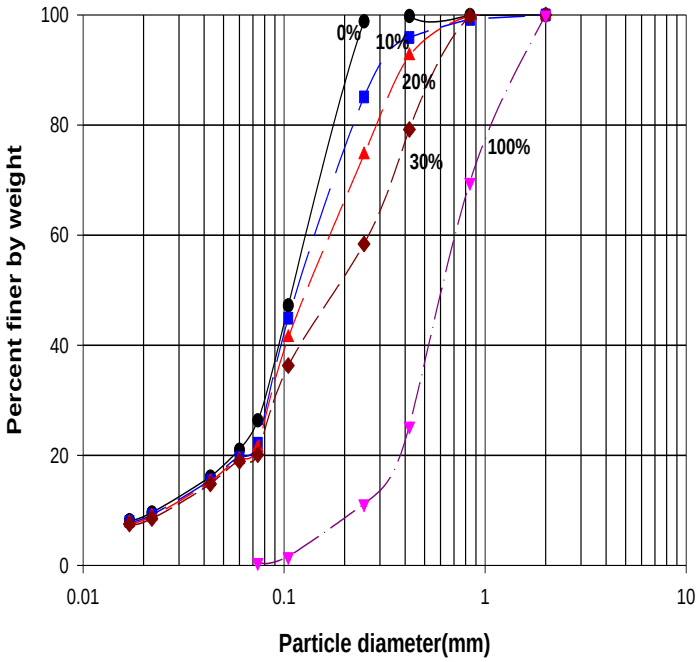

Fig. 6.1 Particle size distribution curves of specimen

Photo 6.1 Sample for ultrasonic experiment

6.2.2 Ultrasonic experimental device

An experimental device consists of transmitter, receiver, amplifier, pulse transmitter, and time counter etc (Photo 6.2). As shown in Photo 6.2, sample, transmitter, and receiver were installed in the acrylic container having kerosene and the velocity of dilatational wave and shear wave of frozen sample by the temperature variation of acrylic container with the range

of -10 degree Celsius ~ 0 degree Celsius was measured. Time counter was used to measure T, the repetitive cycle of ultrasonic pulse. This device was based on the frequency of 2MHz. Also, the temperature of frozen soil was measured to the extent of 1/50 degree Celsius using thermister and was automatically recorded in computer through GPIB.

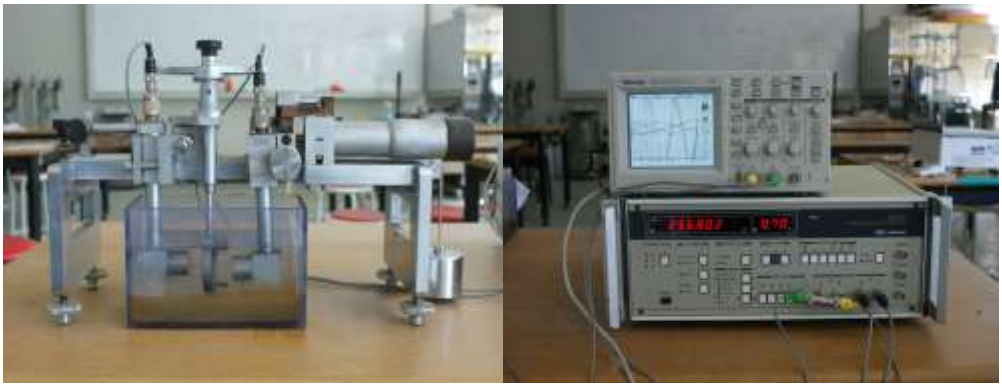

Photo 6.2 Ultrasonic experimental device

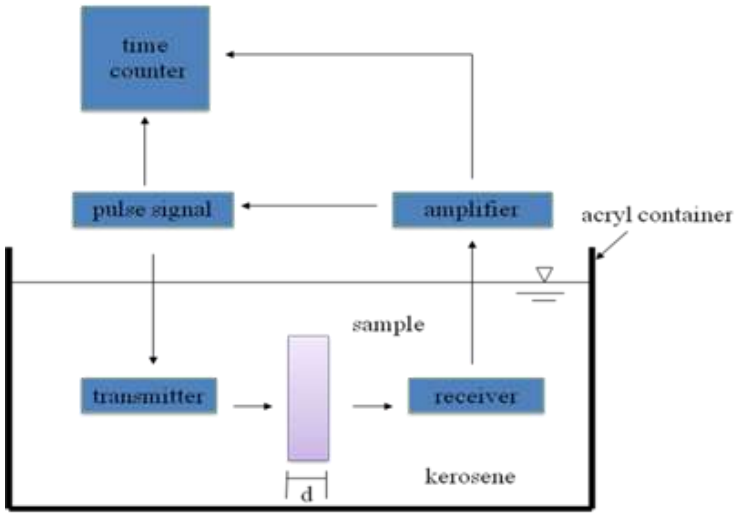

Fig. 6.2 Schematic diagram of ultrasonic experimental device

After a sample was made with a diameter of 35mm and thickness of 5mm under the condition of optimum moisture content and maximum dry density in accordance with JIS A 1210 (compaction test) for this experiment, it was frozen for 12 hours in a cold room after it was rapidly cooled into -20 degree Celsius to minimize volumetric expansion of a specimen

by freezing. First of all, a sample was fixed in ultrasonic experimental device set as -10 degree Celsius and signaling cycle (T) was measured with time counter after verifying that the temperature of the sample became -10 degree Celsius. Subsequently, after raising the temperature of kerosene up to the measuring temperature, circulation cycle (T) was measured again. With this manipulation with the range of -10 degree Celsius ~0 degree Celsius, the velocity of elastic wave of a sample was measured.

6.2.3 Unconfined compressive test device

When making a sample (diameter: 5cm, height: 10cm) for unconfined compressive test by compacting in the metal mold, the compaction condition of a sample is identical with the case of ultrasonic sample. To minimize volumetric expansion of specimen by freezing, it was frozen for 12 hours in a cold room after it was rapidly cooled with the temperature of -20 degree Celsius. Before conducting the experiment, the volume and weight of the sample were measured and it was placed for 12 hours under the condition of the established temperature; -10, -8, -6, -4, -2, -1 degree Celsius. The strain rate was based on 1mm/min and the axial stress was measured by load cell. At this time, the measured maximum stress was considered as an unconfined compressive strength.

6.3 Principle and method of measurement of elastic wave velocity

6.3.1 Measurement of dilatational wave velocity

As shown in Fig. 6.2, the cycle, T, is the time that ultrasonic pulse created from pulse transmitter returns through transmitter → sample → receiver → amplifier → pulse transmitter. The cycle, T, is defined from propagation time (t) and delayed time (te) of electric circuit system between a transmitter and a receiver as below:

$$T = t + t \tag{6.1}$$

It is required to measure elastic wave velocity of kerosene for the measurement of elastic wave velocity of specimen in the liquid. First of all, the repetitive cycle (T_1) of ultrasonic pulse is measured when the distance between a transmitter and a receiver is L_1 (Fig. 6.3). From the Eq. (6.1), T_1 can be presented as the formula below:

$$T_1 = t_1 + te_1 \tag{6.2}$$

A frozen sample with the thickness of d and the distance (L_1) between a transmitter and a receiver was perpendicularly fixed to the direction of elastic wave (the incident angle = 0°) and then T_2, ultrasonic repetitive cycle, was measured (Fig. 6.4). The measured cycle, T_2, is comprised of kerosene (L_1-d), each wave time t_2, tp and delayed time of electric circuit system (te) and can be expressed as the formula below:

$$T_2 = t_2 + tp + te \tag{6.3}$$

For the arrangement of them using the Eq. (6.2) and (6.3), it can be as follows:

$$T_1 - T_2 = (t_1 - t_2) - tp \tag{6.4}$$

Where, if t_1, t_2, tp is identified as the distance L_1, $L_{1\text{-}d}$, d corresponding to ultrasonic velocity of kerosene (V_k), dilatational wave velocity of a sample (V_p) respectively, it could be expressed as the Eq. (6.5) below and from the Eq. (6.5), dilatational wave velocity that is transferred to a sample can be calculated with the Eq. (6.6).

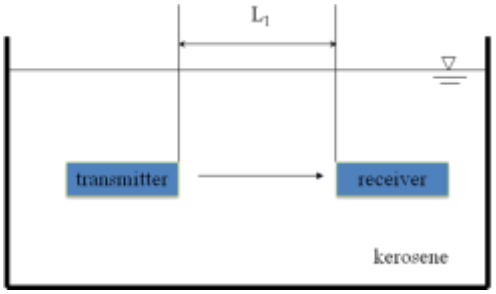

Fig. 6.3 The cycle T_1 at the distance (L_1) between a transmitter and a receiver

$$T_1 - T_2 = \left(\frac{L_1}{V_k} - \frac{L_1 - d}{V_k}\right) - \frac{d}{V_p} = \left(\frac{1}{V_k} - \frac{1}{V_p}\right) \times d \tag{6.5}$$

$$V_p = \frac{1}{\frac{1}{V_k} - \frac{T_1 - T_2}{d}} \tag{6.6}$$

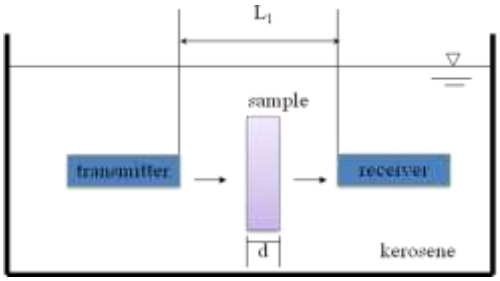

Fig. 6.4 Measurement of circulation cycle T_2 (the incident angle=0°)

6.3.2 Measurement of shear wave velocity

The shear wave velocity is measured by using the property of wave refraction. In the case that the incident angle of elastic wave from kerosene to a sample is 0°, only dilatational wave exists for elastic wave created in a sample. However, if the incident angle is more than 0°, the shear wave is created in addition to dilatational wave. Since the wave velocity in a sample is faster than in kerosene, dilatational wave and shear wave is transmitted in the refracted direction in a sample (Fig 6.5).

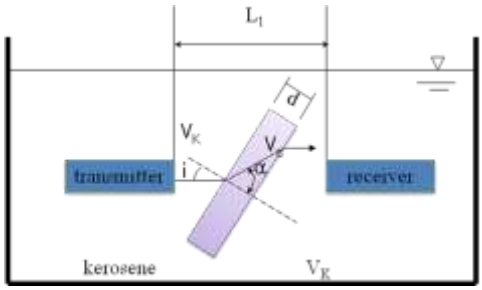

Fig. 6.5 Measurement of circulation cycle T_3 (the incident angle= i°)

As shown in Fig. 6.5, in the case that the incident angle is not perpendicular to a sample, the dilatational wave and the shear wave simultaneously created in a sample. This wave refraction can be expressed by Snell's law below:

$$\frac{\sin i}{\sin \alpha} = \frac{V_k}{V_s} \tag{6.7}$$

Where, i is the incident angle, α is rotation angle, V_k is ultrasonic velocity of kerosene, and V_s is the shear wave velocity of sample.

As for the Eq. (6.7), if the incident angle is gradually raised from 0°, it can reach 90°of the rotation angle at a certain incident angle, which causes the dilatational wave to be completely reflected without passing through a sample. This incident angle is called as the critical incident angle. In the case that the incident angle is greater than the critical angle of the dilatational wave, only the shear wave can be transmitted to a sample and the shear wave cycle, T_3, can be presented as below from the geometric relationship in Fig. 6.5.

$$T_3 = te + \frac{L_1 - \frac{d \cdot \cos(i-\alpha)}{\cos i}}{V_k} + \frac{\frac{d}{\cos i}}{V_s} \tag{6.8}$$

For the arrangement of them from the Eq. (6.8) and (6.2), the shear wave velocity (V_s) is the formula as follows:

$$V_s = \frac{1}{\frac{\cos(i-\alpha)}{V_k} - \frac{(T_1 - T_3)\cos i}{d}} \tag{6.9}$$

The velocity of the dilatational wave and the shear wave of frozen soil mixed with tire powder was obtained by measuring T_1, T_2, T_3 which are the repetitive cycle of elastic wave.

6.4 Results of experiment and considerations

6.4.1 Ultrasonic experiment

(1) Determination of critical incident angle

As stated in the previous sections, the elastic wave velocity (V_p, V_s) was measured with the dilatational wave velocity in the case that the circulation cycle T_3 is less than the critical incident angle and with the shear wave velocity in the case of being more than the critical incident angle. Fig 6.6 shows an instance of elastic wave velocity and the incident angle of sandy loam (which has 0% of the mixing ratio with tire powder) frozen at -10 degree Celsius.

Fig. 6.6 shows that the elastic wave velocity is rapidly changing from 3.91~3.60 km/sec to 1.32~1.21 km/sec at the boundary of being 20°for the incident angle (i). As a result of it, the

critical incident angle of shear wave of sandy loam can be found around 20°. In the case that

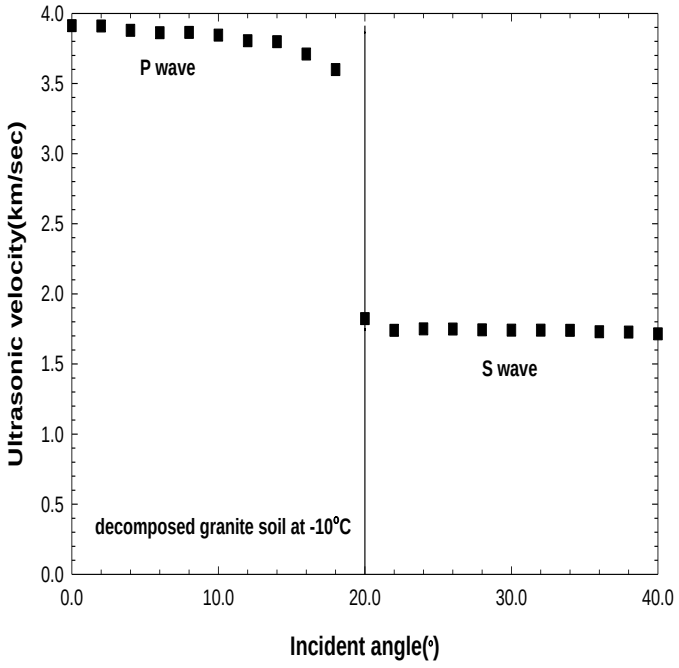

Fig. 6.6 Relationship between the elastic wave velocity and the incident angle

the incident angle is more than 20°in the Eq. (6.7), the rotation angle(α) of the dilatational wave becomes 90°, which results in no longitudinal wave in refraction wave and the existence of only the shear wave (Fig. 6.5). This study was carried out with 24°which is greater than 20° for the incident angle (i), considering the experimental variance, where 0° was used to measure the dilatational wave.

(2)Temperature and elastic wave velocity

Figs. 6.7 and 6.8 show the relationship between the temperature and the velocity of the dilatational and shear wave for four kinds of samples with the mixing ratio of tire powder as 0, 10, 20, 30%.

From the result of Fig. 6.7 and 6.8, it can be found that the velocity of the dilatational and shear wave is dramatically increased with temperature down to -2 degree Celsius and subsequently, it is gently increased to -10 degree Celsius. This behavior conforms well to the result of Christ[10], Thimus[11] and it is considered that the main reason of this result is the reduction of the amount of unfrozen water in freezing soil by the decline of temperature. In other words, it shows that it can be affected by the phase change of water with the low elastic

wave velocity into ices with the high elastic wave velocity as the temperature lowers. Since

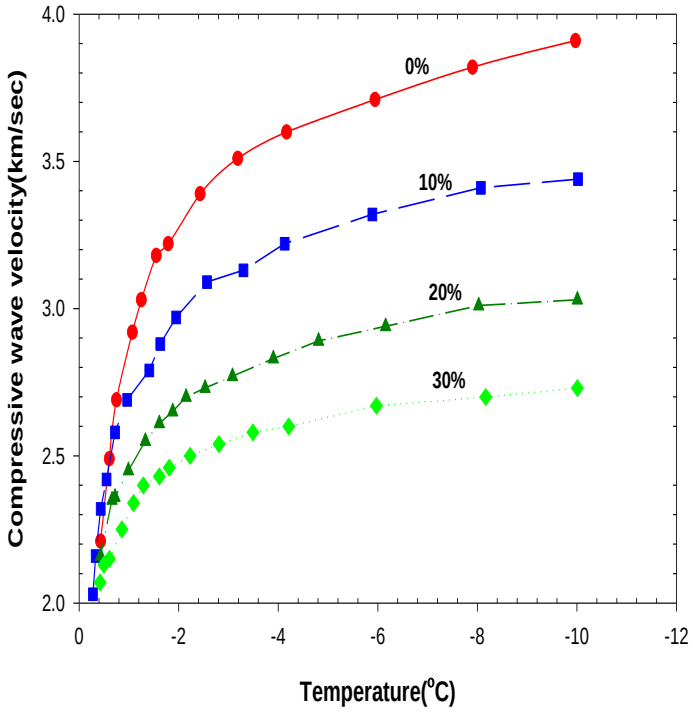

Fig. 6.7 Relationship between the dilatational wave velocity and the temperature

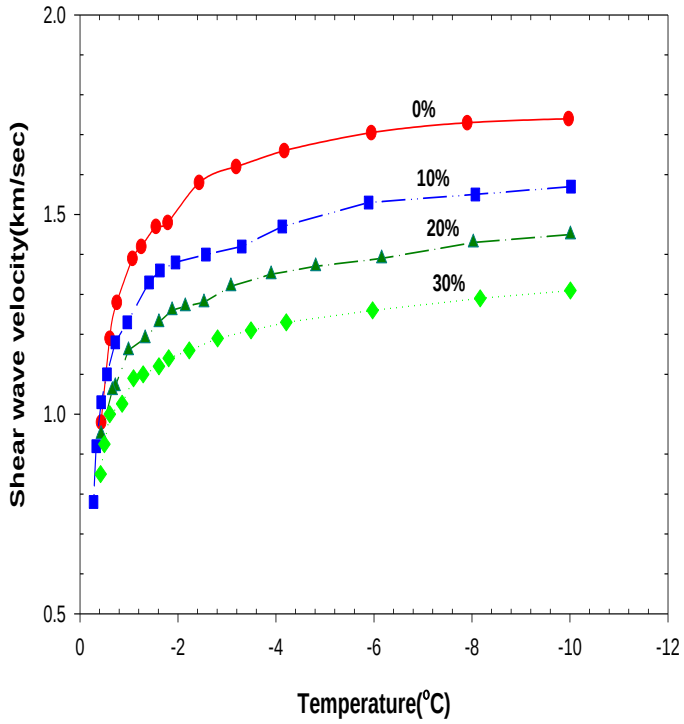

Fig. 6.8 Relationship between the shear wave velocity and the temperature

the dilatational wave depends on a solid (soil + ice) or the status of mutual contact of the part of liquid or the ratio that voids occupy[12], the less the amount of unfrozen water is and the more densely a solid (soil + ice) contact, the higher the velocity is.

Meanwhile, since the shear wave is transmitted by the mutual vibration of elastic bodies, it reflects the coupling status or structure of reciprocal particles[8]. Besides, since the shear wave is not transmitted through pore water (unfrozen water) of a sample, it is affected by the shape and location of soil particles or the change of ice content. By the decline of temperature, as the phase change is proceeding from unfrozen water into ices, the connecting route is increasing among soil particles that have shear strength and consequently, it is considered that the shear wave velocity is increased by the reduction of propagation route of the shear wave as much as it is increased[9].

In a present stage, it is difficult to assume the elastic wave velocity of frozen soil with the geometric component ratio including soil particles, ices, unfrozen water, air, etc. that comprise the frozen soil and especially, in the case of ices, the elastic wave velocity by rising temperature is almost consistent up to nearly 0 degree Celsius[13]. However, in the case of frozen soil, unfrozen water is increasing as the temperature approaches to 0 degree Celsius and consequently, it is considered to be a factor of decrease of elastic wave velocity.

(3) Relationship between the temperature and unfrozen water

The clear theoretical analysis regarding how the presence of unfrozen water affects the elastic wave velocity is not yet existed but it is considered that the measurement of elastic wave velocity is effective as a method of assuming quantitatively the amount of unfrozen water. To verify this validation, Fig. 6.9 shows the relationship between the amount of unfrozen water and temperature for the same sample using NMR.

The amount of unfrozen water was rapidly decreased as the decline of temperature between 0 degree Celsius and -2 degree Celsius but it was gently decreased at below -2 degree Celsius. When the relationship between the amount of unfrozen water and temperature shown in Fig.6. 9 is expressed with the Eq. (6.10) of exponential function, constants a, and b of that were obtained by a least square from the measured value and a correlation coefficient r at that time are shown in Table 6.2. The curves in Fig 6.9 show the amount of unfrozen water (θ_u) calculated by using these coefficients.

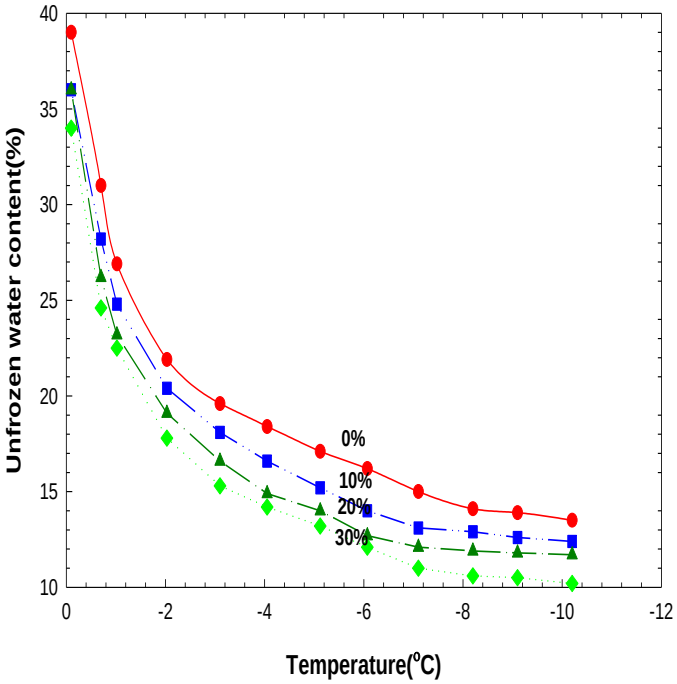

Fig. 6.9 Relationship between temperature and the amount of unfrozen water

Table 6.2 Experimental constants of amount of unfrozen water a, b and a correlation coefficient r

Mixing ratio (%)	a	b	r
0	25.15	-0.247	0.971
10	22.97	-0.254	0.970
20	21.68	-0.268	0.982
30	20.36	-0.281	0.976

$$\theta_u = a \cdot |T|^b \qquad (6.10)$$

Where, θ_u is the amount of unfrozen water (%), T is the absolute value of sample temperature (degree Celsius), a, b are experimental constants.

As shown in Table 6.2, it was found that each correlation coefficient is 0.970~0.982 in the field of freezing soil at below 0 degree Celsius for four kinds of sample used in this experiment. From these results, it can be found that the relationship between sample

temperature (T) and the amount of unfrozen water can be expressed as the Eq. (6.10).

(4) Relationship between elastic wave velocity and the amount of unfrozen water

Fig. 6.9 shows that the greater the mixing rate of tire powder is, the less amount of unfrozen water it has. Since tire powder are consisted of rubber, it is impossible to form adsorbed water on the powder surface in terms of properties of rubber. Therefore, it is considered that the amount of unfrozen water per unit volume of mixed soil decreases in proportion to the increase of mixing ratio of tire powder.

From the measurement result of the dilatational wave and the shear wave (Figs. 6.7 and 6. 8) and the amount of unfrozen water in Fig. 6.9, Figs. 6.10 and 6.11 show the relationship between elastic wave velocity and the amount of unfrozen water corresponding to the same temperature.

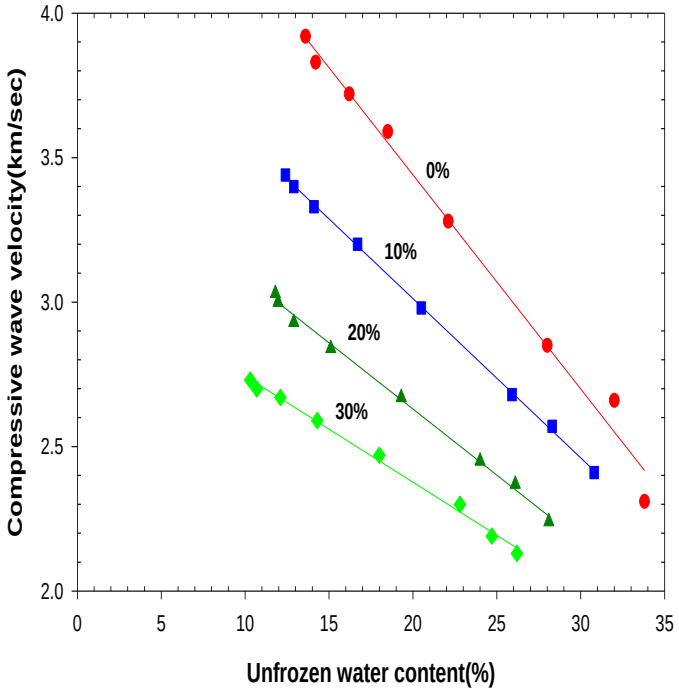

Fig. 6.10 Relationship between the dilatational wave velocity and the amount of unfrozen water

The propagation velocity of the dilatational and shear wave can be expressed with the function of unfrozen water such as the Eq. (6.11) through regression analysis of results of Figs. 6.10 and 6.11.

$$V = c \cdot \theta_u + d \tag{6.11}$$

Where, V is the velocity of the dilatational and shear wave (km/sec), θ_u is the amount of unfrozen water (%), and c, d are the experimental constants.

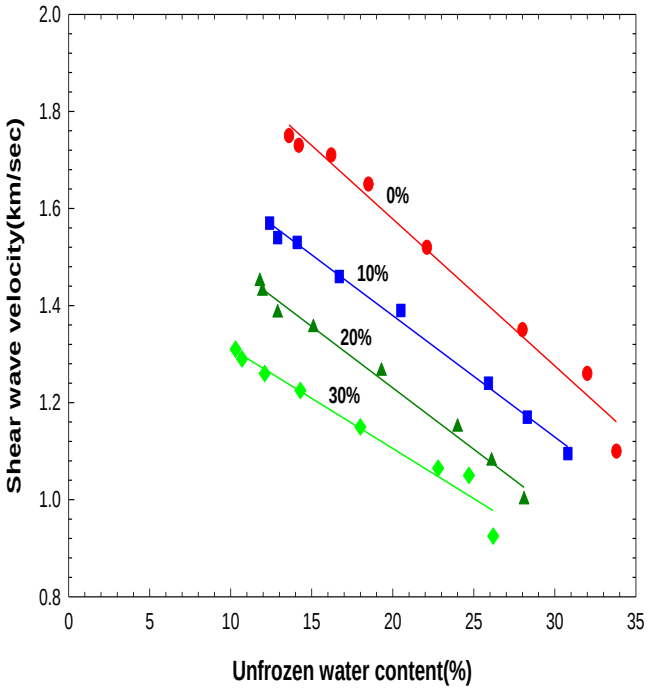

Fig. 6.11 Relationship between the shear wave velocity and the amount of unfrozen water

Each experimental constant c, d and a correlation coefficient r of the dilatational and shear wave applied to the Eq. (6.11) are shown in Table 6.3 and 6.4. As shown in Table 6.3 and 6.4, a high correlation exists between elastic wave velocity and the amount of unfrozen water. Christ[14] suggested that the dilatational wave is affected by the amount of unfrozen water and the shear wave by ice content and soil matrix but this experiment could not verify the influence of ice content and soil matrix on the shear wave. It is shown that in the case of mixed soil with used tire powder, both the dilatational and shear wave can be applied to the assumption of the amount of unfrozen water with the temperature range of 0°C~-10°C in Table 6.3 and 6.4 For instance, it can be found that as the amount of unfrozen water increases by 1%, the dilatational wave decreases around 36.4 (30%) ~74.1(0%) m/sec and the shear

wave around 40.8 (30%) ~ 60.6 (0%) m/sec in Figs. 6.10 and 6.11.

Table 6.3 Experimental constants c, d of the dilatational wave velocity and a correlation coefficient r

Mixing ratio (%)	c	d	r
0	-0.074	4.92	0.995
10	-0.055	4.12	0.999
20	-0.046	3.55	0.998
30	-0.037	3.11	0.997

Table 6.4 Experimental constants c, d of the shear wave velocity and a correlation coefficient r

Mixing ratio (%)	c	d	r
0	-0.030	2.18	0.991
10	-0.025	1.88	0.998
20	-0.025	1.74	0.995
30	-0.021	1.52	0.981

6.4.2 Unconfined compressive test

Fig. 6.12 shows the relationship between unconfined compressive strength and temperature for the four kinds of mixed soil. It can be found that the unconfined compressive strength increased with the decline of temperature and decreased in proportional to the increase of mixing rate of used tire powder. For example, in the case of frozen soil, it was verified that there was about three times difference compared with the strength of 210.7kN/m^2 at -1 degree Celsius and 573.3kN/m^2 at -10 degree Celsius. It can be found that this difference in strength results from the increase of adfreeze strength between soil particles and ices by the phase change of unfrozen water into ices as the temperature lowers.

Besides, compared with unconfined compressive strength by the mixing rate of tire powder, as the mixing rate increases from 0% to 30% at -10 degree Celsius, the strength decreased from 573.3kN/m^2 to 333.2kN/m^2. In other words, it shows that the strength reduces by around 7.5kN/m^2 with the 1% increase of tire powder. When tire powder is compared with soil particles, the former has a deformation, low surface-activity and low adfreeze force. Therefore, it is considered that as the mixing rate of tire powder increases, the decline of physical and chemical coherence and interlocking between soil particles and tire powder is

the main factor of strength reduction

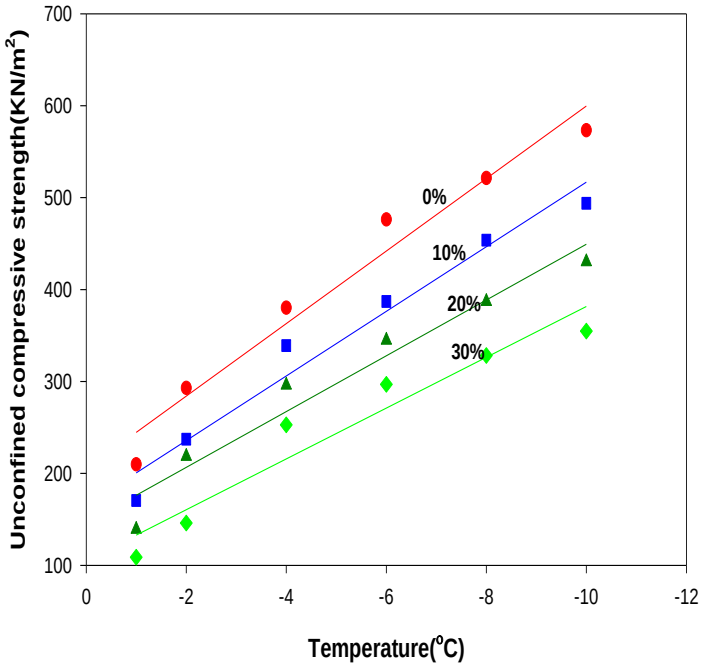

Fig. 6.12 Changes of temperature and unconfined compressive strength

From the results of the shear wave velocity in Fig. 6.8 and unconfined compressive test in Fig. 6.12, Fig. 6.13 shows the relationship between unconfined compressive strength and the shear wave velocity corresponding to the same temperature. Since the propagation of shear wave among soil matrix is affected by mutual vibration of elastic bodies, the connection status and structure of reciprocal particles so that the propagation velocity of shear wave has a close relationship with unconfined compressive strength[13]. As shown in Fig. 6.13, it shows that linear relationship exists between unconfined compressive strength (qu) and the shear wave velocity (Vs) of freezing soil. The correlation between the shear wave velocity and unconfined compressive strength for the mixed soil with used tire powder with the temperature range of -1℃ ~-10℃ can be expressed with the Eq. (6.12).

$$qu = a \cdot Vs + b \tag{6.12}$$

Where, qu is unconfined compressive strength (kN/m^2), Vs is the shear wave velocity (km/sec), and a, b are experimental constants determined by the mixing rate of used tire and

temperature

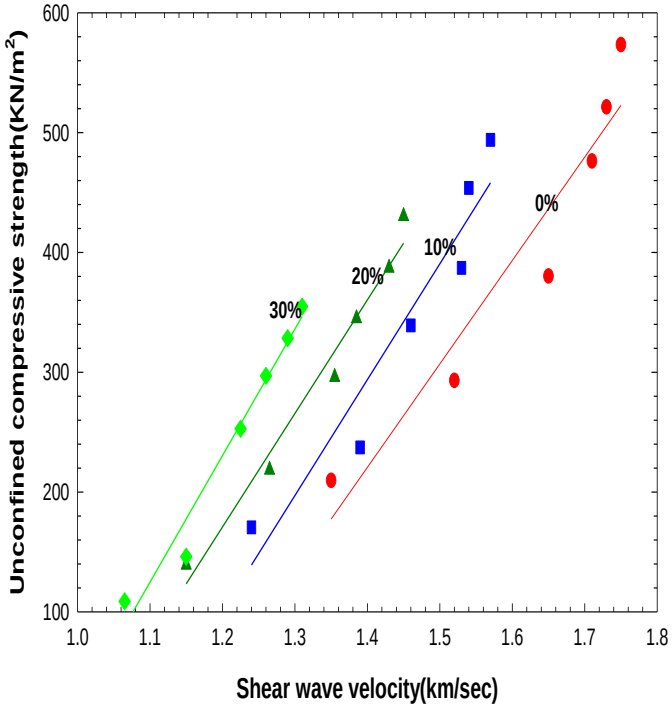

Fig. 6.13 Relationship between unconfined compressive strength (qu) and the shear wave velocity (Vs)

6.4.3 Dynamic elastic constant of frozen soil

The frozen soil used for this experiment consists of soil particles, tire powder, ices and unfrozen water but it can be assumed as a sequential uniform elastic body with a macroscopic view. When freezing soil is macroscopically viewed here, dynamic elastic modulus (E), dynamic shear modulus (G), and Poisson's ratio (μ) were obtained from the Eqs. (13) ~ (15) deducted from the propagation theory of elastic wave and the measured values of the dilatational and shear wave velocity.

$$E = \frac{\rho Vs^2(3Vp^2 - 4Vs^2)}{Vp^2 - Vs^2} \tag{6.13}$$

$$G = \rho Vs^2 \tag{6.14}$$

$$\mu = \frac{Vp^2 - Vs^2}{2(Vp^2 - Vs^2)} \tag{6.15}$$

Where, Vs is the shear wave velocity, Vp is the dilatational velocity, and ρ is the density of freezing soil.

Dynamic elastic modulus (E) and dynamic shear modulus (G) of tire powder calculated were shown in Fig. 6.14 and 6.15 by substituting the density of each specimen, the velocity of the dilatational and shear wave for the Eqs. (6.13) ~ (6.15).

It is shown that dynamic elastic modulus (E) and dynamic shear modulus (G) depend on temperature and the mixing rate of tire powder. Besides, dynamic elastic modulus (E) and dynamic shear modulus (G) rapidly increased with the decline of temperature within 0 ~ -2 degree Celsius but it shows the tendency to increase gently at below -2 degree Celsius and as the mixing rate of tire powder increased, it decreased. It is considered that the increase of dynamic elastic modulus (E) and dynamic shear modulus (G) result from the increase of coherence between soil particles and ice by the phase change of unfrozen water into ice as the freezing temperature of a specimen lowers. Meanwhile, it is considered that the deformation property of tire powder and the reduction of freeze strength are the main factor of the decrease of dynamic elastic modulus (E) and dynamic shear modulus (G) by the increase of the mixing rate of tire powder.

The behavior of dynamic shear modulus(E) and dynamic elastic modulus(G) by the decrease of freezing temperature in Figs. 6.14 and 6.15 shows the similar tendency with the result of Sheng et al.[15] using ultrasonic method, of Wilson[16] through cyclic triaxial technique, and of Kaplar[17] using resonant frequency method. For instance, Wilson[16] obtained (2.7~15.8)GPa for dynamic shear modulus(E) and (0.7~5.5)GPa for dynamic elastic modulus(G) with the temperature range of (-1.5~-10 degree Celsius). Besides, Kaplar[17] obtained (12.0~25.0)GPa for dynamic shear modulus(E) for many kinds of silt soil within the temperature range of (-1.0 ~-25.0 degree Celsius).

It is shown of Poisson's ratio (μ) in Fig. 6.16 that was calculated on four kinds of freezing soil with different mixing rate of tire powder. From the result of Fig. 6.16, even though there is error in data, the overall trend shows that the value of Poisson's ratio is consistent with the range of (0.35~0.37) except for the case of being at above -0.5 degree Celsius and the influence of mixing rate of tire powder is small.

The result of Fig. 6.16 shows the identical trend with the result of measurement for frozen silt by Christ[9] but the value obtained in this study was found to be rather greater. Meanwhile, Wang et al. [18] reported that Poisson's ratio (μ) of frozen loess is about 0.27 which is

consistent regardless of the change of temperature through ultrasonic experiment. In contrast

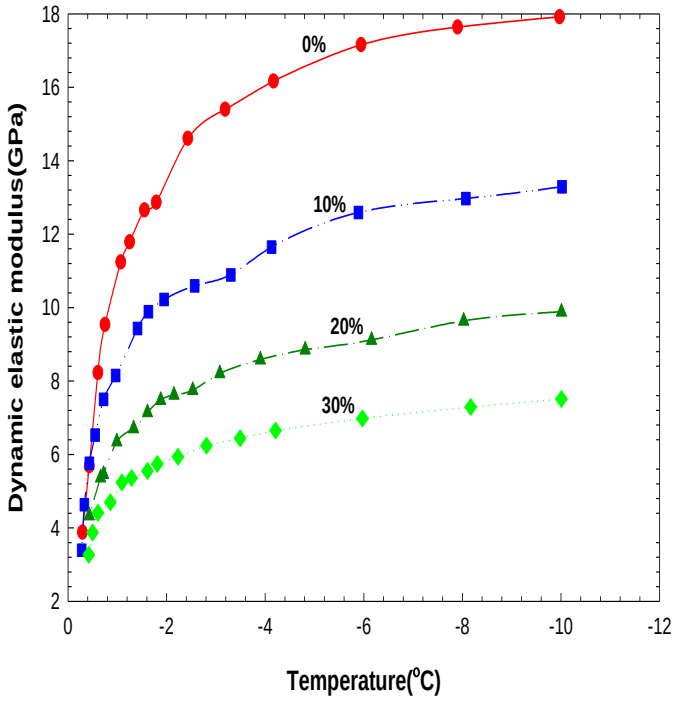

Fig. 6.14 Relationship between dynamic shear modulus and temperature

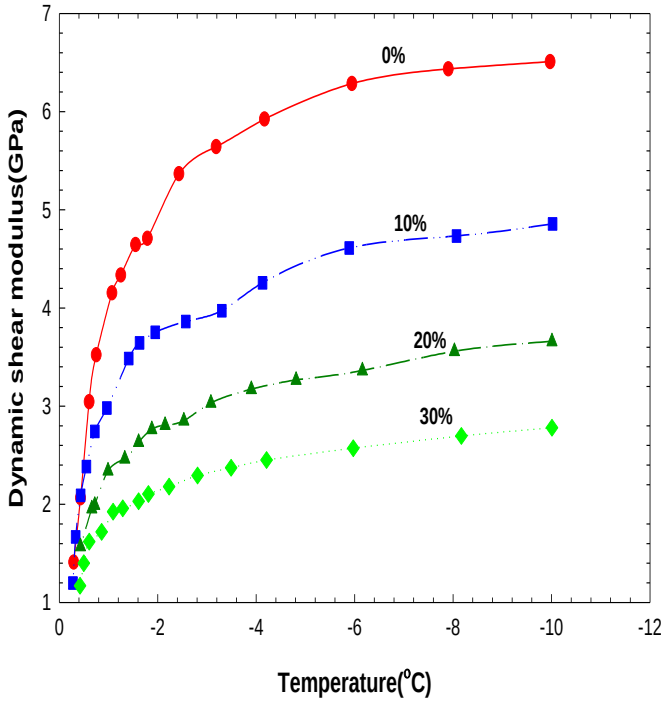

Fig. 6.15 Relationship between dynamic elastic modulus and temperature

of these results, Nakano et al. [19] reported that Poisson's ratio increased from 0.178 (-2 degree Celsius) to 0.292 (-14 degree Celsius) with the decline of freezing temperature.

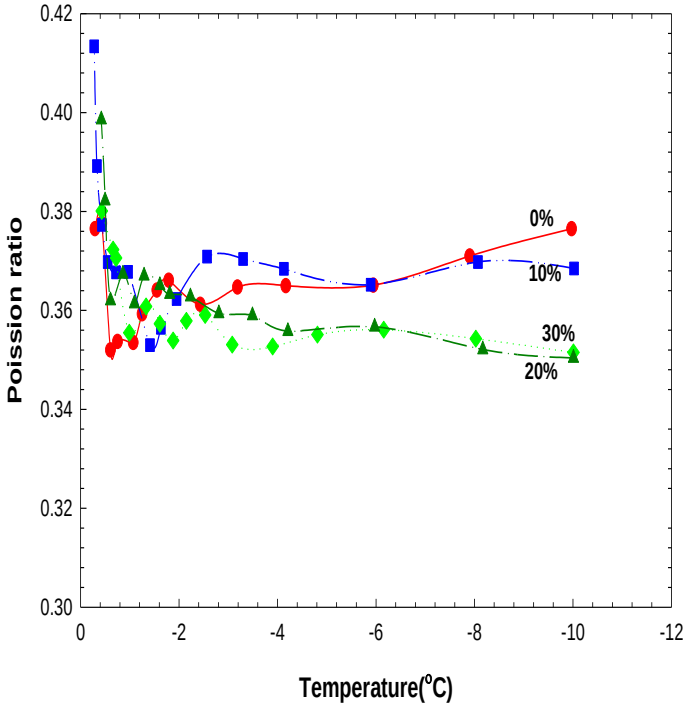

Fig. 6.16 Relationship between Poisson's ratio (μ) and temperature

As for the disparate research results of Poisson's ratio (μ), Stephenson[20] points out that Poisson's ratio (μ) is ultimately sensitive to the change of ultrasonic velocity. It is considered that the error of experiment results in Fig. 16 resulted mainly from the difficulty in regulating temperature of a sample and kerosene during the experiment, the formation of non-uniformed pore ice within a sample, and the difficulty in manufacturing homogeneous sample. Besides, as known in Fig. 6.16, as the temperature approaches closely to -0.5 degree Celsius, Poisson's ratio (μ) rapidly increased. It is considered that this phenomenon indicates that the rupture of pore ice started with the increase of unfrozen water of a sample by the rising of temperature.

6.5 Summary

This study stipulated dynamic properties of freezing soil mixed with tire powder. Using ultrasonic pulse method, elastic wave velocity was measured within the temperature range of below 0 and an elastic wave constant was calculated from the elastic wave velocity and associated properties were analyzed. Arranged from the results obtained from this study, they are as follows:

1. Elastic wave velocity of frozen soil decreased in accordance with the rising of temperature and the increase of mixing ratio of tire powder, especially, elastic wave velocity (dilatational wave, shear wave) rapidly decreased at the temperature below -2 degree Celsius. From this result, it was verified that the change of elastic wave velocity has a close relationship with variance of unfrozen water in frozen soil by the change of temperature.

2. It was confirmed that the linear relationship exists with high correlation between elastic wave velocity (dilatational wave, shear wave) and the amount of unfrozen water, and between shear wave velocity and unconfined compressive strength.

3. Unconfined compressive strength of frozen soil increased with the decline of temperature and decreased as the mixing ratio of used tire powder increased. It is considered that this increase of strength mainly resulted from the phase change of unfrozen water into ice by the decline of freezing temperature and from the increase of adfreeze strength between a specimen and ice. In addition, it is judged that the decline of strength by the increase of mixing rate resulted from the decrease of interlocking among particles and adfreeze force by the increase of mixing rate of tire powder that has a deformation property.

4. The value of dynamic shear modulus (E) and dynamic elastic modulus (G) deduced from the measured elastic wave velocity increased with the decline of temperature, and decreased with the increase of mixing ratio of tire powder. Besides, Poisson's ratio was consistent with the range of 0.35~0.37 and it was shown that there was no big influence of temperature and mixing rate of used tire. However, as it approached to -0.5 degree Celsius,

Poisson's ratio (μ) rapidly increased.

References

1) Eaton, R. A., Robert, R. J. and Humphrey, D. N.: Gravel road sections insulated with scrap tire chip, CRREL Special Report 94-21, pp.1-43 (1994)
2) Humphrey, D. N., Chen, L. H. and Eaton, R. A.: Laboratory and field measurement of the thermal conductivity of tire chips for used surged insulation, Transportation Research Board 76rh Annual Meeting, pp.1-27 (1997)
3) Kim, H.S., Suzuki, T. Fukuda, M., Seo, S.Y., and Yamashita, S.: Field experiments for reducing frost susceptibility using recycled tire powder, Journal of the Korean Geotechnical Society, Vol. 26, No. 4, pp. 5-14 (2010)
4) Satoshi M., Kazuyz Y. and Hideo K.: Deformation characteristics of cement-treated mixed sand with tire-chips, 44th proceedings of the Japanese Geotechnical Engineering, pp.533-534 (2008)
5) Kim, H.S., Seo, S.Y., Nakamura, D., Fukuda, M., Yamashita, S. and Suzuki, T.: Frost-heaving characteristics of soil mixed with discarded tire powder, Journal of the Korean Geotechnical Society, Vol. 26, No. 4, pp. 15-26 (2010)
6) Juichi, Y., Kazutoshi, O., Tadayuki, Y., Norimasa, K., Yuji, M. and Motoki, T.: Shear and liquefaction behavior of waste tire rubber chips, Journal of Japan Geotechnical Society, Vol. 4, No. 1, pp. 81-90 (2009)
7) Yoshiak K., Takeshi N. and Yoshino M.: Failure mechanism of cement treated clay with tire chips and change of its permeability under shear deformation, Journal of Japan Geotechnical Society, Vol. 1, No. 2, pp. 19-32 (2006)
8) Fukuda, M. and Inoue, M.: On the dynamic Moduli of frozen soils, Low temperature science, Series A, Physical Science, Vol. 31, pp.245-259 (1973)
9) Nakano, Y. and Arnold, R.: Acoustic properties of frozen Ottawa sand, Water Resources Research, Vol. 9, N0. 1, pp. 178-184 (1973)
10) Christ, M. and Park, J.B.: Ultrasonic technique as tool for determining physical and mechanical properties of frozen soil, Cold Regions and Technology, 58, pp.136-142 (2009)

11) Thimus, J. Fr., Aguirre-Puente, J. and Cohen-Tenoudji, Fr.: Determination of unfrozen water content of an overconsolidated clay down to -160℃ by sonic approaches-comparison with classical methods, Ground Freezing 91, pp. 83-88 (1991)
12) Gassmann, F.: Elastic waves through a packing of spheres, Geophys. Vol. 16, pp. 673-685 (1951)
13) Inoue, M. and Kinosita, S.: Mechanical properties of frozen soil, Low Temperature Science, Series A, Physical science, Vol. 33, pp.243-253 (1975)
14) Christ, M., Kim, Y.J. and Park, J. B.: The influence of temperature and cycles on acoustic and mechanical properties of Frozen soil, KSCE Journal of Civil Engineering, Vol. 13, No. 3, pp. 153-159 (2009)
15) Sheng, Y., Fukuda, M. and Imamura, T.: The effect of unfrozen water content on dynamic properties of partially frozen soil, Refrigeration Science and Technology Proceeding, pp. 112-119 (1998)
16) Wilson, C.R.: Dynamic properties of naturally frozen Fairbanks silt", Master thesis, Oregon State University (1982)
17) Kaplar, C.W.: Laboratory determination of the dynamic moduli of frozen soils and ice, Proceedings of the Permafrost International Conference, National Academy of Science, National Research Council, Publication No.1278, pp.293-301 (1963)
18) Wang, D.Y., Zhu, Y.L., Ma, W. and Niu, Y. H.: Application of ultrasonic technology for physical-mechanical properties of frozen soils, Cold Regions Science and Technology, Vol. 44, pp. 12-19 (2006)
19) Nakano, Y., Martin, R.J. and Smith, M.: Ultrasonic velocities of the dilatational and shear waves in frozen soils, Water Resources Research 8(4), pp. 1024-1030 (1972)
20) Stephenson, R.W.: Ultrasonic testing for determining dynamic soil moduli, Dynamic Geotechnical Testing, ASTM STP 654, pp. 179-195 (1978)

Chapter 7 Laboratory Frost-Heaving Characteristics of Soil Mixed with Discarded Tire Powder

7.1 Introduction

The combination of the recycling of discarded tires and action against frost heave is an unprecedented application, but sufficient verification of the effectiveness has not yet been made. Conventionally, the replacement method was employed as one measure against the frost heave of roads when frost heave is anticipated in the existing materials; the road base or bed is replaced with a frost heave resistant material. According to Ifukube[1)], the replacement depth should be 70 percent of the maximum freezing depth of a place. Accordingly, the actual consumption of sand or gravel used as the frost-heave-resistant replacement material is very high. In addition, regional development makes it more difficult to obtain high-quality materials and increases road construction costs. Against this background, attention is paid to the development of new granular materials and to the technological development of producing a frost heave resistant material by mixing local soil with an appropriate granular material.

The above means that if waste tire powder could be used as a frost heave resistant material in place of sand or gravel, two effects would be expected: the recycling of the waste resources and the development of a new frost heave suppressing material. Humphery et al.[2)] reported the feasibility of using waste tires featuring low thermal conductivity as a material suppressing the frost heave of roads through a field test in which tire chips (up to 10 cm square) were laid under the ground to a certain thickness. The test results showed that the rubber reduced the freezing depth thanks to its heat insulation effect, but a serious problem was pointed out the tire chip was easier to compress than soil, resulting in a high risk of destroying the road surface.

In this research, we mixed soil with waste tire powder that has lower compressibility comparing to tire chips to construct soils, and measured the rate of frost heave and SP value in three seasons from 1996 to 1999. Through these measurements, we confirmed the frost heave suppressing effect of the waste tire powder[3)].

In parallel with the field experiment described above, we conducted a laboratory experiment to study the relationship between the mixing ratio of waste tire powder and the

frost susceptibility. Specifically, we conducted a ramping frost heave experiment where the freezing speed kept constant to prevent the boundary conditions from varying depending on the unfrozen water content, thermal conductivity, and sample length.

7.2 Characteristics of soil and discarded tire powder samples

Samples used for the frost heave experiment were soil collected in the vicinity of Tomakomai City, Hokkaido Japan. The collected soil contained a large amount of sand with large grain size and its specific surface area was very large-54 m^2/g[4]. We utilized liquid nitrogen (LN_2) to freeze discarded tires at -120 degrees Celsius for 15 minute, and then used a crusher to pulverize them. Subsequently, we used a strong magnet to remove metals from the powder, and passed the powder through a sieve to use only powder having a grain size of 1 mm or less.

In this test, we made four kinds of samples having different soil contents (in weight): 100% soil, 95% soil + 5% powder, 70% soil + 30% powder, and 40% soil + 60% powder. Fig. 7.1 shows the particle size distribution of each sample, and Table 1 indicates the results of a physical test

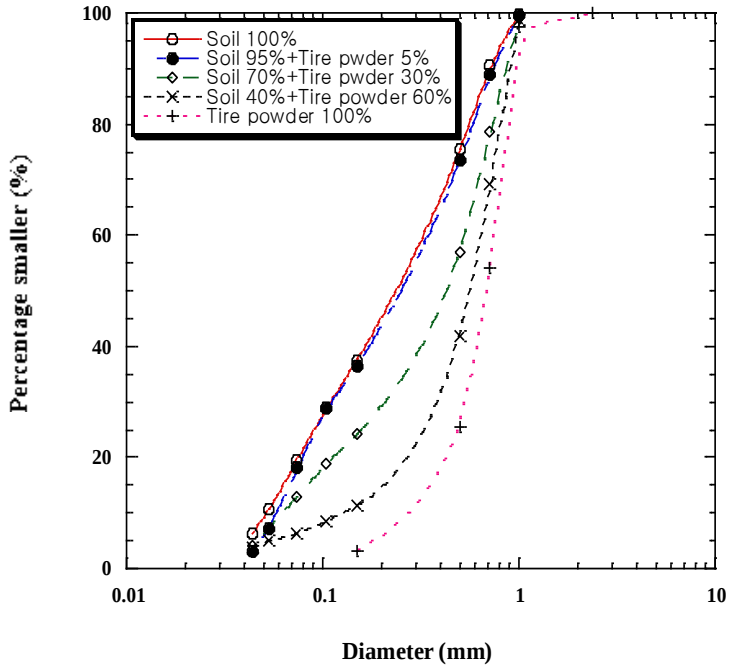

Fig. 7.1 Particle size distribution curve of each sample

Table 7.1 Basic physical properties of each sample

Soil + Tire powder	S100%	S95%+TP5%	S70%+TP30%	S40%+TP60%	TP100%
Dry density(g/cm^3)	1.16	1.15	1.11	1.02	-
Permeability(cm/sec)	4.03×10^{-6}	6.93×10^{-6}	9.45×10^{-6}	1.15×10^{-5}	-
Specific gravity	2.66	2.49	1.97	1.55	1.12

7.3 Outline of the experiment

7.3.1 Frost heave experiment

(1) Experimental apparatus

The schematic diagram of one dimensional frost heaving apparatus is given Fig. 7.2. An acrylic cylindrical cell which has 10 cm in inner diameter, 1 cm in thickness, and 15 cm in height was filled with each sample.

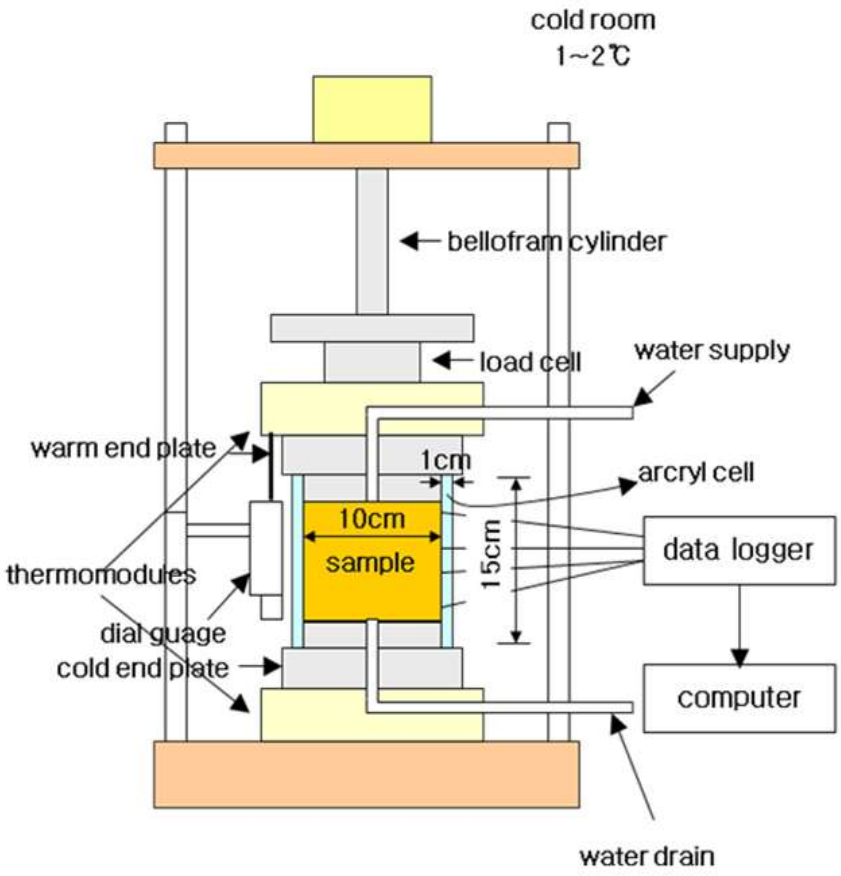

Fig. 7.2 Frost heave apparatus

The apparatus was placed in a low-temperature thermostatic chamber whose temperature was set at 4 ± 2 degrees Celsius. To control the temperatures of both ends of the sample, thermo-modules were arranged on the upper and lower ends of the cell. In addition, the the plate temperatures were measured during testing with platinum resistance temperature sensors (precision: 0.01 degrees Celsius) inserted into the upper and lower plates. Changes in the temperature of each sample were also measured with seven thermocouples (precision: 0.1 degrees Celsius) that were embedded in the cell wall and that were aligned 1 cm apart from each other. To reduce the friction between the sample and cell container during testing, Silicon oil was applied to the inner wall of the cell. Moreover, to minimize a frictional effect produced by the frozen sample adhering to the frozen cell, the soil was frozen from bottom to top, and water was supplied from the top with a burette. To create a one-dimensional heat flow in the sample during testing, the acrylic cell was wound by 5 cm thick sponge around to cut off heat flow in the radial direction.

(2) Experiment method

Each sample was frozen from the bottom by the ramped freezing method featuring a constant difference between the two end temperatures and a constant temperature gradient. After adding water to the dry sample until the water content became 70 percent, sample was kept in a vacuum pump for 24 hours for perfect saturation. The cell was filled with the sample, gradually pressurized it at from 20 kPa up to 100 kPa, and then reduced the pressure to 25 kPa for expansion. The initial state of the sample was completed when the expansion ended.

Table 7.2 Experiment conditions

Test type	Ramped freezing
Overburden pressure	25kPa
Temperature of upper plate	3℃-0.042t
Temperature of lower plate	0℃-0.042t
Temperature gradient	0.4℃/cm
Experiment duration	72hr.

During measurement, hydrostatic pressure was used to supply water from the lower plate and discharge it from the upper plate, and found the coefficient of permeability of each mixed

soil in the cell. After that, frost heave experiment was started. To prevent the supercooling of pore water in the soil, the lower plate was cooled down at less than -5 degrees Celsius for a short time to form ice cores. After confirming the formation of ice, an initial temperature was set to both ends of the sample and the experiment was started. Every hour, the amount of frost heave, the amount of heave by water, and temperatures at both ends were measured. After the experiment ended, to check changes in the water content distribution of the sample, sample was sliced into pieces 1 cm thick to measure the water content. Table 2 shows the conditions of this experiment. For example, "3-0.042t" of the notations shown in the table indicates that the initial temperature is 3 degrees Celsius and then it reduces at a rate of 0.042 degrees per hour.

7.4 Experiment results

Fig. 7.3 presents an example of variations in amount of the frost heave and the heave by water over elapsed time. Where, the latter is given by dividing the volume of water intake (cm^3) by the cross section (cm^2) of the sample. The frost heave and the heave by water are represented as a straight line, which accurately reproduces a phenomenon in which the soil shows a frost heave accompanying water intake. In addition, the figure shows that the frost heave is slightly larger than the heave by water. This difference is because when absorbed pore water changes to ice on the ice lens growing surface, the volume expands by nine percent. In this experiment, as shown in Fig. 7.4, we reduced the temperatures T_C and T_W of the upper and lower ends at a constant rate while keeping the difference between the two constant. As a result, the freezing front moved at a constant speed. Fig. 7.4 also shows that when the temperature T_W of the upper end falls below zero 72 hours after the start of the experiment, the frost heave stops growing, because pore water in the supply pipe in the upper plate is frozen, resulting in a stop of water supply. Therefore, the experiment was ended at that point.

Fig. 7.5 shows the relationship between the amount of frost heave and time when Tomakomai soil is mixed with discarded tire powder. The amount of frost heave increases linearly over time except in the initial stage of the experiment.

The higher the mixing ratio of tire powder, that is non-frost heaving characteristics, the smaller the amount of frost heave, resulting in a reduction in the rate of frost heave.

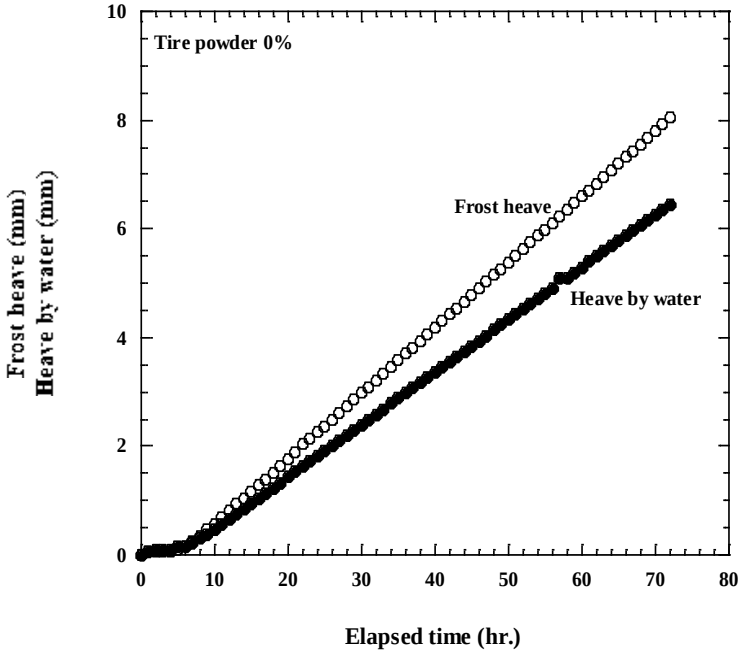

Fig. 7.3 Variations in amount of frost heave and heave by water

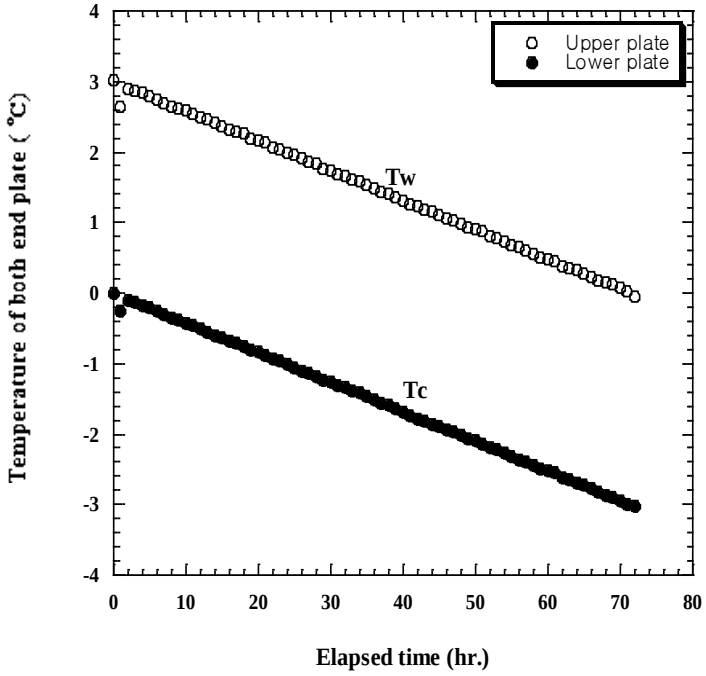

Fig. 7.4 Variations in end temperatures T_W and T_C over elapsed time

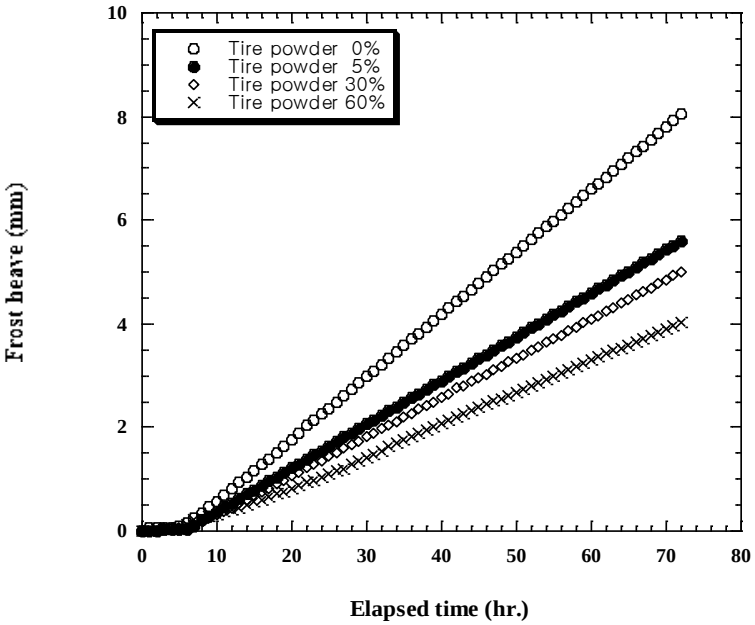

Fig. 7.5 Variations in frost heave mixed with tire powder over elapsed time

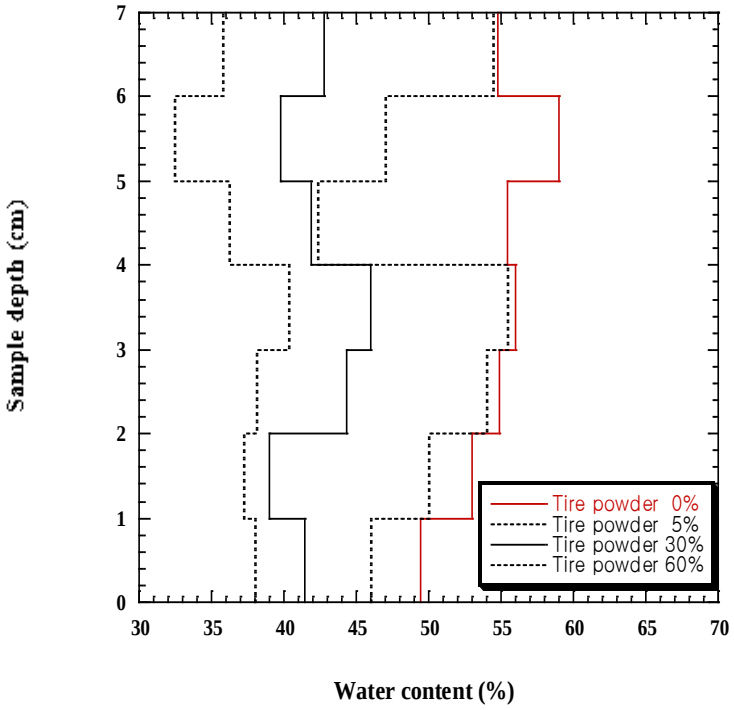

Fig. 7.6 Water content distribution after experiment

Fig. 7.6 shows results from cutting the extracted sample into pieces 1 cm thick after the frost heave experiment, and measuring the water content on a layer basis. Frozen soil includes soil grains, unfrozen water, and ice, but the last two contents cannot be identified separately. Accordingly, the ice was regarded as the water and the total amount of water was found. As shown in Fig. 7.6, no common tendency in the water content distribution with respect to the sample height direction was found. However, as the mixing ratio of tire powder contained in the mixed soil increases, the moisture ratio of the sample decreases.

7.5 Consideration

7.5.1 Volumetric ratio of voids in the soil and tire powder

To investigate the effect of mixing of discarded tires on the suppression of a frost heave, the volume of water in void of two kinds of grains (soil and waste tire powder) having different physical properties must be known. First, we can derive V_S (volume of the soil in the sample), V_T (volume of the tire in the sample), V_W (volume of the water), W_S (weight of the soil in the sample), and W_T (weight of the tire in the sample) from the three phases of the soil by using the post-test physical properties of each mixed soil listed in Table 7.1. Table 7.3 shows the resulting values.

Table 7.3 Volume and weight of each ample

Mixing ratio（%）	0	5	30	60	V=588.8cm^3
Vs(cm^3)	256.8	245.1	205.1	199.8	
Vw(cm^3)	332.0	316.9	257.0	201.3	
V_T(cm^3)	0	26.8	126.7	187.6	
Ws(g)	683.0	604.9	506.6	375.4	
W_T(g)	0	32.2	152.1	225.2	

Fig. 7.7 is a schematic diagram showing the cross-sectional states of the non-mixed and mixed soils. Assuming that the dry density of the soil component in both samples is constant regardless of the mixing ratio of tire powder in the figure, we use the following equation to find the volume of water in the soil and tire powder voids while increasing the mixing ratio. Fig. 7.7 (a) suggests that V_{SW} (volume of pore water in the soil void) and V_{TW} (volume of pore water in the tire powder void) can be given by the following equations:

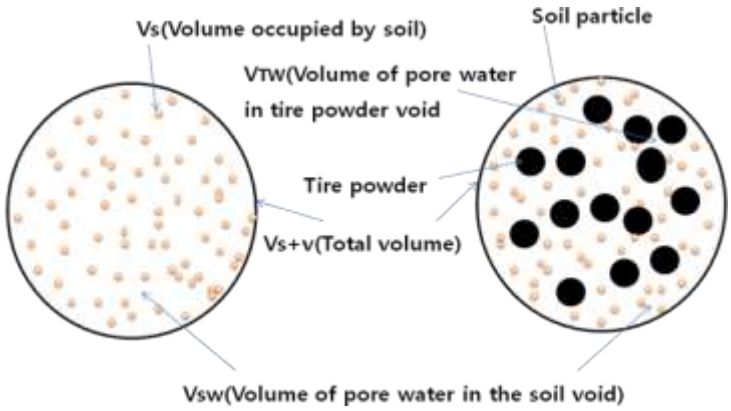

(a) Non-mixed soil (b) Mixed soil

Fig. 7.7 Cross-sectional states of non-mixed and mixed soils

$$V_{SW} = V_{S+V} - V_S \tag{7.1}$$

$$V_{TW} = V_W - V_{SW} \tag{7.2}$$

where, V_{S+V} is the total volume of the soil component. Table 7.4 lists the volume of pore water in the soil and tire powder that is derived from Eqs. (7.1) and (7.2).

Table 7.4 Volume of pore water in soil and tire powder

Mixing ratio (%)	0	5	30	60
V_{SW} (cm^3)	332.0	310.8	231.6	123.8
V_{TW} (cm^3)	-	6.1	25.4	77.5
V_W (cm^3)	332.0	316.9	257.0	201.3
Permeability (cm/sec)	4.03×10^{-6}	6.93×10^{-6}	9.45×10^{-6}	1.15×10^{-5}

Table 7.4 shows that V_{SW} reduces from 332.0 to 123.8 cm when the mixing ratio increases from zero to 60 percent, while V_{TW} rises from zero to 77.5 cm^3. Although V_W decreases from 332.0 to 201.3 cm^3 with an increase in the mixing ratio, the coefficient of permeability increases gradually. Fig. 7.8 illustrates the relationship between the mixing ratio and permeable cross section. Believing that the powder less than 1 mm in diameter has characteristics similar to sand; therefore, the higher the mixing ratio of tire powder, the larger the permeable cross section at temperatures above zero, resulting in an increase in permeability.

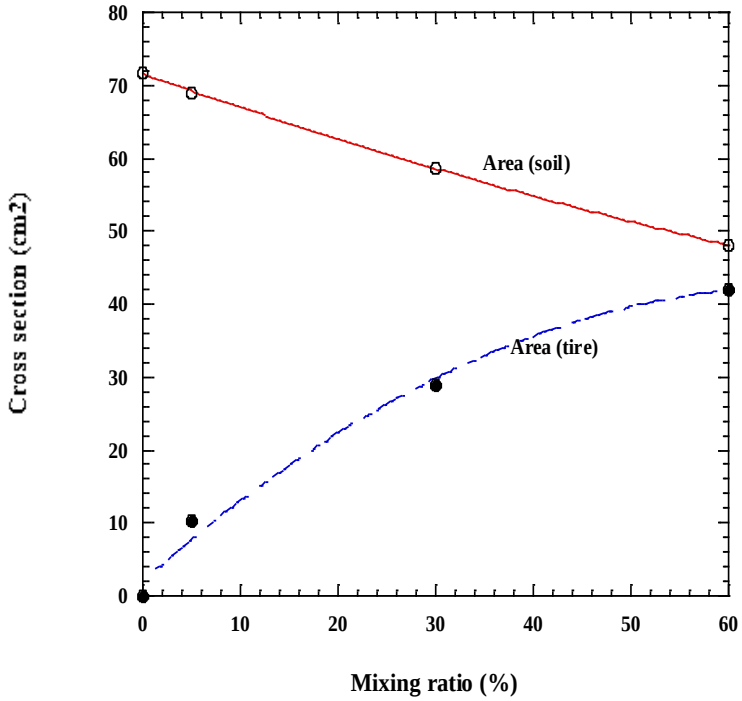

Fig. 7.8 Variation in mixing ratio and permeable cross section

The coefficient of permeability is said to relate to the area of water rather than to the volume of water. We find the permeable cross sections shown in Fig. 7.8 by applying V_S and V_T derived from the three phases of the soil as well as V_{SW} and V_{TW} shown in Table 7.4 to Eqs. (7.3) and (7.4) shown below to find the water volume, and converting it with Eq. (7.5).

$$V_{soil} = V_S + V_{SW} \tag{7.3}$$

$$V_{powder} = V_T + V_{TW} \tag{7.4}$$

$$A_{(soil,\ powder)} = V_{(soil,\ powder)}^{2/3} \tag{7.5}$$

Where, V_{soil} is the volume of the soil component of the sample and V_{powder} is the volume of tire powder. As shown in Fig. 7.8, as the mixing ratio of tire powder is increased, the soil

area Asoil decreases but the powder area A_{powder} increases.

At temperatures above zero, $A_{soil} + A_{powder}$ shown in Fig. 7.8 is the permeable area. Fig. 7.9 illustrates the relationship between total permeable area and mixing ratio. At temperatures above zero, the permeable area rises from 71.8 to 90.2 cm^2 with an increase in the mixing ratio (see Fig. 7.9 +Temperature).

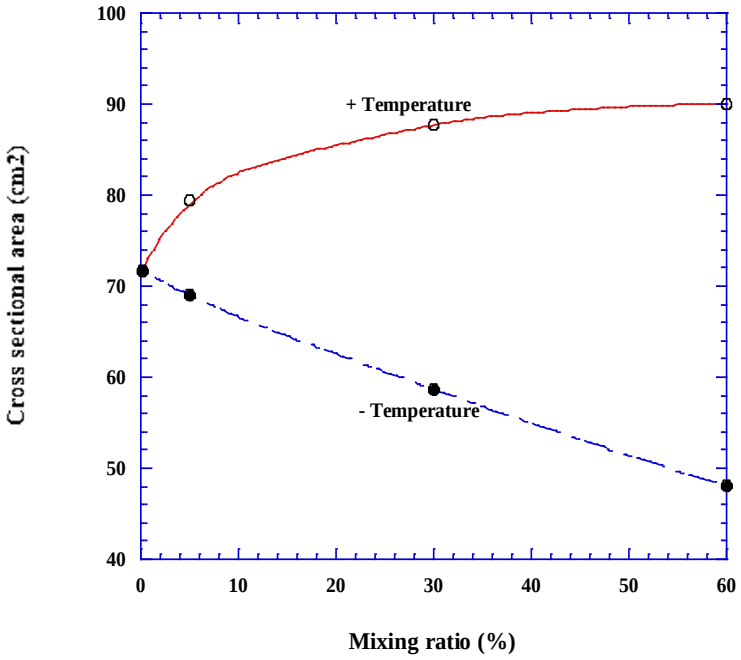

Fig. 7.9 Permeable area of soil

Believing that the tire powder has sand-like characteristics and is water-repellent; therefore, it contains no unfrozen water at temperatures below zero. As a result, water included in powder voids is completely changed to ice at temperatures below zero, which is likely to stop the flow of water. In this case, water can flow only through the soil; therefore, as the mixing ratio increases, the permeable cross-section decreases. The permeable area at temperatures below zero is only A_{soil} shown in Fig. 7.8, which tends to be inversely proportional to the mixing ratio. For example, mixing ratios of zero and 60 percent present permeable areas of 71.8 and 48.1 cm^2 respectively (see Fig. 7.9 -Temperature), which correspond to a reduction of about 43 percent. According to Figs. 7.8 and 7.9 showing the relationship between

permeable area and mixing ratio, as the mixing ratio increases at temperatures below zero, the permeable area decreases, resulting in a reduction in permeability (see Table 7.4).

7.5.2Variations of unsaturated coefficient of permeability in an unfrozen state

When the temperature falls below zero, ice is formed in soil voids. This pore ice decreases the water flowing area by the corresponding area. The coefficient of permeability of the frozen fringe where pore ice is present is very difficult to measure. However, we expect that using a method of finding the unsaturated coefficient of permeability at temperatures above zero enables calculation of the coefficient of permeability of the frozen fringe.

According to Black and Tice[5)], if two kinds of cohesive soil have the same density and water content—the unfrozen water content at low temperatures is the same as the water content in an unsaturated state at the normal temperature—then the two pore water distributions are consistent with each other as shown in Fig. 7.10.

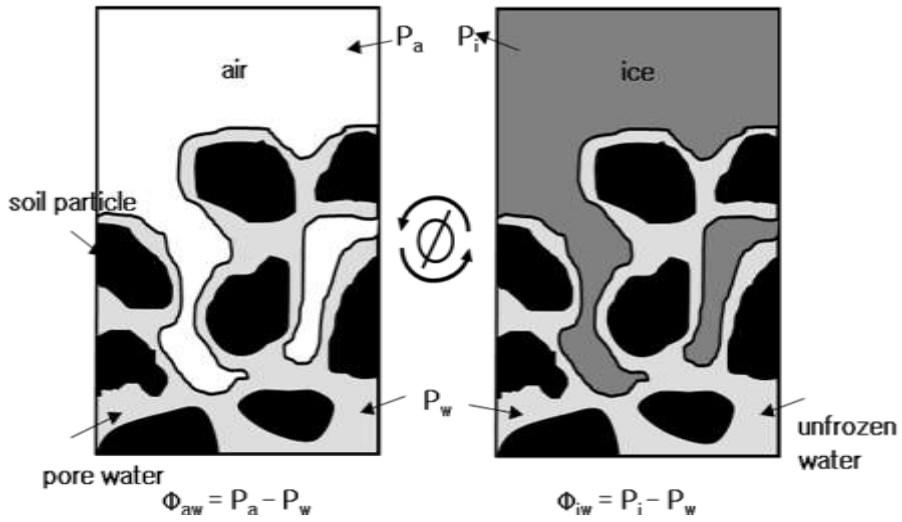

(a) Unsaturated soil at normal temperature (b) Frozen soil

Fig. 7.10 Distributions of unfrozen and pore water at the same water content[5)]

They compare the unfrozen water content measured with the pulse NMR system and the water retention curve derived from the pF test. Black and Tice claim that the following relation holds between the temperature of a freezing state and the air pressure at normal temperature.

$$\phi_{aw} = \phi_{iw} \tag{7.6}$$

$$\phi_{aw}(kPa) = -1{,}110\ (\text{kPa/°C}) \cdot T_S\ (°C) \tag{7.7}$$

where, ϕ is the pressure difference (kPa), T_S is the growing temperature of ice lens, and the subscripts a, w, and i represent air, water, and ice, respectively. If the frozen soil temperature is -1 degree Celsius, the sample has a pore ice distribution in the soil, which is equivalent to an air distribution in the pF test at a pressure of 1,110 kPa. This is the modified Clausius-Clapeyron equation.

Fukuda and Tice[6] show the following experimental equation to represent the unsaturated coefficient of permeability of the same Tomakomai soil as that used in this research as a capillarity potential function:

$$-\log_{10}(K) = A + B / \phi_{aw} \tag{7.8}$$

where, K is the unsaturated coefficient of permeability (cm/sec), ϕ is the capillarity potential (pF), and A and B are factors (9.549 and -6.614 respectively).

Substituting equation (8) into equation (9) and converting kPa to g/cm^2 produces equation (10) below.

$$-\log_{10}(K) = 9.549 - 6.614 / (-1{,}110 \cdot 10 \cdot Ts)\ (g/cm^2) \tag{7.9}$$

Eq. (7.9) shows that the relationship between the unsaturated coefficient of permeability and the pF is changed to that between the former and the temperature. Accordingly, we must determine the growing temperature T_S of ice lens. However, we could not measure T_S in this research, so we used Eq. (7.9) and the temperature range of -0.25 to -1.0 degrees Celsius-the developing and growing temperatures of ice lens formed in ordinary soil-to find the unsaturated coefficient of permeability[7]. Fig. 7.11 shows the resulting Kuu curve.

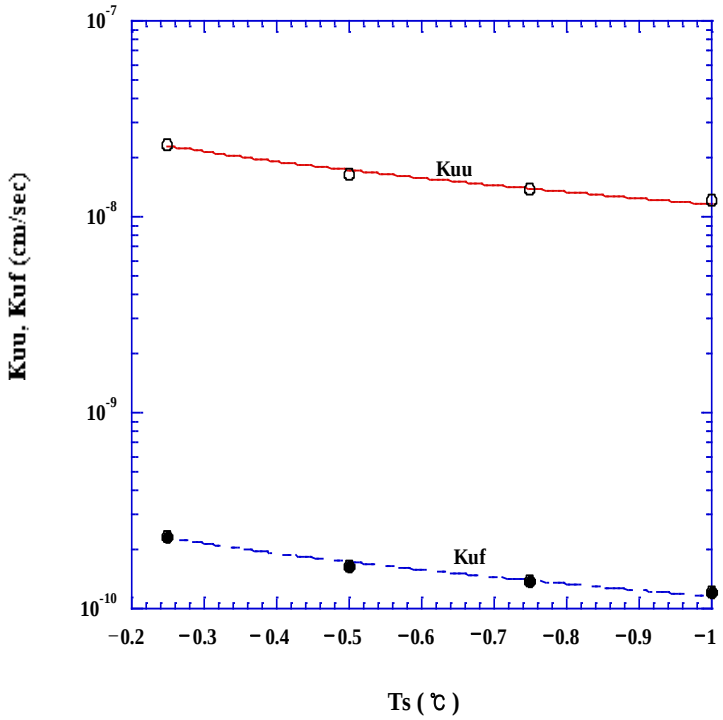

Fig. 7.11 T_S and unsaturated coefficients of permeability in unfrozen and frozen states

7.5.3 Variations of unsaturated coefficient of permeability in a frozen state

In the calculation of the unsaturated coefficient of permeability in an unfrozen state in the previous subsection, we assume that air exists instead of ice. When air is present in a void, the friction between the air and water can be ignored, but in the presence of ice instead of air, the resulting resistance between the ice and water lowers the speed of the flow of water. This means that finding the coefficient of permeability of the frozen fringe requires taking the resistance of ice into consideration. According to research conducted by Burt and Williams[8], the resistance corresponds to 10^{-2} times of an unfrozen permeability coefficient. This is the ice-impeding factor. In this research, we apply the value to the coefficient of permeability (Kuu curve) shown in Fig. 7.11 to find the unsaturated coefficient of permeability of the frozen fringe (Kuf curve).

7.5.4 Apparent unsaturated coefficient of permeability of the mixed soil

In Subsection 7.5.1, we told that water was present as free water in the discarded tire powder at temperatures above zero. However, when the temperature fell below zero, pore water was frozen, resulting in no water flow. Accordingly, the coefficient of permeability of the frozen fringe of the mixed soil is derived from changes in the cross sections of the soil and tire powder, which depend on the mixing ratio of the latter as shown in Fig. 7.8. Fig. 7.12 indicates changes in the coefficient of permeability when the temperature range is -0.25 to -1.0 degrees Celsius and the mixing ratio is 0, 5, 30, or 60 percent.

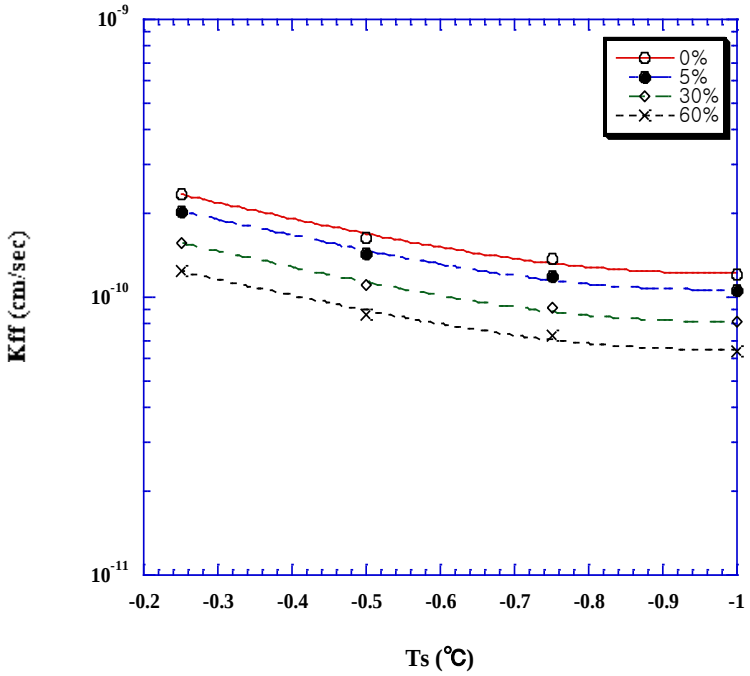

Fig. 7.12 Unsaturated coefficient of permeability of frozen fringe

As shown in Fig. 7.8, the cross sections (permeable areas) of the soil and tire powder are 69 cm^2 and 10.4 cm^2, respectively, if the mixing ratio is, for example, five percent. The soil component accounts for an 87% share of the entire cross section. Multiplying the ratio of the resulting cross section of the soil by Kuf in Fig. 7.11 on a powder mixing ratio basis yields the coefficient of permeability shown in Fig. 7.12. As the temperature T_S changes from -0.25 to-1 degrees Celsius, the tire powder mixing ratio increases but the coefficient of permeability decreases.

Fig. 7.13 shows the relationship between the coefficient of permeability of the mixed soil (Fig. 7.12) and the mixing ratio with the growing temperature T_S of ice lens parameterized.

So long as T_S is within the range of -0.25 to -1 degrees Celsius, increasing the mixing ratio tends to decrease the coefficient of permeability K_{ff}. We think that the reason why a temperature reduction decreases the coefficient of permeability is that the speed of water flowing through the frozen fringe is lowered due to decrease of unfrozen water (Fig. 5.8).

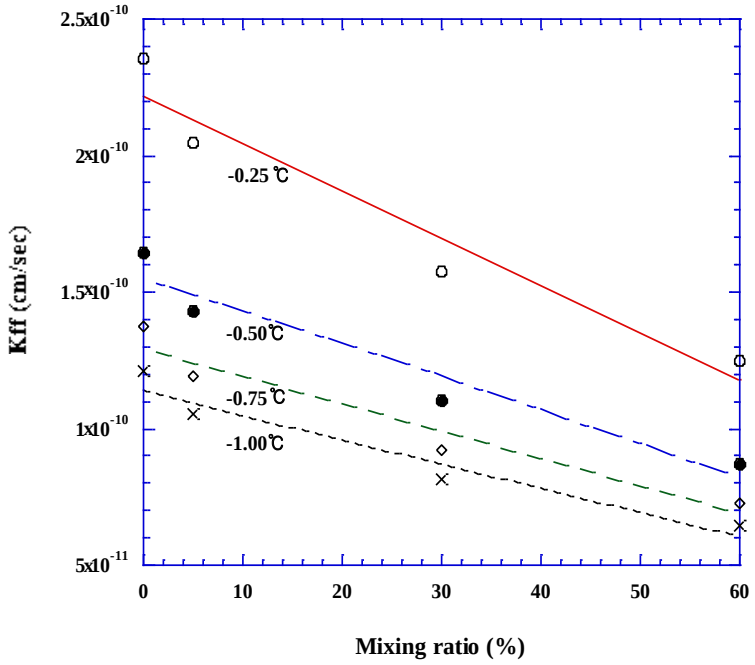

Fig. 7.13 Unsaturated coefficient of permeability and mixing ratio

7.5.5 Unsaturated coefficient of permeability and water intake rate

Fig. 7.14 shows the relationship between the unsaturated coefficient of permeability (K_{ff}) of the frozen fringe and the water intake rate (dw/dt). The latter is given by dividing the amount of frost heave shown in Fig. 7.5 by a bulk modulus of 1.09 when water is frozen-the displacement per unit time.

Water in the tire powder is completely frozen at temperatures below zero, eliminating any water flowing route. Assuming that only the soil component shows a frost heave and the pressure gradient (dpw/dx) of the soil is constant regardless of the mixing ratio, the water intake rate is represented by the following equation including the unsaturated coefficient of permeability:

$$\frac{dw}{dt} = K_{ff} \cdot \frac{dpw}{dx} \tag{7.10}$$

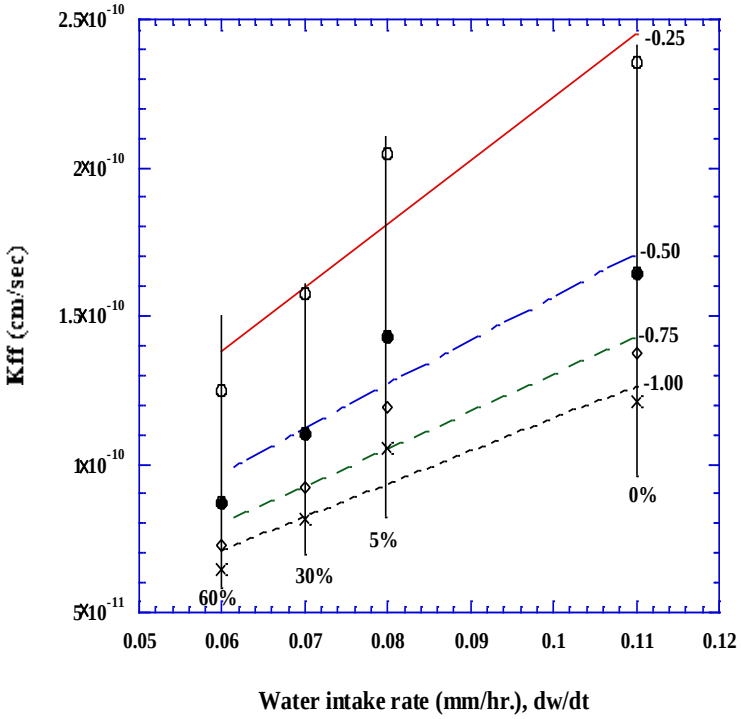

Fig. 7.14 Relationship between coefficient of permeability and water intake rate

If the pressure gradient is constant in Eq. (7.10), a linear relationship exists between the coefficient of permeability and the water intake rate (see Fig. 7.14). Fig. 7.14 indicates that increasing the amount of tire powder mixed reduces the coefficient of permeability, resulting in a fall in the water intake rate.

7.6 Summary

Through field tests, we have confirmed that mixing of tire powder has the effect of suppressing frost heave. To clarify the mechanism of this effect, we used the same tire powder to conduct three kinds of laboratory experiments: unfrozen water content, thermal conductivity, and frost heave. We employed a ramping test as the third one to maintain the frost heaving speed constant regardless of test conditions, such as the length and weight of samples.

In this research, we focused on changes in the coefficient of permeability caused by mixing of tire powder, and first found it in an unsaturated state. In the presence of ice, we took the ice-impeding factor into consideration to derive the coefficient of permeability of the frozen fringe from the ratio of the soil and tire powder areas in the mixed soil. The results showed that a linear relationship exists between the water intake rate and the coefficient of permeability. Accordingly, we have concluded that the frost heave reduces thanks to a fall in the permeability and a reduction in the unfrozen water content of the soil mixed with tire powder.

In addition, we calculated the volumetric ratio of the soil and tire powder to quantify the moisture amount of soil and tire powder pores. The results show that:

1. At temperatures above zero, as the mixing ratio of tire powder increases, the water content of tire pores rises from zero (at a mixing ratio of 0 percent) to 77.5 cm^3 (at 60 percent). When the temperature falls below zero, water in the tire powder completely changes to pore ice at zero degrees, eliminating any water passing route. As the tire powder content increases, the unfrozen water in the soil component decreases.

2. When we take the cross-section ratio into consideration and increase the mixing ratio of tire powder from zero to 60 percent, the coefficient of permeability of the frozen fringe decreases; for example, from 1.64×10^{-10} to 8.71×10^{-11} cm/sec at a temperature of −0.5 degrees Celsius.

3. The temperature range in which a frozen fringe is present may be from −0.25 to −1.0 degrees Celsius, at which a linear relationship exists between the coefficient of permeability and the water intake rate.

References

1) Ifukube, M.: Studies on frost heave, frost penetration and ratio of replacement to prevent frost damage of roads in Hokkaido, Report of the Civil Engineering Research Institute, No. 74 (1962)
2) Humphrey, D. N., Chen, L. H. and Eaton, R. A.: Laboratory and field measurement of the thermal conductivity of tire chips for used surged insulation, Transportation Research Board 76rh Annual Meeting, pp.1-27, pp.33-85 (1997)
3) Kim, H.S., Suzuki, T., Fukuda, M., Seo, S.Y., and Yamashita, S.,: Field experiments for reducing frost susceptibility using recycled tire powder, Journal of the Korean Geotechnical Society, Volume 26, No. 4, pp.5-14 (2010)
4) Kinosita, S.: Effects of initial soil-water conditions on frost heaving characteristics, Engineering Geology, 13, pp.41-52 (1979)
5) Black, P.B. and Tice, A.R.: Comparison of soil freezing curve and soil water curve data for Windsor sandy roam, CRREL Report 88-16, pp.1-9 (1988)
6) Fukuda, M. and Tice, J.N: Pore-water pressure profile of a freezing soil, Frost I Jord NR. 21, pp.31-36 (1980)
7) Sato, M. and Akagawa, S.: Experimental verification on proposed ice lens initiation process, Technical report 42, Hokkaido branch, Japanese Geotechnical Society, pp.277-282 (2002)
8) Burt, T.P. and Williams, P.J.: Hydraulic conductivity in frozen soil, Earth Surface Processes 1, pp.349-360 (1970)

Chapter 8 Conclusions

The following conclusions are drawn from the experimental investigation on the studies on Engineering Properties of Soil Mixed with Discarded Tire Powder as a new frost heave restraint material.

Field Frost Heave Test Using Discarded Tire Powder (Chapter 4)

1) The frost heave reductions achieved by mixing powdered tires into soil were not due to the insulating effect of rubber.

2) The frost front in the mixed section penetrated deeper than in the non-mixed section. This may be a latent heat diminution effect caused by water-repellent properties of the rubber and decreased specific surface area in the mixed soil.

3) Our 3-year field experiment found that mixing soil with granulated tires (20% by weight) reduced the frost heave ratio by about 75%.

4) The segregation potential (SP) value of the soil decreased 65% by mixing 20% tire powder by weight into the soil. This large SP difference explains how the frost heave of mixed soil is restrained by the addition of powdered tires.

Thermal conductivity of discarded tire powder-soil mixture (Chapter 5)

5) Unfrozen water content in frozen soil was measured using Pulsed NMR equipment. As the result, relations between temperature and unfrozen water content were expressed into exponent of temperature for the area below 0 degree Celsius.

6) As powder mixing ratio increases thermal conductivity decreased, with 1% increase of mixing ratio based on -20 degree Celsius thermal conductivity decreased 0.029W/m.K, and at +10 degree Celsius, it was about 0.016W/m.K mean, around half of thermal conductivity at -20 degree Celsius. Also, at the same mixing ratio, very similar thermal conductivity was measured regardless of the particle size.

7) By developing the two-phase model of thermal conductivity for unfrozen soil, soil particles and water, proposed by Woodside, we proposed three-phase model consisting of soil particle, ice and unfrozen water, which can be applied also to frozen soil area, as well as a concrete method of calculation for three-phase model.

Dynamics Characteristics of Frozen Soil with Discarded Tire Powder (Chapter 6)

8) Elastic wave velocity of freezing soil decreased in accordance with the rising of temperature and the increase of mixing rate of used tire powder an especially, elastic wave velocity (dilatational wave, shear wave) rapidly decreased at the temperature below -2 degree Celsius. From this result, it was verified that the change of elastic wave velocity has a close relationship with variance of unfrozen water in freezing soil by the change of temperature.

9) It was confirmed that the linear relationship exists with high correlation between elastic wave velocity (dilatational wave, shear wave) and the amount of unfrozen water, and between shear wave velocity and unconfined compressive strength.

10) Unconfined compressive strength of freezing soil increased with the decline of temperature and decreased as the mixing rate of used tire powder increased. It is considered that this increase of strength mainly resulted from the phase change of unfrozen water into ice by the decline of freezing temperature and from the increase of freeze strength between a specimen and ice. Besides, it is judged that the decline of strength by the increase of mixing rate resulted from the decrease of interlocking among particles and freeze force by the increase of mixing rate of tire powder that has a big transforming property.

11) The value of dynamic shear modulus (E) and dynamic elastic modulus(G) deduced from the measured elastic wave velocity increased with the decline of temperature, and decreased with the increase of mixing rate of used tire. Besides, Poisson's ratio was consistent with the range of 0.35~0.37 and it was shown that there was no big influence of temperature and mixing rate of used tire. However, as it approached to -0.5 degree

Celsius, Poisson's ratio (μ) rapidly increased.

Laboratory frost-heaving characteristics of soil mixed with discarded tire Powder (Chapter 7)

12) At temperatures above zero, as the mixing ratio of tire powder increases, the water content of tire pores rises from zero (at a mixing ratio of 0 percent) to 77.5 cm^3 (at 60 percent). When the temperature falls below zero, water in the tire powder completely changes to pore ice at zero degrees, eliminating any water passing route. As the tire powder content increases, the unfrozen water in the soil component decreases.

13) When we take the cross-section ratio into consideration and increase the mixing ratio of tire powder from zero to 60 percent, the coefficient of permeability of the frozen fringe decreases; for example, from 1.64×10^{-10} to 8.71×10^{-11} cm/sec at a temperature of −0.5 degrees Celsius.

14) The temperature range in which a frozen fringe is present may be from −0.25 to −1.0 degrees Celsius, at which a linear relationship exists between the coefficient of permeability and the water intake rate.